

CORROSION OF CARBON STEEL IN ACIDIC SALT SOLUTIONS UNDER FLOW CONDITIONS

A Thesis

**Submitted to the College of Engineering of Alnahrain University
in Partial Fulfillment of the Requirements for the
Degree of Master of Science in
Chemical Engineering**

by

SARA ALI SADEK

(B.Sc. in Chemical Engineering 2010)

Safar

1434

December

2012

Certification

I certify that this thesis entitled "**Corrosion of Carbon Steel in Acidic Salt Solutions under Flow Conditions**" was prepared by **Sara Ali Sadek** under my supervision at Alnahrain University / College of Engineering in partial fulfillment of the requirements for the degree of Master of Science in Chemical Engineering.

Signature:



Name: **Asst. Prof. Dr. Basim O. Hasan**

(Supervisor)

Date: 27/12/2012

Signature:



Name: **Asst. Prof. Dr. Basim O. Hasan**

(Head of Department)

Date: 27/12/2012

Certificate

We certify, as an examining committee, that we have read this thesis entitled “**Corrosion of Carbon Steel in Acidic Salt Solutions under Flow Conditions**”, examined the student **Sara Ali Sadek** in its content and found it meets the standard of thesis for the degree of Master of Science in Chemical Engineering.

Signature:

Name: **Asst. Prof. Dr. Basim O. Hasan**

(Supervisor)

Date: 27 / 12 / 2012

Signature:

Name: **Asst. Prof. Dr. Shaker Saleh Bahar**

(Member)

Date: 7 / 1 / 2013

Signature:

Name: **Dr. Sarmad Talib Najim**

(Member)

Date: 27 / 12 / 2012

Signature:

Name: **Asst. Prof. Dr. Mohammed Hliyil Hafiz**

(Chairman)

Date: 8 / 01 / 2013

Approval of the College of Engineering

Signature:

Name: **Prof. Dr. Muhsin J. Jweeg**
(Dean)

Date:

13 / 1 / 2013

Abstract

Corrosion of carbon steel in acid (HCl) - salt (Na_2SO_4) solutions under flow conditions was investigated for a range of rotation velocity, 0 – 2000 rpm, and temperature, 32 °C- 52 °C, by using rotating cylinder electrode (RCE). The corrosion rate was determined by using both weight loss method and electrochemical polarization technique. Different acid and salt concentrations were used from range 0.01 M to 0.4 M for salt and 0.5 % to 5 % (v/v) for acid with different oxygen concentrations provided by pumping air through the corrosive solution. Indole and cetyl trimethyl ammonium bromides (CTAB) inhibitors were used in concentrations of 2.74×10^{-3} M for CTAB and 1.7×10^{-3} to 3.4×10^{-3} M for indole. The effects of time (or corrosion product formation), and oxygen concentration through air bubbling in the solutions were also investigated.

The results showed that increasing the rotational velocity leads to an increase in the corrosion rate for all solutions investigated. Also, the corrosion rate in salt solutions had unstable trend with salt concentrations and temperature. In acid solutions, increasing the temperature and acid concentrations leads to an increase in the corrosion rate. Generally, the corrosion rate that represented by limiting current density decreased with time depending on rotational velocity and temperature. It was found that, adding air bubbles (i.e. by using air pump) leads to a considerable increase in the corrosion rates depending on rotational velocity, temperature, and time. High effect of oxygen concentration was noted in cases of acid solutions and in case of high rotational velocity.

Using statistical analysis (STATISTICA version 5.0), empirical correlations for the corrosion rate as a function of the velocity, temperature, concentrations, and time were obtained and discussed.

Indole and CTAB showed very good inhibition efficiency in most conditions investigated with the former exhibited better inhibition efficiency arriving up to 88 % at low rotational velocities decreasing with flow velocity increase. In addition, indole inhibitor reveals excellent inhibition efficiency for high temperatures, while in CTAB solution increasing the temperature leads to decrease the inhibition efficiency.

List of Contents

Contents		Page
Abstract		I
List of Contents		III
Nomenclature		VII
Greek Symbols		VIII
Abbreviations		IX
List of Tables		X
List of Figures		XIV

Chapter One : Introduction

1.1	Introduction	1
1.2	The Scope of Present Work	5

Chapter Two: Corrosion Phenomena

2.1	Electrochemical Aspects of Corrosion	6
2.2	Corrosion Classifications	7
2.2.1	Dry Corrosion	8
2.2.2	Wet Corrosion	8
2.3	Forms of Corrosion Attack	8
2.3.1	Uniform Corrosion	8
2.3.2	Galvanic Corrosion	9
2.3.3	Localized Corrosion	10
2.3.4	Pitting Corrosion	10

2.3.5	Selective Dissolution	10
2.3.6	Conjoint Action of Corrosion and a Mechanical Factor	11
2.4	Factors Effecting Corrosion Rate	11
2.4.1	Effect of PH	11
2.4.2	Effect of Temperature	12
2.4.3	Effect of Dissolved Oxygen	13
2.4.4	Effect of Dissolved Salts	14
2.4.5	Effect of Velocity	15
2.5	Limiting Current Density	17
2.6	Polarization Concept	18
2.7	Polarization Types	19
2.7.1	Activation Polarization	19
2.7.2	Concentration Polarization	20
2.7.3	Combined Polarization	21
2.7.4	Resistance Polarization	22
2.8	Corrosion of Iron in Acid	23
2.9	Corrosion Inhibitors	24
2.10	Classification of Inhibitors	25
2.10.1	Inorganic Inhibitors	25
2.10.2	Organic Anionic	26
2.10.3	Organic Cationic	26
2.11	Inhibitors for Acid Solutions	26
2.12	Indole Inhibitor (I)	28
2.13	Cetyl Trimethyl Ammonium Bromides Inhibitor (CTAB)	29

2.14	Literature Review	30
------	-------------------	----

Chapter Three: Experimental Works

3.1	Introduction	40
3.2	The Solutions	41
3.3	Materials	42
3.4	Experimental Apparatus	42
3.5	Density Measurements	48
3.6	Experimental Procedures	49
3.6.1	Weight Loss Experiments	49
3.6.2	Polarization Experiments	50

Chapter Four: Results

Chapter five: Discussions

5.1	Effect of Velocity on the Corrosion rate	77
5.2	Effect of Velocity and Temperature on Limiting Current Density	79
5.3	Effect of Corrosion Product Formation on Limiting Current Density (LCD)	84
5.4	Effect of Salt Concentration on LCD	89
5.5	Comparison of Corrosion Rate in Presence and Absence of Air Bubbling	91
5.6	Effect of Parameters on Mass Transfer Coefficient (k) and Diffusion Layer Thickness (δ)	93

5.7	Acid-Salt Solution	98
5.7.1	Effect of Velocity on Corrosion Current (i_{corr})	98
5.7.2	Effect of Temperature and Concentration	101
5.8	Addition of Inhibitors	105
5.8.1	Indole	106
5.8.1.1	Effect of Velocity on IE	106
5.8.1.2	Effect of Temperature on IE	109
5.8.2	Cetyl Trimethyl Ammonium Bromides Inhibitor (CTAB)	110
5.8.2.1	Effect of Velocity on IE of CTAB	110
5.8.2.2	Effect of Temperature on IE of CTAB	111

Chapter Six: Conclusions and Suggestions for Future Work

6.1	Conclusions	114
6.2	Suggestions for Future Work	115

References		116
-------------------	--	-----

Appendices

Appendix -A-		A-1
Appendix -B-		B-1
Appendix -C-		C-1
Appendix -D-		D-1

Nomenclature

Symbol	Meaning	Units
A	Surface area of specimen	m^2
C_b	Bulk concentration	ppm (mg/L)
CR	Corrosion rate	$gm/m^2 \cdot day$
d_i	Inside diameter of specimens	cm
d_o	Outside diameter of specimens	cm
D_{O_2}	Diffusivity of oxygen	m^2/s
E	Electrode potential	V
E_a	Activation energy	kJ/mol
$E_{corr.}$	Corrosion potential	V
F	Faraday No. (96487)	Columb/equivalent
I	Current	A
i	Total current density	A/m^2
$i_{corr.}$	Corrosion current density	A/m^2
i_c, i_a	Cathodic and anodic current density	A/m^2
IE	Inhibition efficiency (%)	dimensionless
i_{H_2}	Current density of hydrogen evolution	A/m^2
i_L	Limiting current density	A/m^2
i_o	Exchange current density	A/m^2
i_{O_2}	Oxygen current density	A/m^2
k	Mass transfer coefficient	m/s
L	Length of specimens	cm
mpy	Mils per year	Mils/ year
N_{Fe}	molar flux of iron	mole/ $m^2 \cdot s$

N_{O_2}	Molar flux of oxygen	mole /m ² .s
R	Gas constant (8.314)	J /mol. K
Re	Reynolds number	dimensionless
R_f	Films resistance	Ω . cm
$R_{sol.}$	Electric resistance of solution	Ω . cm
t	Immersion time	h.
T	Temperature	°C
u	Revolution per minute	rpm
Z	Number of electrons transferred	...
ΔW	Weight loss	gm

Greek symbols

Symbol	Meaning	Units
μ	Fluid viscosity	kg/m. s
ρ	Fluid density	kg/m ³
β_a, β_c	Anodic and cathodic Tafel slope	mV/ decade
δ	Thickness of diffusion layer	m
η	Polarization overpotential	mV
η^T	Total overpotential	mV
η^A	Activation overpotential	mV
η^C	Concentration overpotential	mV
η^R	Resistance overpotential	mV

Abbreviations

Abbreviation

Meaning

C.S	Carbon steel
LCD	Limiting current density
SCE	Standard calomel electrode
RCE	Rotating cylinder electrode
gmd	Gram per square meter per day
I	Indole
CTAB	Cetyl Trimethyl Ammonium Bromides
EIS	Electrochemical impedance spectroscopy
PDP	potentiodynamic polarization
APTT	4-amino-5-phenyl-4H-1, 2, 4-trizole-3-thiol
HE	Hydrogen evolution
ML	Mass loss
H ₄ L ³	1,7- bis (2- hydroxy benzamido)-4-azaheptane
SDS	Sodium dodecyl sulfate
QL	Quinoline
QLD	Quinaldine
QLDA	Quinaldic acid
P4	2-phenylthieno (3, 2-b) quinoxaline
P1	Ethyl [4-(2-chlorobenzyl)-3-Methyl-6-oxopyridazin-1(6H)-y1]
WL	Weight loss

List of Tables

Table	Title	Page
4-1	Corrosion rate of carbon steel in 0.2 M Na ₂ SO ₄ at 32 °C for 4 h of immersions time by using weight loss method	55
4-2	Corrosion rate of carbon steel in 0.2 M Na ₂ SO ₄ with 5 % vol HCl at 32 °C for 4 h by using weight loss method	56
4-3	Corrosion rate of carbon steel in 0.2 M Na ₂ SO ₄ mixed with 5 % vol HCl with addition of air bubbles at 32 °C for 4 h of immersions time by using weight loss method.	57
4-4	Measured oxygen solubility at different sodium sulphate concentrations and temperatures.	71
4-5	Measured oxygen solubility in 0.2 M Na ₂ SO ₄ with addition of air bubbles.	72
4-6	Measured oxygen solubility in different acid salt mixture at different temperatures.	72
4-7	Measured oxygen solubility in 0.2 M Na ₂ SO ₄ + 5 % HCl with addition of air bubbles at different velocities and at 32 °C.	72
4-8	Measured oxygen solubility in 0.2 M Na ₂ SO ₄ + 1 % HCl with addition of air bubbles at different velocities and temperatures.	73
4-9	Measured pH values for different salt and acid salt mixtures at different concentrations.	73
4-10	Measured conductivity values of different Na ₂ SO ₄ concentrations at different temperatures.	74

4-11	Corrosion of carbon steel pipe in 0.1M Na ₂ SO ₄ + 1 % HCl (uninhibited solution) for 2h immersion time by using weight loss method.	74
4-12	Corrosion of carbon steel pipe in 0.1M Na ₂ SO ₄ + 1 % HCl with 1.7×10 ⁻³ M indole for 2h immersion time by using weight loss method.	75
4-13	Corrosion of carbon steel pipe in 0.1M Na ₂ SO ₄ + 1 % HCl with 3.4×10 ⁻³ M indole at 32 °C for 2h immersion time by using weight loss method.	75
4-14	Corrosion of carbon steel pipe in 0.1M Na ₂ SO ₄ + 1 %HCl with 2.74×10 ⁻³ M CTAB for 2h immersion time by using weight loss method.	76
A-1	Measured density of the solutions used in experiments	A-1
A-2	Viscosity of the pure water	A-1
A-3	Diffusivity of oxygen in pure water	A-2
A-4	Corrosion of carbon steel in 0.2 M Na ₂ SO ₄ and 32 °C	A-2
A-5	Corrosion of carbon steel in 0.2 M Na ₂ SO ₄ and 42 °C	A-2
A-6	Corrosion of carbon steel in 0.2 M Na ₂ SO ₄ and 52 °C	A-3
A-7	Corrosion of carbon steel in 0.2 M Na ₂ SO ₄ with addition of air bubbles and 32 °C	A-3
A-8	Corrosion of carbon steel in 0.2 M Na ₂ SO ₄ with addition of air bubbles and 42 °C	A-3
A-9	Corrosion of carbon steel in 0.2 M Na ₂ SO ₄ with addition of air bubbles and 52 °C	A-4
A-10	Corrosion of carbon steel in 0.2 M Na ₂ SO ₄ at 32 °C	A-4

	for immersion time of 2 h and velocity of 250 rpm	
A-11	Corrosion of carbon steel in 0.2 M Na ₂ SO ₄ at 32 °C for immersion time of 2 h and velocity of 1000 rpm	A-4
A-12	Corrosion of carbon steel in 0.2 M Na ₂ SO ₄ at 32 °C for immersion time of 2 h and velocity of 2000 rpm	A-5
A-13	Corrosion of carbon steel in 0.2 M Na ₂ SO ₄ at 42 °C for immersion time of 2 h and velocity of 250 rpm	A-5
A-14	Corrosion of carbon steel in 0.2 M Na ₂ SO ₄ at 52 °C for immersion time of 2 h and velocity of 250 rpm	A-5
A-15	Corrosion of carbon steel in 0.2 M Na ₂ SO ₄ with addition of air bubbles at 32 °C for immersion time of 2 h and velocity of 250 rpm	A-6
A-16	Corrosion of carbon steel in 0.2 M Na ₂ SO ₄ with addition of air bubbles at 32 °C for immersion time of 2 h and velocity of 750 rpm	A-6
A-17	Corrosion of carbon steel in 0.2 M Na ₂ SO ₄ with addition of air bubbles at 32 °C for immersion time of 2 h and velocity of 2000 rpm	A-6
A-18	Corrosion of carbon steel in 0.2 M Na ₂ SO ₄ with addition of air bubbles at 42 °C for immersion time of 2 h and velocity of 250 rpm	A-7
A-19	Corrosion of carbon steel in 0.2 M Na ₂ SO ₄ with addition of air bubbles at 52 °C for immersion time of 2 h and velocity of 250 rpm	A-7
A-20	Corrosion of carbon steel in 0.01 M Na ₂ SO ₄ at different temperatures and velocity of 750 rpm	A-7
A-21	Corrosion of carbon steel in 0.025 M Na ₂ SO ₄ at different temperatures and velocity of 750 rpm	A-8
A-22	Corrosion of carbon steel in 0.05 M Na ₂ SO ₄ at different temperatures and velocity of 750 rpm	A-8

A-23	Corrosion of carbon steel in 0.1 M Na ₂ SO ₄ at different temperatures and velocity of 750 rpm	A-8
A-24	Corrosion of carbon steel in 0.4 M Na ₂ SO ₄ at different temperatures and velocity of 750 rpm	A-9
B-1	Corrosion of carbon steel in 0.01 M Na ₂ SO ₄ + 1 % HCl	B-1
B-2	Corrosion of carbon steel in 0.05 M Na ₂ SO ₄ + 1 % HCl at velocity of 250 rpm	B-1
B-3	Corrosion of carbon steel in 0.2 M Na ₂ SO ₄ + 1 % HCl at velocity of 250 rpm	B-2
B-4	Corrosion of carbon steel in 0.2 M Na ₂ SO ₄ + 0.5 % HCl at velocity of 250 rpm	B-2
B-5	Corrosion of carbon steel in 0.2 M Na ₂ SO ₄ + 3 % HCl at velocity of 250 rpm	B-2
B-6	Corrosion of carbon steel in 0.2 M Na ₂ SO ₄ + 1 % HCl with addition of air bubbles	B-3
D-1	Data for polarization experiments in 0.2 M Na ₂ SO ₄ at 32 °C	D-1
D-2	Data for polarization experiments in 0.2 M Na ₂ SO ₄ + 1 % HCl at 250 rpm	D-2

List of Figures

Figure	Title	Page
2- 1	Electrochemical corrosion of metal	6
2- 2	Uniform corrosion	9
2- 3	Effect of pH on corrosion rate of iron	12
2- 4	Indole	29
3- 1	Rotating shaft and specimen insallation	43
3- 2	Air pump and oxygen bubbles	44
3- 3	PH meter	45
3- 4	Conductivity meter	45
3- 5	Dissolved oxygen meter	46
3 - 6	Desiccator	46
3- 7	Balance	46
3- 8	Schematic illustrates of experimental apparatus.	47
3- 9	Experimental rig picture	48
3- 10	Density testing	48
3- 11	Typical polarization curve	51
3- 12	Anodic and cathodic polarization curves with Tafel slopes in acid solution	53
4-1	Cathodic polarization curves in 0.2 M Na ₂ SO ₄ at 32 °C	58
4-2	Cathodic polarization curves in 0.2 M Na ₂ SO ₄ at 42 °C	58
4-3	Cathodic polarization curves in 0.2 M Na ₂ SO ₄ at 52 °C	59
4-4	Cathodic polarization curves in 0.2 M Na ₂ SO ₄ with air bubbles at 32 °C	59
4-5	Cathodic polarization curves in 0.2 M Na ₂ SO ₄ with air bubbles at 42 °C	60
4-6	Cathodic polarization curves in 0.2 M Na ₂ SO ₄ with air bubbles at 52 °C	60
4-7	Cathodic polarization curves in 0.2 M Na ₂ SO ₄ at 250 rpm at 32 °C for 2h	61
4-8	Cathodic polarization curves in 0.2 M Na ₂ SO ₄ at 250 rpm at 42 °C for 2h	61

4-9	Cathodic polarization curves in 0.2 M Na ₂ SO ₄ at 250 rpm at 52 °C for 2h	61
4- 10	Cathodic polarization curves in 0.2 M Na ₂ SO ₄ at 32°C for 1000 rpm & 2h	62
4- 11	Cathodic polarization curves in 0.2 M Na ₂ SO ₄ at 32°C for 2000 rpm & 2h	62
4-12	Cathodic polarization curves in 0.2 M Na ₂ SO ₄ with air bubbles at 250 rpm, 32 °C and 2h	63
4-13	Cathodic polarization curves in 0.2 M Na ₂ SO ₄ with air bubbles at 250 rpm, 42 °C and 2h	63
4-14	Cathodic polarization curves in 0.2 M Na ₂ SO ₄ with air bubbles at 250 rpm, 52 °C and 2h	63
4-15	Cathodic polarization curves in 0.2 M Na ₂ SO ₄ with air bubbles at 32 °C for 750 rpm and 2h	64
4-16	Cathodic polarization curves in 0.2 M Na ₂ SO ₄ with air bubbles at 32 °C for 2000 rpm and 2h	64
4-17	Cathodic polarization curves in 0.01 M Na ₂ SO ₄ at 750 rpm	65
4-18	Cathodic polarization curves in 0.025 M Na ₂ SO ₄ at 750 rpm	65
4-19	Cathodic polarization curves in 0.05 M Na ₂ SO ₄ at 750 rpm	65
4-20	Cathodic polarization curves in 0. 1 M Na ₂ SO ₄ at 750 rpm	65
4-21	Cathodic polarization curves in 0. 4 M Na ₂ SO ₄ at 750 rpm	66
4-22	Anodic and cathodic polarization curves in 0.01 M Na ₂ SO ₄ with 1 % HCl at 32 °C and different velocities	67
4-23	Anodic and cathodic polarization curves in 0.01 M Na ₂ SO ₄ with 1 % HCl at 250 rpm and different temperatures	67
4.24	Polarization curves at 250 rpm in 0.05 M Na ₂ SO ₄ + 1 % HCl	68
4.25	Polarization curves at 250 rpm in 0.2 M Na ₂ SO ₄ + 1 % HCl	68
4.26	Polarization curves at 250 rpm in 0.2 M Na ₂ SO ₄ + 0.5 % HCl	69

4.27	Polarization curves at 250 rpm in 0.2 M Na ₂ SO ₄ + 3 % HCl	69
4.28	Polarization curves at 32 °C and different u in 0.2 M Na ₂ SO ₄ + 1 % HCl with air bubbles	70
4.29	Polarization curves at 250 rpm and different T in 0.2 M Na ₂ SO ₄ + 1 % HCl with air bubbles	71
5-1	Variation of corrosion rate with velocity at 32 °C and 4 h immersion time	77
5-2	Variation velocity and temperature on i_L in 0.2 M Na ₂ SO ₄	80
5-3	Variation of i_L with velocity at different temperatures in 0.2 M Na ₂ SO ₄ with addition of air bubbles.	81
5-4	E_{corr} vs. u in 0.2 M Na ₂ SO ₄	83
5-5	E_{corr} vs. u in 0.2 M Na ₂ SO ₄ with air bubbles.	83
5-6	Variation of i_L with time in 0.2 M Na ₂ SO ₄ at 250 rpm	85
5-7	Variation of i_L with time at 32 °C and different velocities in 0.2 M Na ₂ SO ₄	87
5-8	Variation of i_L with time in 0.2 M Na ₂ SO ₄ with addition of air bubbles at 250 rpm and different temperatures.	88
5-9	Effect of time on the i_L at the three velocities and 32 °C in 0.2 M Na ₂ SO ₄ in presence of air bubbles.	89
5-10	Effect of sodium sulphate concentrations on the i_L at 750 rpm	90
5-11	Conductivity versus Na ₂ SO ₄ concentrations.	90
5-12	i_L vs. .time with and without using air bubbles at 32 °C and 250 rpm.	92
5-13	i_L vs. .time with and without using air bubbles at 32 °C and 250 rpm.	92
5-14	i_L vs. time with and without air bubbling at 52 °C and 250 rpm	92
5-15	Variation of k with u at 32 °C by using W.L. method	94

5-16	Variation of δ with u at 32 °C by using W.L. method	94
5-17	Variation of K with u in 0.2 M Na ₂ SO ₄	95
5-18	Variation of δ with u in 0.2 M Na ₂ SO ₄	95
5-19	Variation of K with u in 0.2 M Na ₂ SO ₄ with air bubbles	95
5-20	Variation of δ with u in 0.2 M Na ₂ SO ₄ with air bubbles	95
5-21	Variation of K with t at 32 °C	95
5-22	Variation of δ with t at 32 °C	95
5-23	Variation of K with t at 250rpm	96
5-24	Variation of δ with t at 250 rpm	96
5-25	Variation of K with t at 250rpm in 0.2 M Na ₂ SO ₄ with air bubbles	96
5-26	Variation of δ with t at 250 rpm in 0.2 M Na ₂ SO ₄ with air bubbles	96
5-27	Variation of K with t at 32 °C in 0.2 M Na ₂ SO ₄ with air bubbles	96
5-28	Variation of δ with t at 32 °C in 0.2 M Na ₂ SO ₄ with air bubbles	96
5-29	Variation of K with T at different salt concentration	97
5-30	Variation of δ with T at different salt concentration	97
5-31	Variation of i_{corr} with velocity at 32 °C in 0.01M Na ₂ SO ₄ +1 % HCl	99
5-32	Variation of i_{corr} with velocity at 32 °C in 0.2 M Na ₂ SO ₄ +1 % HCl and in 0.2 M Na ₂ SO ₄ both with addition of air bubbles.	100
5-33	Variation of i_{corr} with T at 250 rpm in 1% HCl with different salt concentrations	103
5-34	Variation of i_{corr} with T in 0.2 M Na ₂ SO ₄ with different acid concentrations at 250 rpm	103
5-35	Variation of i_{corr} with T at 250 rpm in 0.2 M Na ₂ SO ₄ + 1% HCl with and without addition of air bubbles.	104

5-36	Variation of CR with velocity in presence of indole.	106
5-37	Variation of IE % with u at 32 °C	107
5-38	Variation of IE with T at 0 rpm in 0.1 M Na ₂ SO ₄ + 1 % HCl + 1.7×10 ⁻³ M (200 ppm) indole	110
5-39	Variation of IE with u at 32 °C in CTAB solution	110
5-40	Variation of IE with T at 0 rpm in 0.1 M Na ₂ SO ₄ + 1% HCl + 2.74×10 ⁻³ M (1000 ppm) CTAB	112
C-1	Polarization curve in 0.2 M Na ₂ SO ₄ at 32 °C and 0 rpm	C-1
C-2	Polarization curve in 0.2 M Na ₂ SO ₄ at 42 °C and 0 rpm	C-1
C-3	Polarization curve in 0.2 M Na ₂ SO ₄ at 52 °C and 0 rpm	C-2
C-4	Polarization curve in 0.2 M Na ₂ SO ₄ with air bubbles at 32 °C and 0 rpm	C-2
C-5	Polarization curve in 0.2 M Na ₂ SO ₄ with air bubbles at 42 °C and 0 rpm	C-3
C-6	Polarization curve in 0.2 M Na ₂ SO ₄ with air bubbles at 52 °C and 0 rpm	C-3
C-7	Variation of E _{corr} with time at different u and 32 °C	C-4
C-8	Variation of E _{corr} with time at different T and 250 rpm	C-4
C-9	Variation of E _{corr} with time at different u and 32 °C in 0.2 M Na ₂ SO ₄ with air bubbles	C-4
C-10	Variation of E _{corr} with time at different T and 250 rpm in 0.2 M Na ₂ SO ₄ with air bubbles	C-4
C-11	Variation of E _{corr} with T at 750 rpm in different salt solutions	C-5
C-12	Variation of E _{corr} with u at 32 °C	C-5
C-13	Variation of E _{corr} with T at 250 rpm in different acid salt solution with and without air bubbles	C-5
C-14	Variation of E _{corr} with T at 250 rpm in different acid salt solution	C-5

Chapter One

Introduction

1.1 Introduction

The most accepted definition for corrosion is the destruction of material due to a chemical reaction of the material with its environment. Generally, this destruction takes place on its surface in the form of material dissolution or redeposit ion in some other forms. Metallic systems are the predominant materials of construction, and as a class, are generally susceptible to corrosion. Consequently, the bulk of corrosion science focuses upon metals and alloys [Guthrie and Gretchen, 2002].

Corrosion usually begins at the surface of material and occurs because of the spontaneous tendency of the materials to return to their thermodynamic stable state or to one of the forms in which they were originally found. Metals are generally prone to corrosion because most of them occur naturally as ores, which is the most stable state of low energy and there is a net decrease in free energy ΔG from metallic to oxidized state [Ogunleye et. al., 2011].

Carbon steel, the most widely used engineering material, accounts for approximately 85% of the annual steel production worldwide. Despite its relatively limited corrosion resistance, carbon steel is used in large tonnages in marine applications, chemical processing, petroleum production and refining, construction and metal processing equipment [Fouda et.al, 2011].

Sulphate corrosion is one of the most ordinary and widest kinds of chemical corrosion. There are plenty of sulphate ions in coastal areas which can cause great damages to concrete structures. [Liang et. al., 2011]

There are many investigations for corrosion of carbon steel in neutral aerated salt solutions, especially in sodium chloride (NaCl) solution. Little investigation has been found for corrosion of carbon steel in Na₂SO₄ salt solution. Generally corrosion of turbine caused by a thin film deposit of fused salt (sodium sulphate) on alloy surface (carbon steel) is an example of corrosion in sodium sulphate [Bornstein and Decrescente, 1971; Goebel et. al., 1973]. During combustion in the gas turbine, sulfur from the fuel reacts with sodium chloride from ingested air at elevated temperatures to form sodium sulphate. The sodium sulphate then deposits on the hot-section components, such as nozzle guide vanes and rotor blades, resulting in accelerated oxidation attack. This is commonly referred to as “hot corrosion” [Stringer, 2007]. Sodium sulphate also causes corrosion in boiler that used sodium sulfite (Na₂SO₃) as oxygen scavenger when Na₂SO₃ reacted with oxygen at low temperature and pressure it forms sodium sulphate that causes serious attack to the tubes of the boiler [Huijbregts, 2007]. Sodium sulphate is also present in considerable amount in the water accompanying petroleum drawn from underground.

Salts dissolved in water have a marked influence on the corrosivity of water. At extremely low concentrations of dissolved salts, different anions and cations show varying degrees of influence on the corrosivity of the water. The anions most commonly found in water are chloride, sulphate and bicarbonate. The sulphate ion has a greater effect on the corrosivity of the water than the chloride ion, and the bicarbonate ion shows inhibitive tendencies. Generally, the corrosivity of waters containing dissolved salts increases with increasing salt

concentration until a maximum is reached, and then the corrosivity decreases. This may be attributed to increased electro-conductivity because of the increased salt content, until the salt concentration is great enough to cause an appreciable decrease in the oxygen solubility, resulting in a decreased rate of depolarization [Revie and Uhlig 2008].

The following reactions occur as the result of the corrosion of carbon steel in sodium sulphate (Na_2SO_4) aqueous solutions:



The morphology of the corrosion attack occurring on the surface of mild steel after a certain exposure can be regarded as partially uniform. This attack started in isolated locations and then spread laterally without developing any pits. The effect of SO_4^{-2} on the rate of oxidation of iron in mildly alkaline solutions results from its ability to form soluble complexes with Fe^{+2} or Fe^{+3} ions. Also it was found that sulphate ions accelerate the active dissolution of iron and the films formed in sulphate solutions result from supersaturated solutions of iron salts, most probably iron hydroxysulphate. This implies that iron dissolves in sulphate solutions at a high rate, creating a supersaturated solution and allowing precipitation of a non protective film [Peralta et. al. 2002].

Corrosion of mild steel is a fundamental academic and industrial concern that has received considerable amount of attention. However, most equipment in industries is usually corroded owing to the general aggression of acid solutions. Some of the important fields of application of acid solutions in industries being acid pickling of iron and steel, chemical cleaning, ore production and oil well acidification [Obi-Egbedi et. al. 2011].

Hydrochloric acid is the most difficult of the common acids to handle from the standpoints of corrosion and materials of constructions. Extreme care is required in the selection of materials to handle the acid by itself, even in relatively dilute concentrations or in process solutions containing appreciable amount of hydrochloric acid. This acid is very corrosive to most of the common metals and alloys. Metals are exposed to the action of acids in many different ways and for many different reasons. One of the most commonly used acids in today's industrialized world is hydrochloric acid HCl. The wide use of this acid has led to the concentration on the corrosive effects of this acid on carbon steel, which is a versatile component in many industrial structures [Khadom et. al., 2009].

In order to prevent or minimize corrosion rates of metallic materials corrosion, inhibitors are usually used in the industry. Organic, inorganic, or a mixture of both inhibitors can inhibit corrosion by either chemisorptions on the metal surface or reacting with metal ions and forming a barrier-type precipitate on its surface [Al-Sehaibani 2000]. Because of the toxic nature and/or high cost of some chemicals currently in use as inhibitors, it is necessary to develop environmentally acceptable and inexpensive ones [Nahl'e et. al., 2010].

The corrosion of carbon steel in neutral environments is of practical importance, therefore it is considered by many studies. It is widely recognized that the corrosion of carbon steel may be accounted for by the anodic reaction as in equation 1.1 and cathodic reaction in presence of oxygen,



In many corrosion problems, there is strong evidence that the rate of uniform corrosion is controlled by mass transfer rate. This is true whether the corrosion fluid remains static or in fast motion with respect to the metal surface. However, molecular diffusion is not the only factor which influences the rate of corrosion. In addition, in turbulent fluids, the rate of transport of eddy diffusion appears to participate in the control of the overall transfer rate [Brodkey and Hershey, 1989]

It is accepted that the corrosion of mild steel in aerated water is controlled by the rate of cathodic reduction of oxygen and hence by the oxygen transport from the main stream solution to the reacting surface, generally if a metal is corroding under cathodic control it is apparent that the velocity of the solution will be more significant when diffusion of the cathodic reactant is rate controlling, although temperature may still have an effect. On the other hand if the cathodic process requires high activation energy, temperature will have the most significant effect. The effects of concentration, velocity and temperature are complex and it will become evident that these factors can frequently outweigh the thermodynamic and kinetic considerations [Shreir et. al., 2000].

1.2 The Scope of Present Work

The aim of this work is to study the influence of velocity, temperature, time, presence of air bubbles, and using of different corrosion inhibitors on corrosion rate of commercial carbon steel pipe in different concentrations of sodium sulphate (Na_2SO_4) and hydrochloric acid (HCl) solutions for rotating cylinder electrode (RCE) using both weight loss method and electrochemical polarization technique.

Chapter Two

Corrosion Phenomena

2.1 Electrochemical Aspects of Corrosion

Corrosion in aqueous environment and atmospheric environment is an electrochemical process because corrosion involves the transfer of electrons between a metal surface and an aqueous electrolyte solution [Zvandasara, 2009]. The current flows from a higher potential to a lower one. Hence, there are two reactions taking place simultaneously in the system. One reaction occurs as the electrons are discharged from the surface, called the anode. The released electrons are consumed in the other circuit of the corrosion cell shown schematically in Fig. 2-1. The corrosion cell consists of the following four components: anode, cathode, electrolyte, and Electronic connector. Several cathodic reactions are possible depending on what reducible species are present in the solution. Typical reactions are the reduction of dissolved oxygen gas or the reduction of hydrogen ions



However, if oxygen is present, two other reactions may occur:

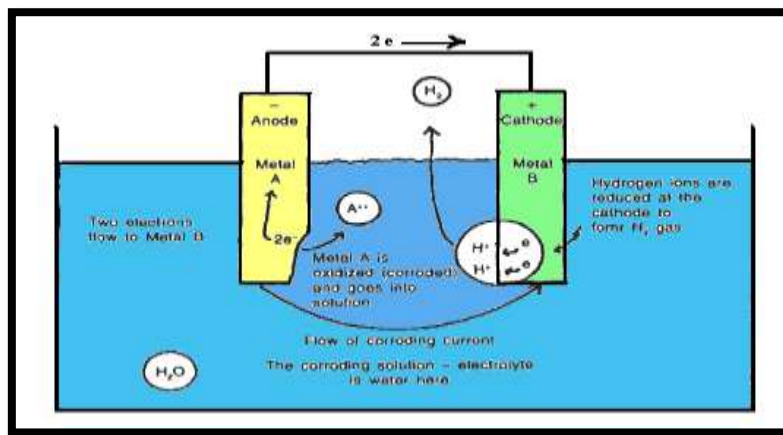
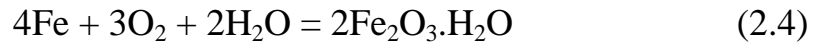


Figure 2-1 Electrochemical corrosion of metal [Lyon, 1996]

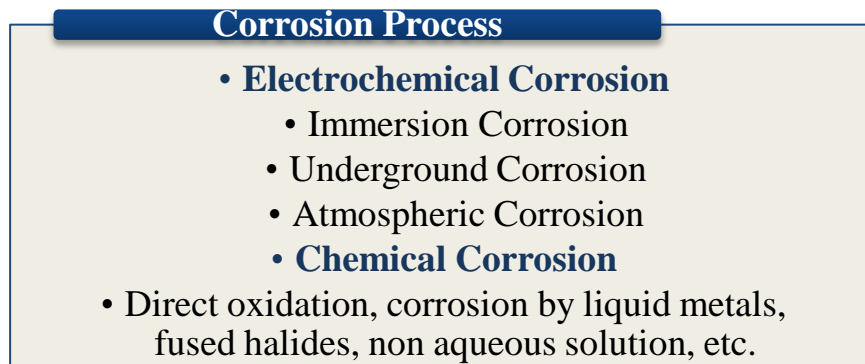
Most corrosion of steel can be considered as an electrochemical process which occurs in stages. Initial attack occurs at anodic areas on the surface, where ferrous ions go into solution. Electrons are released from the anode and move through the metallic structure to the adjacent cathodic sites on the surface where they combine with oxygen and water to form hydroxyl ions. These react with the ferrous ions from the anode to produce ferrous hydroxide which itself is further oxidized in air to produce hydrated ferric oxide, red rust the sum of these reactions is described by the following equation [Robert et. al., 2003]:



Iron and steel + oxygen + water = rust

2.2 Corrosion Classifications

Corrosion process can be conveniently classified as follows [Syed, 2006]



Also a logical and scientific classification of corrosion processes, although desirable, is by no means simple, owing to the enormous variety of corrosive environments and the diversity of corrosion reactions, but the broad classification of corrosion reactions into 'wet' or 'dry' is now generally accepted, and the terms are in common use. The term 'wet' includes all reactions in which an aqueous solution is involved in the reaction mechanism; implicit in the term 'dry' is the absence of water [Heitz, 1974; Shreir et. al., 2000].

2.2.1 Dry Corrosion

These are generally metal/gas or metal/vapor reactions involving nonmetals such as oxygen, halogens, hydrogen sulphide, sulphur vapor, etc. and oxidation, scaling and tarnishing are the more important forms. A characteristic of these reactions is that the initial oxidation of the metal, reduction of the non-metal, and formation of compound must occur at one and the same place at the metal/non-metal interface [Heitz, 1974; Shreir et. al., 2000].

2.2.2 Wet Corrosion

In wet corrosion the oxidation of the metal and reduction of a species in solution (electron acceptor or oxidizing agent) occur at different areas on the metal surface with consequent electron transfer through the metal from the anode (metal oxidized) to the cathode (electron acceptor reduced) the thermodynamically stable phases formed at the metal/solution interface may be solid compounds or hydrated ions (cations or anions) which may be transported away from the interface by processes such as migration, diffusion and convection [Heitz, 1974; Shreir et. al., 2000].

2.3 Forms of Corrosion Attack

Corrosion may take various forms and may combine other forms of damage (erosion, wear, fatigue, etc.) to cause equipment failure.

2.3.1 Uniform Corrosion

Uniform corrosion, as the name suggests, occurs over the majority of the surface of a metal at a steady and often predictable rate. Although it is unsightly its predictability facilitates easy control, the most basic method being to make the

material thick enough to function for the lifetime of the component. All homogeneous metals without differences in potential between any points on their surfaces are subjected to this type of general attack under some conditions. Uniform corrosion is usually characterized by a chemical or electrochemical attack over the entire exposed surface, Fig. 2-2 Metal corrodes in an even and regular manner becoming thinner, and consequently leads to failure due to reduction of the material's load-carrying capabilities. The rate of penetration or the thinning of a structural member can be used directly to predict the service life of a given component. Therefore, the expression mils penetration per year (mpy) is used to express corrosion resistance directly in terms of penetration. This expression can be calculated by the following [Revie and Uhlig, 2008]

$$mpy = \frac{534 \Delta w}{\rho A t} \quad (2.5)$$

Uniform corrosion can be prevented or reduced by using the following methods singly or in combination: proper selection of materials for the types of service environments and conditions proper selection of inhibitor proper selection of coatings cathodic protection [Lyon, 1996].

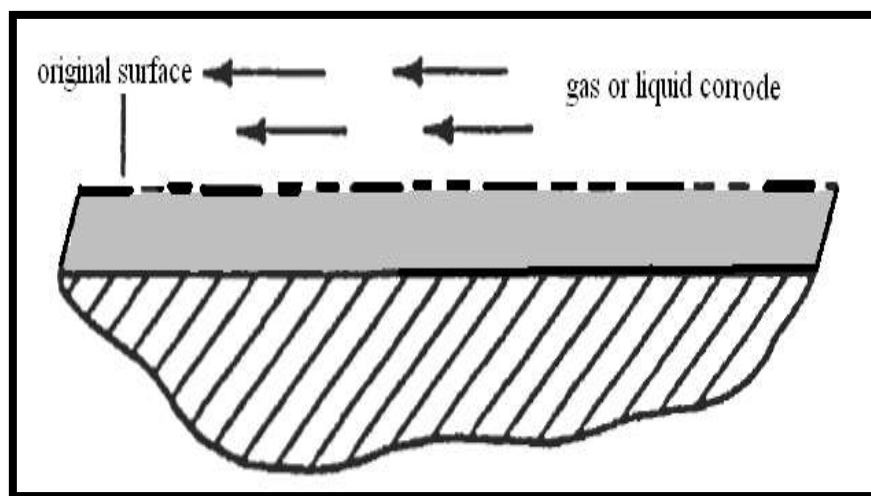


Figure 2-2 Uniform corrosion [Lyon, 1996].

This type of corrosion can be common in oxidation and tarnishing, active dissolution in acids, anodic oxidation and passivity, chemical and electrochemical polishing, atmospheric and immersed corrosion in certain cases. [Lyon, 1996]

2.3.2 Galvanic Corrosion

Galvanic corrosion occurs when two dissimilar metals or alloys come into electronic contact in a conductive solution the more anodic one corrodes. [Lyon, 1996]

2.3.3 Localized Corrosion

Certain areas of the metal surface corrode at higher rates than others due to 'heterogeneities' in the metal, the environment or in the geometry of the structure as a whole. Attack can range from being slightly localized to pitting. Examples of crevice corrosion are filiform corrosion, deposit attack, bimetallic corrosion, intergranular corrosion, and weld decay.

2.3.4 Pitting Corrosion

Highly localized attack at specific areas resulting in small pits that penetrate into the metal and may lead to perforation. Pitting of passive metals such as the stainless steels and aluminum alloys occurs in the presence of specific ions such as chlorine ions.

2.3.5 Selective Dissolution

One component of an alloy (usually the most active) is selectively removed from an alloy such as dezincification, dealuminification and graphitization.

2.3.6 Conjoint Action of Corrosion and a Mechanical Factor

Localized attack or fracture due to the synergistic action of a mechanical factor and corrosion for examples, Erosion – corrosion, fretting corrosion, impingement attack, cavitations damage, stress corrosion cracking, hydrogen cracking, and corrosion fatigue [Shreir et.al, 2000].

2.4 Factors Effecting Corrosion Rate

2.4.1 Effect of PH

The effect of the pH of solution to which iron or steel is exposed is influenced by temperature. The potential of hydrogen or symbol pH is defined as the negative logarithm of the hydrogen concentration, represented as $[H^+]$ in moles/liter.

$$pH = - \log [H^+] \quad (2. 6)$$

The pH value is used to represent the acidity of a solution. First, consider the exposure of iron to aerated water at room temperature (aerated water will contain dissolved oxygen). The corrosion rate for iron as a function of pH is illustrated in Fig. 2- 3. In the range of pH = 4 to pH =10, the corrosion rate of iron is relatively independent of the pH of the solution. In this pH range, the corrosion rate is governed largely by the rate at which oxygen reacts with absorbed atomic hydrogen, thereby depolarizing the surface and allowing the reduction reaction to continue. For pH values below 4.0, ferrous oxide (FeO) is soluble. Thus, the oxide dissolves as it is formed rather than depositing on the metal surface to form a film. In the absence of the protective oxide film, the metal surface is in direct contact with the acid solution, and the corrosion reaction proceeds at a greater rate than it does at higher pH values. It is also observed that hydrogen is produced in acid solutions below a pH of 4, indicating that the corrosion rate no longer depends entirely on depolarization by oxygen, but on a combination of the two factors [hydrogen evolution and oxygen reduction reaction (depolarization)]. For pH values

above about pH 10, the corrosion rate is observed to fall as pH is increased. This is believed to be due to an increase in the rate of the reaction of oxygen with Fe(OH)₂ (Hydrated FeO) in the oxide layer to form the more protective Fe₂O₃ [Gedeon, 2000]. Iron is weakly amphoteric, at very high temperatures such as those encountered in boilers, the corrosion rate increases with increasing basicity. PH has no effect on noble metals such as gold and platinum, but amphoteric metals dissolve rapidly in either acidic or basic solutions such as aluminum and zinc [Perry and Green, 1997].

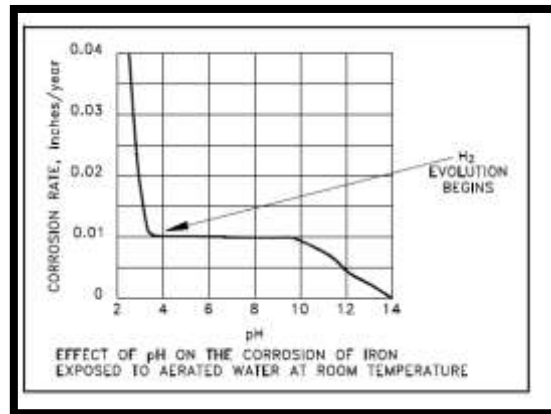


Figure 2-3 Effect of pH on corrosion rate of iron[Gedeon, 2000]

2.4.2 Effect of Temperature

Temperature is one of the critical environmental parameters in corrosion studies because of its severe effects on physicochemical and electrochemical reaction rates. Accordingly, passive film stability and solubility, pitting and crevice corrosion behavior are known to be closely related to temperature [Ashida et. al., 2007]. Temperature gives such a great effect on the rate of corrosion on metal, in case of corrosion in a neutral solution, the increase of temperature has a favorable effect on the overpotential of oxygen depolarization and the rate of oxygen diffusion, but it leads to a decrease of oxygen solubility. In case of corrosion in an acid medium, the corrosion rate increases with temperature

increase because the hydrogen evolution overpotential decreases [Amin et. al., 2011]. When corrosion is controlled by the diffusion of oxygen, the corrosion rate at a given oxygen concentration approximately doubles for every 30 °C rise in temperature [Eid, 1989]. In a closed system, oxygen cannot escape and the corrosion rate continues to increase with temperature until all the oxygen is consumed. When corrosion is attended by hydrogen evolution, the rate of increase will increase more than double for every 30 °C rise in temperature [Wan et. al., 2011]. The corrosion of mild steel in aerated water at varying temperatures is influenced in general by the manner in which temperature affects i - the specific reaction rates of the various corrosion reactions ii - oxygen solubility in the water iii - rate of transfer of dissolved oxygen through the liquid film and the product layer and iv - the nature of corrosion product [Mahato et.al, 1968a]. The studies of Rajappa et.al [1998], Sun et.al [2003], and George and Netic [2004] indicated that the corrosion rate increase with the temperature increase.

2.4.3 Effect of Dissolved Oxygen

The most prevalent and at the same time the most potent of the common corrosive agents is dissolved oxygen. Oxygen in any form of water, be it humidity, rain, drinking water, or sea water, has long been recognized as a destroyer of ferrous metals. When present in public water supplies its concentration may range from a few mg/l to as much as 14 mg/l. This is usually small in comparison with other ingredients. It is no more than half the concentration of nitrogen, for example. As the water passes through a distribution system, rarely is more than 1 mg/l of oxygen used up in corroding the metal, except in low-circulation areas or dead ends [Laurie and Edwards, 2000]. Dissolved oxygen is responsible for costly replacement of piping and

equipment by corrosive attack on metals with which it comes in contact. The amount of oxygen that can be held by the water depends on the water temperature, salinity, and pressure. Gas solubility increases with decreasing temperature (colder water holds more oxygen). Gas solubility increases with decreasing salinity (freshwater holds more oxygen than does saltwater). Both the partial pressure and the degree of saturation of oxygen will change with altitude. Finally, gas solubility decreases as pressure decreases. Thus, the amount of oxygen absorbed in water decreases as altitude increases because of the decrease in relative pressure. Dissolved oxygen can destroy the protective hydrogen film that can form on many metals and oxidize dissolved ions into insoluble forms [Revie and Uhlig, 2008]. In corrosion processes where dissolved oxygen acts as depolarizer, transfer phenomena under flowing conditions are very complex due to such unsteady process characteristics of the system as i - building up of corrosion product on the surface ii - growth of the surface roughness iii - changing physico- chemical properties of the corrosion products and iv- changing mechanics of flow [Mahato et.al, 1980].

2.4.4 Effect of Dissolved Salts

The principal ions found in water are calcium, magnesium, sodium, bicarbonate, sulphate, chloride, and nitrate. A few parts per million of iron or manganese may sometimes be present, and there may be traces of potassium salts, whose behavior is very similar to that of sodium salts. From the corrosion point of view, the small quantities of other acid radicals present, e.g., nitrite, phosphate, iodide, bromide, and fluoride, generally have little significance. Larger concentrations of some of these ions, notably nitrite and phosphate, may act as corrosion

inhibitors, but the small quantities present in natural waters will usually have little effect. Chlorides have probably received the most study in relation to their effect on corrosion. Like other ions, they increase the electrical conductivity of the water, so that the flow of corrosion currents will be facilitated. They also reduce the effectiveness of natural protective films, which may be permeable to small ions. Nitrate is very similar to chloride in its effects but is usually present in much smaller concentrations. In practice, high-sulphate waters may attack concrete, and the performance of some inhibitors appears to be adversely affected by the presence of sulfate. Sulphates have also a special role in bacterial corrosion under anaerobic conditions [Roberge, 2000]. Alkali - metal salts e.g., KCl, LiCl, Na₂SO₄, KI, NaBr, etc. affect the corrosion rate of iron and steel in approximately the same manner as sodium chloride. Chlorides appear to be slightly more corrosive in the order Li, Na, and K. Nitrates appear to be slightly less corrosive than chlorides or sulfates at low concentrations (0.2 – 0.25 N), but not necessarily at higher concentrations. The small differences for all these solutions may arise, for example, from their specific effect on the Fe (OH)₂ diffusion - barrier layer, or perhaps from the different adsorptive properties of the ions at a metal surface resulting in differing anode – cathode area ratios or differing overvoltage characteristics for oxygen reduction [Revie and Uhlig, 2008].

2.4.5 Effect of Velocity

Fluid velocity is one of the most important parameters to be considered during corrosion of metals, due to the flow effects on both anodic and cathodic reactions [Musa et. al., 2011]. A corrosion process can be influenced, in different ways, by the relative movement between the metal and the corroding environment. This

relative movement can increase the heat and mass transfer of reactants towards and from the surface of the corroding metal, with a consequent increase in the corrosion rate. Also, if solid particles are present, removal of protective films, erosion and wear on the metallic surface can occur. The corrosion of the metallic structure under turbulent flow is complex, but this problem has been studied mainly [Garnica-Rodriguez et. al., 2009; Genesca et. al., 2010; Mora-Mendoza et. al., 2002; Papavinasam et. al., 2003; Poulson, 1993], where, the flow are very important in the behaviour of the phenomenon processes. Therefore, the influence of flow on the corrosion processes is an important issue to be considered in the design and operation of industrial equipment. The use of the RCE, as a laboratory hydrodynamic test system, has been gaining popularity in corrosion studies [Nesic et. al., 1995, 2000]. This popularity is due to its characteristics, such as, it operates mainly in turbulent flow conditions; it has a well understood mass transfer properties and it is relatively easy to construct and operate [Gabe, 1974; Gabe and Walsh, 1983; Poulson, 1983]. When the RCE is immersed in a fluid and rotated at a very low rotation rate the fluid moves in concentric circles around the cylinder (laminar conditions). As the rotation rate of the cylinder increases the flow pattern is disrupted, cellular flow patterns, known as “Taylor vortices”, appear and the turbulent condition develops. These vortices enhance the mass, momentum and heat transfer at the rotating electrode [Gabe, 1974; Gabe and Walsh, 1983]. Flow affects only those corrosion processes which are controlled by transfer of reactants to, and products from, the metal surface, i.e., mass transfer controlled process [Shreir et. al., 2000; Roberge 2000]. On mild steel and a large number of other metals and alloys, transfer of oxygen to the cathodic area is often rate controlling. Whereas, with relatively noble metals such as copper the rate of diffusion of metal ions away from the surface may be the controlling factor.

Transfer of oxygen to the metal surface is affected by a combination of convection and diffusion. The later predominates at the surface. The effect of flow is to increase the convection in the neighborhood of metal surface, to decrease in the thickness of the diffusion boundary layer and to supply the cathodic reactants, e.g. oxygen at a faster rate [Mahato et.al, 1968b]. In short; the reduction of oxygen becomes a more facile process. It is well known that, in the presence of oxygen in acid solutions, two cathodic reactions take place which are hydrogen evolution reaction (HER) and oxygen reduction reaction. The first reaction, i.e., HER, is an activation controlled process [Fontana, 1986; Revie and Uhlig, 2008]. It was stated earlier, that oxygen transfer to the cathodic area is often rate controlling, i.e., a mass transfer controlled process. Therefore, the effect of flow on the limiting current density (i_L) of the oxygen reduction reaction in acid solutions is to increase i_L as the flow increases [Revie and Uhlig, 2008; Alwash et.al, 1987].

2.5 Limiting Current Density

The limiting current is an important parameter for the characterization of mass transport rates in electrochemical systems. When an electrochemical system operates under limiting current conditions, the reaction proceeds at the maximum rate and hydrodynamic properties can be characterized, facilitating comparison with other electrochemical systems. Mass transport coefficients (k) for certain redox couples calculated from the limiting current values are frequently used in order to characterize the mass transport conditions of electrochemical cells and reactors. The limiting current condition arises when the electro active species in the diffusion boundary layer reacts immediately on contact with the electrode the charged species sinks through the ionic channels of an ion exchange membrane as soon as it contacts its surface. Under these conditions, the current is limited by the rate at which the electro active species reaches the surface. In an electrochemical process,

the definition of the limiting current is when the change of current with potential is minimum or zero, i.e., $d(I)/d(E) = 0$. During the reduction of metal ions, the limiting current is achieved when the concentration of an electro active species at the electrode surface is negligible. The limiting current region can be affected by factors such as the secondary reaction, electrolyte composition (including pH), increase of the electrode area due to metal deposition, changes in the concentration of the electro active species and uneven current and/or potential distribution [Ponce-de-Leo'n et. al., 2007].

2.6 Polarization Concept

The kinetics of a reaction on an electrode surface depends on the electrode potential. Thus, a reaction rate strongly depends on the rate of electron flow to or from a metal-electrolyte interface. If the electrochemical system (electrode and electrolyte) is at equilibrium, then the net rate of reaction is zero. In comparison, reaction rates are governed by chemical kinetics, while corrosion rates are primarily governed by electrochemical kinetics. Thus, electrode reactions are assumed to induce deviations from equilibrium due to the passage of an electrical current through an electrochemical cell causing a change in the working electrode potential [Perez, 2004]. This electrochemical phenomenon is referred to as polarization. In this process, the deviation from equilibrium causes an electrical potential difference between the polarized and the equilibrium (unpolarized) electrode potential known as over potential η . Cathodic polarization η_c means that electrons are supplied to the surface and they build up a negative potential in the metal. Therefore η_c is negative by definition. Anodic polarization η_a is the opposite process [Fontana, 1986].

2.7 Polarization Types

There are three distinct types of polarization and these are additive, as expressed in equation 2. 7 [Roberge, 2000]:

$$\eta^T = \eta^A + \eta^C + \eta^R \quad (2. 7)$$

2.7.1 Activation Polarization

In general, the activation polarization is basically an electrochemical phenomenon related to a charge-transfer mechanism, in which a particular reaction step controls the rate of electron flow from a metal surface undergoing oxidation. This is the case in which the rate of electron flow is controlled by the slowest step in the half-cell reactions. The reaction rate for activation polarization depends on the charge-transfer over-potential as in metal oxidation due to electrons loss [Perez, 2004] Activation polarization is usually the controlling factor during corrosion in strong acids. For example, consider the evolution of hydrogen gas illustrated previously in equation 2.1 the rate at which hydrogen ions are transformed into hydrogen gas is in reality a function of several factors, including the rate of electron transfer from a metal to hydrogen ions. In fact, there is a wide variability in this transfer rate of electrons on various metals and, as a result, the rate of hydrogen evolution from different metal surfaces can vary greatly [Roberge, 2000]. A general representation of the polarization of an electrode supporting one redox system is given in the Butler-Volmer equation 2.8:

$$i_{reaction} = i_o \left\{ \exp \left(\alpha_{reaction} \frac{zF}{RT} \eta_{reaction} \right) - \exp \left[- (1 - \alpha_{reaction}) \frac{zF}{RT} \eta_{reaction} \right] \right\} \quad (2.8)$$

Where: $i_{reaction}$ = anodic or cathodic current

$\alpha_{reaction}$ = charge transfer barrier or symmetry coefficient for the anodic or cathodic reaction, close to 0.5.

$\eta_{\text{reaction}} = E_{\text{applied}} - E_{\text{eq}}$, i.e., positive for anodic polarization and negative for cathodic polarization

When reaction is anodic i.e., η_{reaction} positive, the second term in the Butler- Volmer equation becomes negligible and i_a can be more simply expressed by equation 2.9 and its logarithm equation 2.10

$$i_a = i_o \left[\exp \left(\alpha_a \frac{z F}{R T} \eta_a \right) \right] \quad (2.9)$$

$$\eta_a = b_a \log \left(\frac{i_a}{i_o} \right) \quad (2.10)$$

Where b_a is the Tafel coefficient or Tafel slop that can be obtained from the slope of a plot of η against $\log i$ with the intercept yielding a value for i_o

$$b_a = 2.303 \frac{R T}{\alpha Z F} \quad (2.11)$$

Similarly, when η_{reaction} is cathodic (i.e., negative), the first term in the Butler-Volmer equation becomes negligible and i_c can be more simply expressed by equation 2.12 and its logarithm, equation 2.13, with b_c obtained by plotting η versus $\log i$ equation 2. 14 [Roberge, 2000]:

$$i_c = i_o \left\{ \exp \left[- (1 - \alpha_c) \frac{z F}{R T} \eta_c \right] \right\} \quad (2.12)$$

$$\eta_c = - b_c \log \left(\frac{i_c}{i_o} \right) \quad (2.13)$$

$$b_c = 2.303 \frac{R T}{\alpha Z F} \quad (2.14)$$

2.7.2 Concentration Polarization

Concentration polarization is the polarization component caused by concentration changes in the environment adjacent to the surface. When a chemical species participating in a corrosion process is in short supply, the mass

transport of that species to the corroding surface can become rate controlling. A frequent case of concentration polarization occurs when the cathodic processes depend on the reduction of dissolved oxygen since it is usually in low concentration [Bagotsky, 2006; Roberge, 2000]. Because the rate of the cathodic reaction is proportional to the surface concentration of the reagent, the reaction rate will be limited by a drop in the surface concentration. For a sufficiently fast charge transfer, the surface concentration will fall to zero, and the corrosion process will be totally controlled by mass transport.

Mass transport to a surface is governed by three forces: diffusion, migration, and convection. In the absence of an electric field, the migration term is negligible, and the convection force disappears in stagnant conditions [Roberge, 2000].

η^C can be evaluated using an expression in equation 2.15 derived from the Nernst equation [Roberge, 2000]:

$$\eta^C = \frac{2.303 R T}{Z F} \log \left(1 - \frac{i}{i_L} \right) \quad (2.15)$$

2.7.3 Combined Polarization

Both activation and concentration polarization usually occur at an electrode. At low reaction rates, activation polarization usually controls, while at higher reaction rates, concentration polarization becomes controlling [Fontana, 1986; Revie and Uhlig, 2008]. The total polarization of an electrode is the contribution of activation polarization and concentration polarization:

$$\eta^t = \eta^A + \eta^C \quad (2.16)$$

During reduction process such as hydrogen evolution or oxygen reduction, concentration polarization is important as the reduction rate approaches the limiting diffusion current density. The overall cathodic over potential for activation process is given by [Fontana and Green, 1986]

$$\eta_{red} = -b_c \log \left(\frac{i_c}{i_o} \right) + \frac{2.303 R T}{Z F} \log \left(1 - \frac{i}{i_L} \right) \quad (2.17)$$

For example sometimes, the anodic reaction by which a metal is dissolved is sustained by not one but two significant cathodic reactions, e.g., in an aerated dilute acid, where both oxygen reduction and hydrogen discharge can contribute to the total cathodic current. The corrosion potential then assumes a value at which the anodic current due to dissolution of the metal equals the sum of the currents from the cathodic reactions [Talbot, 1998].

2.7.4 Resistance Polarization

Since in corrosion the resistance of the metallic path for charge transfer is negligible, resistance overpotential η^R is determined by factors associated with the solution or with the metal surface. Thus resistance overpotential may be defined as

$$\eta^R = I (R_{sol.} + R_F) \quad (2.18)$$

Where R_{sol} is the electrical resistance of the solution, which depends on the electrical resistivity (Ω cm) of the solution and the geometry of the corroding system, and R_F is the resistance produced by films or coatings formed on or applied to the surface of the sites. Thus, in addition to the resistivity of the solution, any insulating film deposited either at the cathodic or anodic sites that restricts or completely blocks contact between the metal and the solution will

increase the resistance overpotential, although the resistivity of the solution is unaffected [Shreir et. al., 2000].

2.8 Corrosion of Iron in Acid

In strong acids, such as hydrochloric and sulfuric acids, the diffusion - barrier oxide film on the surface of iron is dissolved below pH 4. In weaker acids, such as acetic or carbonic acids, dissolution of the oxide occurs at a higher pH; hence, the corrosion rate of iron increases accompanied by hydrogen evolution at pH 5 or 6. This difference is explained by the higher total acidity or neutralizing capacity of a partially dissociated acid compared with a totally dissociated acid at a given pH. In other words, at a given pH, there is more available H^+ to react with and dissolve the barrier oxide film using a weak acid compared to a strong acid. The increased corrosion rate of iron as pH decreases is not caused by increased hydrogen evolution alone; in fact, greater accessibility of oxygen to the metal surface on dissolution of the surface oxide favors oxygen depolarization, which is often the more important reason. In more concentrated acids, the rate of hydrogen evolution is so pronounced that oxygen has difficulty in reaching the metal surface. Hence, depolarization in more concentrated acids contributes less to the overall corrosion rate than in dilute acids, in which diffusion of oxygen is impeded to a lesser extent. Potential and polarization measurements indicate that oxygen in small concentrations at the metal surface increases cathodic polarization, thereby decreasing corrosion; in higher concentrations, oxygen acts mainly as a depolarizer, increasing the rate. The important depolarizing action of dissolved oxygen suggests that the velocity of an acid should markedly affect the corrosion rate. This effect is observed, particularly with dilute acids, In addition, the inhibiting effect of dissolved oxygen is observed within a critical velocity range, with the critical velocity becoming higher the more rapid the inherent reaction rate of steel with the

acid. Relative motion of acid with respect to metal sweeps away hydrogen bubbles and reduces the thickness of the stagnant liquid layer at the metal surface, allowing more oxygen to reach the metal surface. In the absence of dissolved oxygen, only hydrogen evolution occurs at cathodic areas, and an effect of velocity is no longer observed. This result is expected because hydrogen overpotential (activation polarization) is insensitive to velocity of the electrolyte. For aerated acid, the minimum rate occurs at higher velocities the more concentrated the acid because the rate of hydrogen evolution is more pronounced, thereby impeding oxygen diffusion to the metal surface [Revie and Uhlig, 2008].

2.9 Corrosion Inhibitors

Corrosion of metals is a serious material degradation problem from both economic and structural integrity standpoints, but it can to some extent be controlled by suitable strategies. Among these, application of inhibitors is one of the most convenient methods to reduce the corrosion rate of metallic materials [Ashassi-Sorkhabi et.al., 2005; Oguzie, 2005; Ashassi-Sorkhabi et.al., 2008; Frateur et.al., 2006; Amin et.al., 2007]. However, because of environmental impact and health risk issues, many of the traditional corrosion inhibitors have to be phased out, and there is an urgent need to develop new corrosion inhibitors that are safe, smart and multifunctional [Zhang et.al., 2011].

Inhibitors intervene in corrosion kinetics in various ways. Some inhibit cathodic reactions, others inhibit anodic reactions and yet others, mixed inhibitors, do both. The detailed mechanisms by which the individual substances produce their effects can be quite complex and is the subject of extensive on-going research [Talbot, 1998].

Corrosion inhibitor can be defined as a chemical substance that, when added in small concentration to an environment, effectively decreases the corrosion rate. The efficiency of an inhibitor can be expressed by a measure of this improvement:

$$IE (\%) = 100 \times \frac{CR_{\text{uninhibited}} - CR_{\text{inhibited}}}{CR_{\text{uninhibited}}} \quad (2.19)$$

In general, the efficiency of an inhibitor increases with an increase in inhibitor concentration. Considerations of cost, toxicity, availability, and environmental friendliness are of considerable importance [Roberge, 2000].

2.10 Classification of Inhibitors

Inhibitors are chemicals used to give the metallic surface a certain level of protection from the environment that surface was exposed to. Inhibitors often work by adsorbing themselves on the metallic surface, protecting the metallic surface by forming a film. Inhibitors are normally distributed from a solution or dispersion. Some are included in a protective coating formulation. Inhibitors slow corrosion processes by

1. Increasing the anodic or cathodic polarization behavior.
2. Reducing the movement or diffusion of ions to the metallic surface
3. Increasing the electrical resistance of the metallic surface

Inhibitors have been classified differently to their chemical functionality [Roberge, 2000].

2.10.1 Inorganic Inhibitors

Usually crystalline salts such as sodium chromate, phosphate, or molybdate. Only the negative anions of these compounds are involved in reducing metal

corrosion. When zinc is used instead of sodium, the zinc cation can add some beneficial effect. These zinc-added compounds are called mixed-charge inhibitors.

2.10.2 Organic Anionic

Sodium sulfonates, phosphonates, or mercaptobenzotriazole (MBT) are used commonly in cooling waters and antifreeze solutions.

2.10.3 Organic Cationic

In their concentrated forms, these are either liquids or waxlike solids. Their active portions are generally large aliphatic or aromatic compounds with positively charged amine groups [Roberge, 2000].

2.11 Inhibitors for Acid Solutions

Corrosion protection of steel in acidic media is of great important both for industrial facilities and theoretical aspects. The use of inhibitor is one of the most practical methods for protection of steel against corrosion in acidic media. Among all inhibitors, the most important are the organic ones, also called adsorption inhibitors [Sanyal, 1981]. They control corrosion, acting over the anodic or the cathodic surface or both. Most commercial acid inhibitors are organic compounds containing hetero atoms such as nitrogen, oxygen, sulphur, phosphor atoms, by which the inhibitor molecules are adsorbed on the metal surface in acidic media, thus resulting adsorption film acts as a barrier separating the metal from the corrosive medium and blocks the active sites [Lgamri et. al.,

2003; Bentiss et. al., 2002; Popova et. al., 2004; Quraishi and Sharma, 2002; Chebabe et. al., 2003; Elayyachy et. al., 2006].

The widespread use of mild steel in many petroleum applications is quite well known. Hydrochloric acid is widely used in petroleum fields for cleaning and descaling of steel alloys. However, generally the corrosion current density is high so in order to reduce the corrosion current density of the metallic material, various types of inhibitors are injected into the system. Specific interaction between functional groups and the metal surface and hetero atoms play an important role in inhibition due to the free electron pairs they possess [Kustu et.al., 2007].

The compounds containing nitrogen can provide excellent inhibition in acid media [Elewady, 2008]. The existing data show that most organic inhibitors get adsorbed on the metal surface by displacing water molecules and form a compact barrier film [Goncalves and Mello, 2001; Al-Sawaad et.al. 2010; Chauhan and Gunasekaran, 2007; Bentiss et.al., 2000; Muralidharan et.al., 1995].

The adsorption process depends on the electronic characteristic of the molecules (adsorbate), the chemical composition of the solution; nature of the metal surface, temperature of the reaction and on the electrochemical potential at the metal–solution interface [Abboud et. al., 2009; Liu et. al., 2009; Ahamad et. al., 2010]. The adsorption requires the existence of attractive forces between the adsorbate and the metal. According to the type of forces, adsorption can be physisorption or chemisorption or a combination of both [Liu et. al., 2009; Touhami et. al., 2000; Khaled et. al., 2010].

The important prerequisites for a compound to be an efficient inhibitor are: (i) it should form a defect free compact barrier film, (ii) it should chemisorbs

on the metal surface, (iii) it should be polymeric or polymerize in situ on the metal and (iv) the barrier thus formed should increase the inner layer thickness [Jeyaprabha et.al., 2006].

The inhibition efficiency of organic compounds is strongly dependent on the structure and chemical properties of the layer formed on the metal surface under particular experimental conditions. The strength of adsorption, and hence, the extent of inhibition is dependent on the nature of the organic compounds and the nature of the metal and the corrosive media [Samide, 2010].

2.12 Indole Inhibitor (I)

Indole C_8H_7N is a heterocyclic compound with a fused structure of the benzene ring with a pyrrole ring chemical structure as shown in Fig.2-4. The benzene ring is fused to a five-membered heterocycle containing one nitrogen atom in ortho-position. It has one lone electron pair, which is delocalized and participates in the aromatic structure of the molecule [Popova et.al, 2007; Lebrini et.al, 2010].

Corrosion inhibition by organic compounds is usually ascribed to adsorption of inhibitor molecules on steel surface to prevent the attack of aggressive ions. There are physisorption and chemisorption depending on the adsorption strength. Adsorption caused by van der Waals and coulombic interaction are belonging to physisorption, whereas that resulted from interaction between the π -electrons of organic molecules and d-orbital of metal belonging to chemisorption. An initial physisorption possibly form a stable polymeric film and turn into chemisorptions [Subramanian, 2002]. Four types of adsorption may take place involving organic molecules at the metal solution interface (i) electrostatic attraction between charged molecules and the charged metal, (ii)

interaction of π electrons with the metal, (iii) interaction of uncharged electron pairs in the molecule with the metal and (iv) a combination of the above [Loto et.al, 2012].

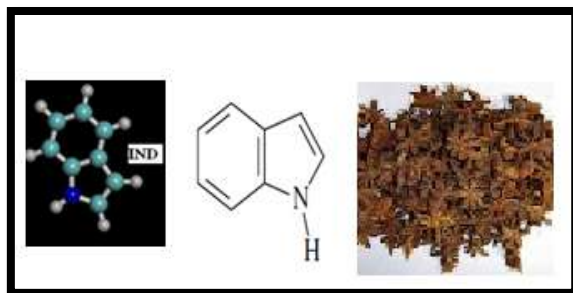
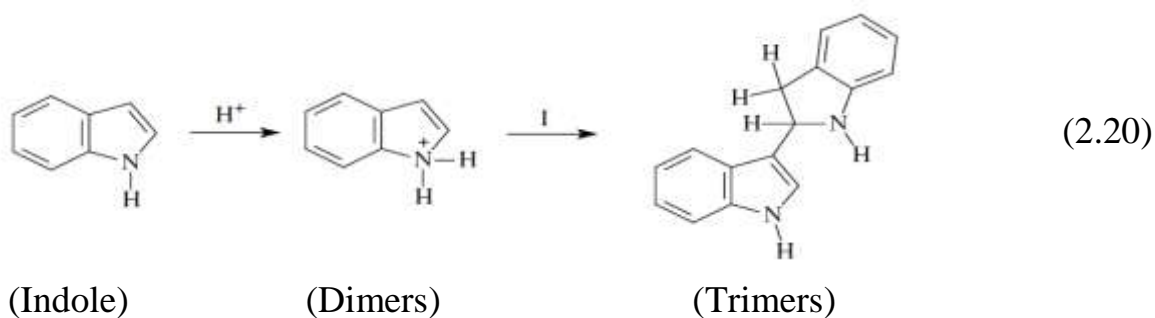


Figure 2-4 Indole [Ismail et.al, 2000; Sanad et.al, 2000; Popova et.al, 2007; Popova, 2007].

Indole is the only compounds which acts as a very weak acid because the lone electron pair is delocalized and participates in the π electron aromatic system. Nevertheless indole can react with acids forming high-molecular compounds (dimers, trimers) instead of salts with a definite composition. The first step is the protonation and a cation is formed. It reacts with an unchanged indole molecule to produce the dimer, and so on [Popova et.al, 2007]:



2.13 Cetyl Trimethyl Ammonium Bromides Inhibitor (CTAB)

Cetyl Trimethyl Ammonium Bromides, having a chemical formula of $\text{CH}_3(\text{CH}_2)_{15}\text{N}^+(\text{CH}_3)_3\text{Br}^-$, The CTAB is a cationic surfactant has many advantages such as high inhibition efficiency, low price, low toxicity and easy production

[Singh et.al, 1993; Bannerjee and Malhotra, 1992; Arab and Noor, 1993; Raspi, 1993]. The adsorption of the surfactant on the metal surface can markedly change the corrosion resisting property of the metal [Bentiss et.al, 2000].

2.14 Literature Review

In addition to the studies stated previously, there are some studies in literature considered the effect of various factors on the corrosion and inhibition of CS in aerated acidic or salt solutions.

Peralta et.al, 2002 they studied of the electrochemical behaviour of a carbon steel electrode in sodium sulphate aqueous solutions by using electrochemical impedance spectroscopy EIS to measure corrosion current densities at high concentrations in the range 0.1–1 wt % Na_2SO_4 , but in the low concentration range, from 0.001 to 0.01 wt%, a scattered Nyquist plot was obtained. Authors concluded that the corrosion rate of mild steel increases significantly above 0.1 wt% Na_2SO_4 and the EIS is the technique that better describes the corrosion of steel in Na_2SO_4 containing solutions.

Andijani et.al, 2002 studied the corrosion behavior of carbon steel in deaerated 1 M NaCl solution at 50 °C for the pH of solution from 4 to 9.5 by adding dilute HCl and NaOH solutions. The readings were taken at different rotation speed and pH. Authors found that the effect of velocity on the corrosion behavior of carbon steel is pH dependent, while the corrosion rates are greatly influenced by rotation speed at pH 4 but the effect of velocity on the corrosion rate decreases as pH increases. This is attributed to the fact that at pH 4 the corrosion rate is mass controlled, where reduction of H^+ is dominant reaction. At higher pH

solution, $[H^+]$ becomes much lower, and therefore reduction of H_2O is predominant and corrosion rate is activation controlled.

Martinez et.al, 2005 studied the electrochemical kinetics results measured during the corrosion of carbon steel immersed in aqueous environments, containing dissolved hydrogen sulfide under turbulent flow conditions. Using rotating cylinder electrode, different velocities were considered at 20 °C in 3.5 % NaCl deaerated solution. The authors found that the turbulent flow increases the corrosion rate and the corrosion mechanism exhibits a significant dependence on mass transfer on the cathodic kinetics. The mass transfer coefficient is flow dependent, because it increases as the rotation rate also increases.

Ochoa et.al, 2005 studied the inhibition mechanism of carbon steel in a 200 ppm NaCl solution at 25 °C by a non-toxic multi-component inhibitor the inhibitive formulation was composed of 50 ppm fatty amines associated with 200 ppm phosphonocarboxylic acid salts. Steady-state current–voltage curves, obtained with a rotating disc electrode with a velocity of 100 and 2000 rpm, revealed that the properties of the protective layer were dependent on the electrode rotation rate and on the immersion time. The cathodic process of oxygen reduction was not modified in the presence of the inhibitive mixture. As expected, the current densities increased when the rotation rate was increased. In the anodic range, original behaviour was observed: the current densities decreased when the electrode rotation rate increased. Two distinct surface areas were visualized on the metal surface and the ratio between the two zones was dependent on the flow conditions.

Hamdy et.al, 2008 studied the effect of solution speed and sulfide ion concentration present as a pollutant in 3.5% NaCl solution on the corrosion rate of

mild steel. The weight loss/gain due to the interaction of the materials with the surrounded environments was calculated after rotating mild steel samples with different speeds and concentrations at room temperature. The authors found that the presence of sulfide ions in NaCl solution enhanced the corrosion attack due to the localized replacement of the protective Fe-oxide film by a non-protective iron sulfide film. On the other hand, increasing the solution speed in presence of sulfide ions increased the corrosion attack which can be explained in the light of the synergistic action between the presence of sulfide and increasing the solution speed.

Osarolube et.al, 2008 studied the corrosion behaviour of mild steel and high carbon steel in various concentrations of nitric acid HNO_3 , hydrochloric acid HCl , and perchloric acid HClO_4 . Corrosion rates evaluated using the weight loss method. Test solutions maintained at room temperature and using different acid solutions range from 0.5 to 3 M. Authors observed that HNO_3 environment was most corrosive to both steels because of its oxidizing nature, followed by HClO_4 acid, and HCl acid. The rate of metal dissolution increased with increasing concentration of the corrosion media and exposure time.

Noor and Al-Moubaraki, 2008 investigated the corrosion behaviour and mechanism for mild steel in solutions of HCl concentration of $0.25\text{-}2.5 \text{ mol dm}^{-3}$ at $25 \text{ }^\circ\text{C}$ by using chemical (hydrogen evolution, HE and Mass loss, ML) and electrochemical (electrochemical impedance spectroscopy, EIS and potentiodynamic polarization, PDP) methods. The chemical results revealed that mild steel corrodes in HCl solutions with a first order reaction having reaction constant of 0.56 and the corrosion rate increases with the increase in acid concentration. Micro structural studies for mild steel after immersion in HCl solutions of different concentrations showed general and pitting corrosion and the

latter becomes more pronounced at higher level of HCl concentration. Accordingly, it was found that charge transfer resistance value decreases while both the double layer capacitance and i_{corr} values increase with increasing HCl concentration. PDP results revealed that the steel dissolution is anodically controlled.

Ali et.al, 2009 studied the corrosion of carbon steel, measured the corrosion current and potentials in 3.5% NaCl solution at 40 °C for different flow conditions Re range 5000 to 15000, by using commercial metal pipe as test specimens cylindrical. The authors found that the corrosion of Fe is under diffusion control since the corrosion current density i_L increases and corrosion potential E_{corr} shifts to less negative with increasing velocity, the limiting diffusion current density is independent of the nature of the cathode material, but it depends on the Reynolds number.

Khadom et.al, 2009 studied the effect of different temperatures and acid concentrations on the corrosion of low carbon steel in hydrochloric acid with a concentration of 1 to 5 M and at 30 to 60 °C were studied by using weight loss method. Nonlinear corrosion rates as a function of temperature and acid concentration equation were estimated with a good prediction corrosion rates values. Authors conclude that the values of activation energy and enthalpy of activation decrease with increase in acid concentration indicating the increasing in reaction rate. The corrosion reaction was approximately first order reaction.

Musa et.al, 2009 studied the stability of layer forming for corrosion inhibitor on mild steel surface under hydrodynamic conditions at 30 °C in aerated 2.5M H_2SO_4 and 0.5M HCl solutions. The hydrodynamic conditions experiments were simulated using the rotating cylinder electrode. The corrosion inhibitor in this study

used was 4×10^{-4} M 4-amino-5-phenyl-4H-1, 2, 4-triazole-3-thiol (APTT). The investigation showed that in both solutions, the corrosion current density decreased and charge transfer resistances were decreased with the flow velocity, while, E_{corr} shifted toward more positive values as the flow velocity increased. The results also revealed that the formation and the development of the inhibitor layer in both pickling solutions were dependent on the respective flow velocities. It was found that the flow can increase the inhibitor mass transport from bulk to electrode surface and on the other hand it leads to more desorption of adsorbed inhibitor molecules which can have a negative effect on surface protection.

Ciubotariu et.al, 2010 investigated the electrochemical corrosion behavior of carbon steel using the EIS technique and potentiodynamic polarization methods. As test solutions sodium chloride, sodium sulphate and sulphuric acid 0.5M concentration were used. The reading was taken for different time of immersion at room temperature and for static condition. Authors observed that the corrosion rate is higher in 0.5M H_2SO_4 , and concluded that the polarization resistance decreases with time in H_2SO_4 because of the possibility of general corrosion with the dissolution of corrosion products while in 0.5M Na_2SO_4 and 0.5M NaCl solutions it increases with time.

Musa et.al, 2010 studied the behavior of corrosion inhibitor 4-amino-5-phenyl-4H-1, 2, 4-triazole-3-thiol (APTT) film under turbulent flow condition in oxygenated and deaerated solutions. Turbulent flow condition experiments were simulated by rotating cylinder electrode. Potentiodynamic polarization and electrochemical impedance spectroscopy (EIS) were used. Experiments were carried out in oxygenated and deaerated 1.0 M HCl with and without 4×10^{-4} M APTT solutions at different electrode rotation rates at 30 °C. Authors conclude that

corrosion current density decreased with addition of APTT in solution, regardless the rotation rate. Inhibition efficiencies were found decreased with rotation rate in oxygenated solution. The formation and the development of the inhibitor film were dependent on the flow rate.

Hasan, 2010 investigated the effect of salt content on the corrosion rate of carbon steel pipe in aerated water under isothermal turbulent flow conditions Re range of 15000-110000 and temperature of 30-60 °C by using weight loss method. Different electrolytic solutions were used having concentration of 0.1, 0.5N NaCl and distilled water. The results revealed that the salt content has considerable effect on the corrosion rate for the whole investigated range of Re and temperature. The highest corrosion rate was encountered in sea water. Also distilled water causes considerable corrosion rate but it is lower than for the whole range of Re and temperature. Also it is found that Re increases the corrosion rate depending on temperature. Temperature affects the corrosion rate by changing two main parameters, oxygen solubility and diffusivity.

El Ouali et.al, 2010 studied the thermodynamic characterization of steel corrosion in HCl in the presence of 2- phenylthieno (3, 2-b) quinoxaline. The influence of inhibitor concentration and temperature on the corrosion behaviour of steel in molar HCl solution has been investigated by weight loss method. Results obtained show that the inhibitory effect of 2-phenylthieno (3, 2-b) quinoxaline (P4) increases with increasing P4 concentration to attain the highest value (95%) at 5×10^{-4} M. The IE% decreases with rise of temperature. The various parameters of activation and adsorption may be a good tool to discuss manner of adsorption of organic compound. Attempt to correlate molecular structure to quantum indices was made.

El Maghraby and Soror, 2010a studied the inhibition effect of cetyl trimethyl ammonium bromide (CTAB) as a cationic surfactant on the corrosion of carbon steel in different HCl concentrations 1 to 2 M at different at different temperatures 20- 45 °C by weight loss, open circuit potential, Tafel polarization and linear polarization methods. The results show that CTAB is a good inhibitor in 2M HCl, and the inhibition efficiency increases with the inhibitor concentration range from 200 to 1000 ppm, while it decreases with increasing the hydrochloric acid concentration more than 2M and temperature. Effect of immersion time was also studied and discussed. Polarization curves show that CTAB is a mixed-type inhibitor in hydrochloric acid. The results obtained from weight loss and polarizations are in good agreement. Authors concluded that the maximum inhibition efficiency is about 87% in 2M HCl solution and its values increase with the inhibitor dose, but decrease with the temperature. CTAB acts as a mixed-type inhibitor in 1M and 2M HCl.

Ebenso et.al, 2010 studied the Quinoline and its derivatives as effective corrosion inhibitors for mild steel in acidic medium. Quinoline (QL) and its derivatives namely quinaldine (QLD) and quinaldic acid (QLDA) were tested as inhibitors for the corrosion of steel in 0.5 M HCl by weight loss method at 30 and 40 °C. Different inhibitors concentrations were used range from 0.001 to 0.1 M. Inhibition efficiency increased with increase in the concentration of inhibitor but decreased with increase in temperature. Results show that the order of inhibition efficiency is QLDA > QLD > QL. The adsorption of the inhibitors on the steel surface obeys Langmuir and kinetic thermodynamic models.

Nessim et.al, 2011 studied the inhibitory effect of some cationic gemini surfactants for carbon steel in sea water. Investigation of corrosion inhibition of carbon steel alloy in sea water by different synthesized gemini surfactants {12-2-12, 14-2-14 and 16-2-16} at 25 °C have been done by using weight loss, potentiodynamic polarization and surface tension measurements, Gemini surfactants inhibitor concentration range from 0 to 6 m mol dm⁻³. The results showed that the inhibition efficiency increases with increasing the concentration of inhibitors. Also, the adsorption ability of the surfactant molecules on carbon steel surface increases with the increase in the hydrocarbon chain length of the surfactant molecule from 12 to 16 and through 14 C atoms; meanwhile, the isotherm of 16-2-16 declares the formation of multilayer onto the used metal surface. The inhibitive action of the studied surfactants follows the order: 16-2-16 > 14-2-14 > 12-2-12.

Nor et.al, 2011 studied the corrosion of carbon steel in high CO₂ environment corrosion has been investigated using a high-pressure high-temperature rotating cylinder electrode (RCE) autoclave and a pipe flow loop system. Corrosion rates are measured via weight loss and by electrochemical methods at various pH from 3 to 5, temperatures range of 25 to 50 °C, near critical and supercritical CO₂ partial pressures and at equivalent fluid velocities from 0 to 1.5 m/s. The authors found that reducing the flow effect at high pressure due to increase the concentration of carbonic acid whose reduction is limited by hydration of dissolved CO₂. The flow velocity was not clearly observed at pH 3 even at low pressure. Because the anodic reaction was under charge transfer control flow has no effect.

Hasan and Sisodia, 2011 investigated the inhibition of corrosion of mild steel using Paniala extract in 1M HCl and 0.5 H₂SO₄ solutions by using weight loss method at 30 °C. The result showed that corrosion rate was significantly decreased

in presence of the extract and inhibition efficiency increased with increasing the concentration of extract. In case of HCl maximum inhibition efficiency (98%) was noticed at 5% v/v inhibitor concentration and in 0.5M H₂SO₄, it was found 95% efficiency at the same concentration of inhibitor. At lower concentration of inhibitor, better inhibition was observed in HCl medium as compared to H₂SO₄. Adsorption of Flacourtia jangomas depends on its chemical composition which has oxygen atoms with lone pair electrons for co-ordinate bonding with metal.

Mobin et.al, 2011 studied the corrosion inhibition characteristics of nitrogen containing amino acid L-tryptophan concentration range from 10 to 500 ppm on mild steel in 0.1 M HCl solution, in the temperature range of 30-50 °C, was studied by weight loss and potentiodynamic polarization measurements. L-tryptophan significantly reduces the corrosion rates of mild steel, the maximum inhibition efficiency being 83% at 50 °C in presence of inhibitor concentration of 500 ppm. The effect of the addition of very small concentrations about 1 ppm of anionic surfactant, sodium dodecyl sulfate (SDS), and of cationic surfactant, cetyl trimethyl ammonium bromide (CTAB), on the corrosion inhibition behavior of L-tryptophan was also studied. The inhibition efficiency significantly improved in presence of both surfactants. The authors calculated thermodynamic parameters for adsorption reveal a strong interaction between the inhibitors and the mild steel surface.

Ortega-Toledo et.al, 2011 this work studied the performance of a simple organic compound, carboxyethylimidazoline, as CO₂ corrosion inhibitor of API X-120 pipeline steel by using different electrochemical techniques such as polarization curves, LPR, EIS and EN measurements under hydrodynamic conditions., whereas the rotation speed were 0 to 2500 rpm. Inhibitor concentration used was 20 ppm at a testing temperature of 50 °C, Testing solution consists of 3% NaCl solution with

CO₂, Different techniques show that for uninhibited solution, the corrosion rate increases with an increase in the rotating speed, but for the inhibited solution, the lowest corrosion rate is obtained at 1000 rpm, but it increases with a further increase in the rotating speed.

Zerga et.al, 2012 investigated the effect of different organic inhibitors on the electrochemical behaviour of steel in molar hydrochloric acid at different concentration of each inhibitor range from 10⁻⁶ to 10⁻³ M at 6 h and 303 K. Authors results showed that the addition of these compounds inhibits the corrosion of steel and the extent of inhibition depends upon the type and concentration of the pyridazine compounds. The inhibition efficiency for four compounds studied increase with the increase in the inhibitor concentrations to attain 100 % at the 10⁻³M of P1. Moreover, the results revealed that the inhibitors act as mixed inhibitors and cathodically predominant.

Belfilali et.al, 2012 investigated the inhibitor effect of 1,7- bis (2- hydroxy benzamido)-4-azaheptane H₄L³ on the corrosion of mild steel in 1M hydrochloric acid t 308 K using weight loss measurements and electrochemical techniques (impedance spectroscopy and polarization curves). All experiments used inhibitor concentration from 10⁻⁶ to 10⁻³ M. Inhibition efficiency is dependent upon the H₄L³ concentration and its inhibition efficiency increases with the increase of concentration of inhibitor to attain 96 % since 10⁻³M. Polarization curves indicate that H₄L³act essentially as mixed inhibitors. EIS measurements show an increase of the transfer resistance with the inhibitor concentration. The corrosion rate increased both in the presence and absence of the inhibitors by increasing the temperature of the system.

Chapter Three

Experimental Works

3.1 Introduction

Experimental work was carried out to determine the corrosion rate of carbon steel pipe under flow conditions for velocity range of 0 to 2000 rpm, temperatures 32, 42, and 52 °C, with Na₂SO₄ concentration range of 0.01 to 0.4 M and HCl concentration range of 0.5 to 5 % (v/v) by volume using weight loss and electrochemical polarization methods. The experimental work was divided into four parts:

1. Weight loss measurements to determine the average corrosion rates under isothermal conditions (T = 32 °C). This was done for determining the corrosion rate of carbon steel in three different solutions: 0.2 M Na₂SO₄, 0.2 M Na₂SO₄ + 5 % HCl, and 0.2 M Na₂SO₄ + 5 % HCl with addition of air bubbles under different values of rotational velocity.
2. Electrochemical polarization measurements on salt to measure the instantaneous corrosion rate using limiting current density technique under different conditions of rotational velocity, Na₂SO₄ concentrations, temperature, time, and in presence of air bubbles (increased O₂ concentration).
3. Electrochemical polarization measurements on acid- salt mixtures to measure the instantaneous corrosion rate using Tafel extrapolation method of anodic and cathodic polarization curves to determine the corrosion current density under various conditions of velocity, concentrations of HCl and Na₂SO₄, temperature, and the effect of presence air bubbles.

4. Weight loss measurements to determine the average corrosion rate on acid salt solution (1% HCl with 0.1 M Na₂SO₄) with addition of indole concentrations of 1.7×10^{-3} and 3.4×10^{-3} M (200 and 400 ppm) and CTAB inhibitors with a concentration of 2.74×10^{-3} M (1000 ppm), were studied the effect of velocity, and temperature.

3.2 The Solutions

Different solutions were used in experiments:

1. The first type of solution consist only Na₂SO₄ solution of different concentrations: 0.01, 0.025, 0.05, 0.1, 0.2, and 0.4 M Na₂SO₄.The concentration of Na₂SO₄ was dissolve in distilled water to obtain the required molarities.
2. The second type consisted salt- acid mixture with different concentrations that were 0.01 M Na₂SO₄+ 1 % HCl, 0.05 M Na₂SO₄+ 1 % HCl, and 0.2 M Na₂SO₄ + 1 % HCl. Also, by using different acid concentrations with constant salt concentration: 3 % HCl+ 0.2 M Na₂SO₄ and 0.5 % HCl + 0.2 M Na₂SO₄.
3. The third solution consisted of indole and cetyl trimethyl ammonium bromides (CTAB) inhibitors to inhibit the corrosion in a solution consisted 0.1 M Na₂SO₄+ 1 % HCl + 1.7×10^{-3} M indole, 0.1 M Na₂SO₄+ 1 % HCl + 3.4×10^{-3} M indole, and 0.1 M Na₂SO₄+ 1 % HCl + 2.74×10^{-3} M CTAB

The salt used was anhydrous sodium sulphate (Na₂SO₄) produced by “Scharlau Company- Spain” having assay of 99.8 % and a molecular weight of 142.04 g / gmole. The hydrochloric acid that used was produced by “Scharlau Company- Spain” having assay of 36.5 % and a molecular weight of 36.64 g / gmole and density of 1.185 g / cm³.

The used indole and CTAB inhibitors were made in England and both have assay of 99 % with molecular weight of 364.45 g / gmole for CTAB and 117.1 g / gmole for indole. The distilled water that used in experiments having a conductivity of 6.63 μ S, pH of 6.86, oxygen solubility of 6.08 ppm at laboratory temperature (27 °C) with a 0.0 % NaCl.

3.3 Materials

Ethanol was used to clean the specimens. It was supplied by FLUKA and having assay of 99.9 %. For the corrosion experiments in Na_2SO_4 there was clear corrosion product layer. A 50 gm thioharnstoff corrosion inhibitor (H_2NCSNH_2) that produced by MERCK company with assay of 99.8 % was added to the cleaning solution with 10 % HCl. Cylindrical carbon steel specimen was prepared to fit the specimen holder with a surface area of 23.5619 cm^2 having a dimension of 30 mm long (L), 22 mm inside diameter (d_i), and 25 mm outside diameter (d_o) that measured by using electronic digital caliper and it serves as a cathode.

3.4 Experimental Apparatus

1. Holder: or rotating shaft made of Teflon on which the carbon steel specimen was placed. The dimensions and shape of RCE is shown in Fig. 3- 1.
2. Power supply and multimeters: power supply was used to provide a constant applied voltage of 5 V between the electrodes. Two multimeters were used, one work as ammeter and measure the current in mA, the other used as voltmeter to measure the potential in V.

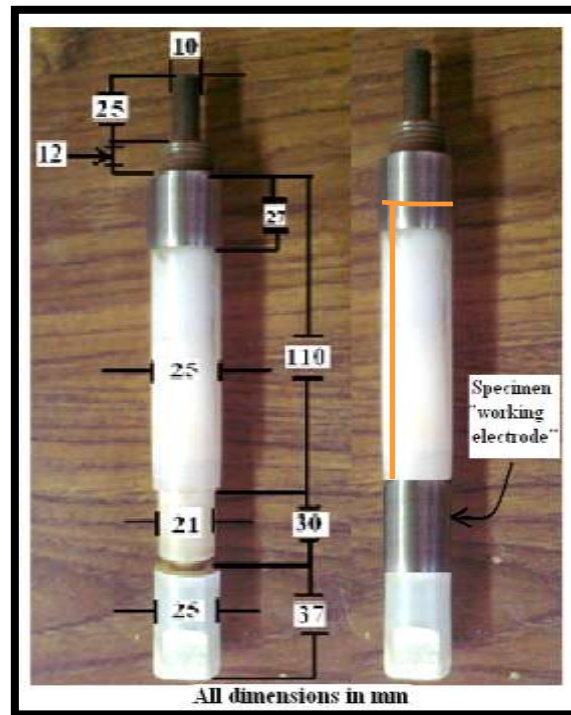


Figure 3- 1 Rotating shaft and specimen insallation

3. Resistance box : or called rheostat type PE 06 RN manufacture by POPULAR company range from 0 to 10^6 Ohm, used to control the current flow
4. Graphite brush was used to attain the electrical connection between the circuit and the rotating specimen.
5. Reference Electrode: was saturated calomel electrode (SCE) used to measure the potentials. The luggin capillary of the reference electrode was placed 2mm downstream of the working electrode.
6. Counter (auxiliary) electrode: made of graphite and serves as anode. The surface area of the counter electrode was made larger than that of the

working electrode ($A_a/A_c = 2.7$) to ensure that the limiting current density occurs on the cathode rather than anode.

7. Stirrer: type of ss10 manufactured by Stuart (UK) which is a rotating motor used to obtain the required rotational velocity that range from 0 to 2000 rpm.
8. Thermometer: of range -10 to 200 °C used to measure the solutions temperature.
9. Water bath: type memmert with temperature controller keep the temperature constant within (± 2 °C) until the solution reached the preset temperature, having temperature range from 10 to 95 °C.
10. Air pump: that joined with bubbles distributor which give air flow rate of 2.5 L / min. Air pump was used to increase the oxygen concentration in the solutions. Fig. 3- 2 shows the air pump and oxygen bubbles around the working electrode.



Figure 3- 2 Air pump and oxygen bubbles.

11. PH – meter: A digital pH meter manufactured by Hanna Instruments Company. Microprocessor pH meter having a range of pH from -2.00 to 16.00 with accuracy of ± 0.01 . Also it contains temperature probe to read the temperature for range of 0 to 100 °C with accuracy of ± 0.5 . The pH meter was calibrated using 4.001 and 7.001 pH buffer solutions. It is shown in Fig. 3-3.
12. Conductivity meter: Auto- ranging microprocessor type HI 2300 Manufactured by Hanna instruments and used to measure the conductivity of the solution at different temperatures and salt concentrations, with conductivity range 0.00 to 500.00 mS, temperature range -9.9 to 120 °C, and accuracy of $\pm 1\%$, ± 0.4 °C for conductivity and temperature respectively. It is shown in Fig. 3-4.

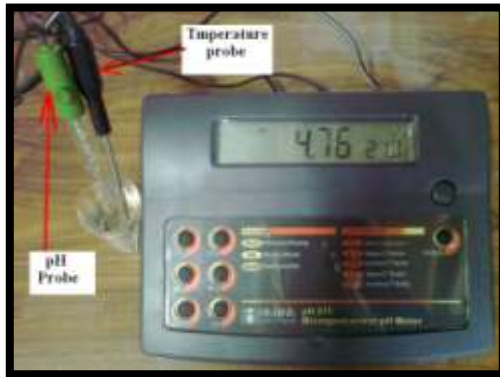


Figure 3- 3 PH meter



Figure 3- 4 Conductivity meter

13. Dissolved oxygen meter: This was used to measure the concentration of oxygen in the solution (C_b) in ppm. Manufactured by Hanna instruments type HI 2400 with accuracy of $\pm 1.5\%$ for range 0.00 to 45.00 ppm. It measures the solubility of oxygen for a range of temperature 0.0 to 50.0 °C with accuracy of ± 0.5 °C. Fig. 3- 5 shows the dissolved oxygen meter.



Figure 3- 5 Dissolved oxygen meter

14. Desiccator: made of Pyrex to keep the specimen from moisture using highly active silica gel as shown Fig. 3-6.
15. Balance: electronic high accuracy 4 decimal places of gram digital balance type Sartorius with maximum weight of 210 g. which have accuracy of 0.1 mg. This was used to weigh the specimens before and after the experiment in weight loss experiments. It is shown in Fig. 3- 7.



Figure 3 - 6 Desiccator.



Figure 3- 7 Balance

16. Beakers: of 2 and 3 liters made of Pyrex in them the test solution was placed.

Figures 3- 8 to 3- 9 illustrated the schematic and Rig Picture of the experimental apparatus respectively.

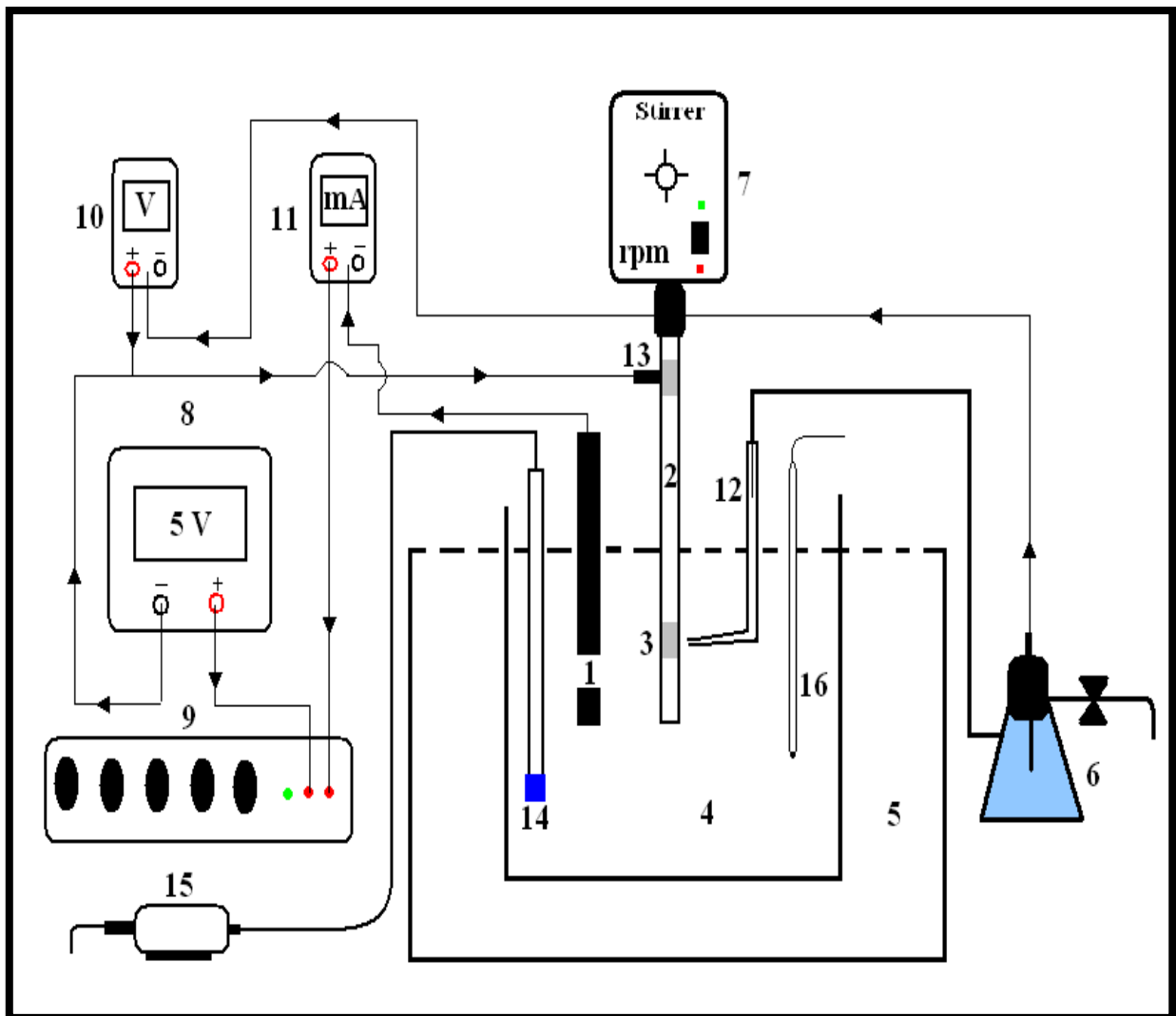


Figure 3- 8 Schematic illustrates of experimental apparatus.

1- Graphite electrode (anode), 2- rotating shaft (holder), 3- working electrode (specimen), 4- beaker , 5- water bath, 6- calomel electrode (reference electrode), 7- stirrer, 8- power supply, 9- resistance box, 10- voltmeter, 11-ammeter, 12- Luggin capillary, 13- brush 14- air distributor, 15- air pump, 16-thermometer.



Figure 3- 9 Experimental rig picture.

3.5 Density Measurements

In present work, the density of solutions was measured at various temperatures and salt concentrations using a picknometer of 10 ml as shown in Fig. 3-10.

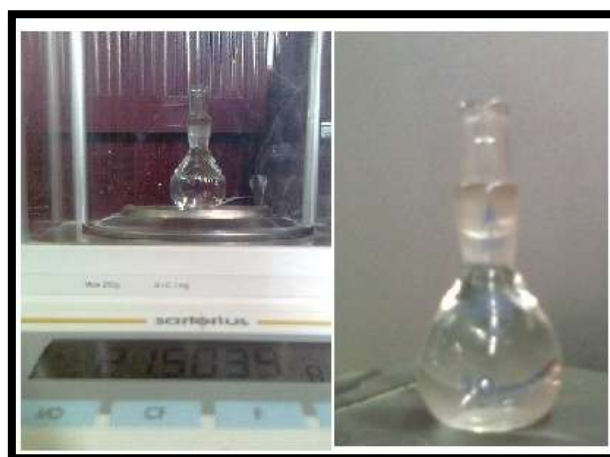


Figure 3-10 Density testing.

3.6 Experimental Procedures

3.6.1 Weight Loss Experiments

Before each experiment, the carbon steel specimen (working electrode) was polished with 120, 180, 220, 400 and 2000 grit silicon carbide papers, washed with brushing by plastic brush with running tap water, immersed in ethanol for 30 second dried with clean tissue, and then dried by using electrical oven to temperature of about 110 °C for 10 minute [Mahato et.al, 1980]. The specimen then was stored in vacuum desiccator over high activity silica gel until use. Then the specimen was weighted to nearest 0.1 mg (w_1) by using digital balance to measure the weight loss. After that the specimen was exposed to corrosion environment for 4 h in salt solutions and for 2 h in acid solutions. At the end of weight loss experiment, the specimen was washed by tap water with brushing to remove the corrosion products that formed on the outside surface and then immersed in 10% hydrochloric acid containing chemical inhibitor (thioharnstoff) for 30 second [Fontana, 1986; Hasan, 2003]. Blank tests showed no appreciable weight loss caused by cleaning with inhibited acidic solution. After that the specimen was washed by tap water, distilled water, dried with clean tissue, rinsed in ethanol and dried by using electrical oven to a temperature about 110 °C for 10 minute. Then the specimen was kept in the desiccator to cool and then weighted (w_2). So that the corrosion rate can be determined using:

$$CR = \frac{\Delta W}{A \times t} \quad (3.1)$$

And the limiting current density can be determined by using the following equation:

$$i_L = z F N_{O_2} \quad (3.2)$$

N_{O_2} = is the molar flux of oxygen which is defined as the moles of O_2 reacted per unit area per unit time ($gmole/m^2.s$). Also, according to reactions in Eq. 1.1 and Eq. 1.3, $N_{O_2} = 0.5 N_{Fe}$. The mass transfer coefficient can be determined from the following equation [Shreir et. al., 2000]:

$$k = \frac{N_{O_2}}{C_b} \quad (3.3)$$

Diffusion layer thickness, δ , can calculate as [Poulson, 1983]:

$$\delta = \frac{D_{O_2}}{K} \quad (3.4)$$

The Reynolds number for a rotating cylinder electrode with outer diameter, d_o (m) was calculated according to the relation:

$$Re = \rho d_o u / \mu \quad (3.5)$$

3. 6. 2 Polarization Experiments

In polarization measurements, after the solution had reached the desired temperature, the electrical circuit was switched on where maximum current pass through the cell because the resistance is very low, the specimen was cathodically polarized from a potential of nearly -1.4 V (vs. SCE) to the corrosion potential (where $i_{app} = 0$) at a rate of $5 - 10$ mV by changing the applied current using rheostat, that is, 5 mV when the change of current with potential is high (near corrosion potential) and 10 mV when the change of current with potential is low, i.e. in the limiting current density region. The current was recorded for step changes in potential. Two minutes were allowed for steady state to be reached after each potential increment [Pickett and Ong,

1974; Slaiman and Hasan, 2010]. For the experiments with air bubbling, the air was pumped at a rate of 2.5 L / min using air pump for 15 minutes before each run and the bubbling was kept until the end of the run. The oxygen concentration was measured for each condition and monitored along the run using dissolved oxygen meter. After collecting the data by recording the current and potential, polarization curve can be drawn by using semi log scale where the x-axis represents the current density (log scale) and the y-axis represents the potential, so that the limiting current density can be obtained from this curve which can be represented by the vertical linear region b to c (after hydrogen evolution region [a to b]) as shown in Fig. 3- 11.

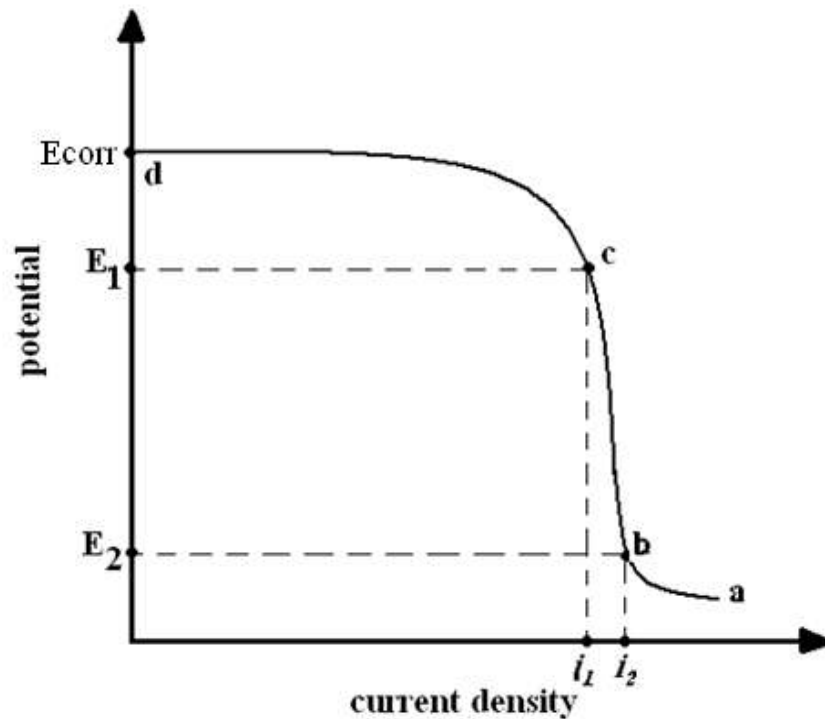


Figure 3- 11 Typical polarization curve [Gabe and Makanjoula in 1986]

Method given by Gabe and Makanjoula [1986] for determines the limiting current as shown below:

$$i_L = \frac{i_1 + i_2}{2} \quad (3.6)$$

The obtained values of i_L represent values for clean surface ($t = 0$), i.e. no corrosion products were formed, since during the polarization experiment no free corrosion occurred (except at low currents near the corrosion potential) because the specimen was cathodically protected. To investigate the influence of time on the instantaneous corrosion rate, the electrical circuit was switched off and the specimen was allowed to corrode freely at a particular velocity and temperature. A free corrosion of the specimen continues for 1 h during this interval corrosion proceeds and the corrosion product forms on the surface of the specimen. At the end of 1 h, the electrical circuit was again switched on and the specimen was polarized to -1.4 V (vs. SCE) and polarization experiment was repeated to obtain the complete polarization curve and new i_L . This value of i_L represents the value at $t = 1$ h. At the end of the second polarization measurement, the electrical circuit was switched off while the specimen was kept corroding in the solution for another 1 h. During this second interval, the specimen will undergo a free corrosion forming additional corrosion products. The specimen was then polarized to -1.4 V (vs. SCE) by switching on the electrical circuit again to repeat the polarization experiment and to obtain new i_L at $t = 2$ h. Each run was carried out in duplicate with third run when the reproducibility was in doubt. The solubility of oxygen at different velocities, temperatures, and salt concentration was measured in ppm at each 15 min using oxygen meter.

For acidic solutions anodic and cathodic polarization curves were needed to measure the i_{corr} . In the anodic polarization, at the end of cathodic polarization curve and arrived to corrosion potential were the current was zero by reversing

the connection to the power supply, i.e. connected the working electrode to (+) and the auxiliary electrode to the (-) of the power supply. The specimen was anodically polarized starting from the corrosion potential obtained from cathodic polarization measurements for clean surface. In the anodic polarization, the temperature and velocity were set at required values to start the polarization at a rate of 5-20 mV to obtain complete anodic polarization curve. Each experiment was carried out in duplicate and each specimen was often used once and when the corrosion is too low it was used twice. Fig. 3-12 shows the anodic and cathodic polarization curves and the way used to measure the corrosion current (i_{corr}) and Tafel slopes β_a , β_c .

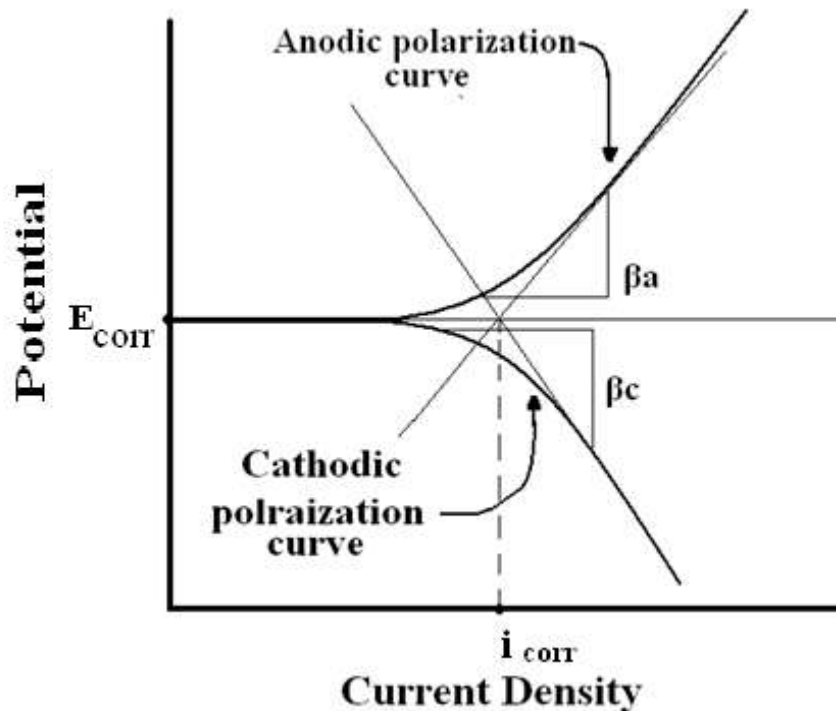


Figure 3- 12 Anodic and cathodic polarization curves with Tafel slopes in acid solution
 [Shreir et.al, 2000].

The total numbers of test runs carried out were:

i- 15 test runs for weight loss determination for salt and acid solutions under isothermal conditions, ii- 48 test runs for cathodic polarization measurements for clean surface ($t=0$) in salt solutions. iii- 10 test runs for cathodic polarization measurements for rough surface ($t =1$ h) in salt solutions. iv- 10 test runs for cathodic polarization measurements for rough surface ($t =2$ h) in salt solutions. v- 24 test runs for anodic polarization measurements in acid salt solutions. vi- 24 test runs for cathodic polarization measurements in acid salt solutions. vii- 19 test runs for weight loss determinations in inhibitors solution. Total number of runs was 150.

Chapter four

Results

This chapter presents the experimental results for the whole investigated ranges of salt and acid concentrations, rotational velocities, temperature, oxygen concentration, time, and inhibitor concentration.

In first part of the experimental work weight loss method was employed to measure the corrosion rate of carbon steel pipe at isothermal conditions ($T = 32$ °C) to study the effect of flow velocity in different solutions.

Table 4-1 shows the corrosion rate of carbon steel expressed in different units in 0.2 M Na_2SO_4 at 32 °C for different rotational velocity with corresponding values of Reynolds number (based on the outer diameter of specimen) at 4 h of immersions time.

Table 4-1 Corrosion rate of carbon steel in 0.2 M Na_2SO_4 at 32 °C for 4 h of immersions time by using weight loss method

u, rpm	u, m/s	Re	$i_L=i_{\text{corr.}}$ A/m²	CR, gmd	CR, mpy	K, ×10⁵ m/s	δ, ×10⁵ m	N_{Fe}, ×10⁵ mol/m².s	N_{O_2}, ×10⁵ mol/m².s
0	0	static	1.074	26.85	49.15	1.42	20.15	0.56	0.28
500	0.655	9409	3.78	94.61	173.19	4.99	5.72	1.96	0.98
1000	1.309	18804	3.93	98.33	179.99	5.19	5.5	2.04	1.02
1500	1.963	28199	4.95	123.7	226.44	6.53	4.37	2.56	1.28
2000	2.618	37609	4.75	118.9	217.62	6.28	4.55	2.46	1.23

Because of the process was under diffusion control, therefore $i_L = i_{corr}$. Also, Table 4-1 lists the values of mass transfer coefficient (calculated using Eq. (3-3)) and molar flux of O_2 (calculated using Eq. (3-2)), then calculated the flux of Fe by $N_{O_2} = 0.5N_{Fe}$. The thickness of diffusion layer (calculated using Eq. (3-4)).

The values of u in m/s were calculated by using the following equation:

$$u \text{ (m/s)} = \frac{\pi \times d_o \times u \text{ (rpm)}}{60} \quad (4.1)$$

The physical properties of viscosity, density, and diffusion coefficient, are presented in Appendix A.

Table 4-2 shows the corrosion rate of carbon steel in 0.2 M Na_2SO_4 mixed with 5 % by volume hydrochloric acid at 32°C and different velocity for 4 h of immersions time here where the $i_{corr} = i_L + i_H$.

Table 4-2 Corrosion rate of carbon steel in 0.2 M Na_2SO_4 with 5 % vol HCl at 32 °C for 4 h by using weight loss method

u, rpm	u, m/s	Re	i_{corr}, A/m²	*i_L, A/m²	i_H, A/m²	CR, gmd	CR, mpy	$N_{Fe} \times 10^5$ mol/m².s	*$N_{O_2} \times 10^5$ mol/m².s	$k \times 10^5$ m/s	$\delta \times 10^5$ m
0	0	Static	7.5	1.07	6.43	187.54	343.30	3.89	0.28	1.48	19.25
500	0.655	9774	13.19	3.78	9.41	329.82	603.76	6.84	0.98	5.23	5.46
1000	1.309	19534	14.09	3.93	10.16	352.35	645	7.30	1.02	5.43	5.26
1500	1.963	29294	20.62	4.95	15.67	515.58	943.82	10.69	1.28	6.84	4.18
2000	2.618	39068	18.42	4.75	13.66	460.50	842.98	9.55	1.23	6.57	4.35

*where the values of i_L and N_{O_2} taken from previous Table 4-1, i.e. they are for O_2 in salt solution before mixing with acid. The hydrogen evolution current is the difference between corrosion current i_{corr} and O_2 reduction currents (i_L).

Table 4-3 lists the corrosion rate of carbon steel in 0.2 M Na_2SO_4 mixed with 5 % by volume hydrochloric acid with addition of air bubbles at 32 °C and different velocity for 4 h of immersions time.

Table 4-3 Corrosion rate of carbon steel in 0.2 M Na_2SO_4 mixed with 5 % vol HCl with addition of air bubbles at 32 °C for 4 h of immersions time by using weight loss method.

u, rpm	u, m/s	Re	i_{corr}, A/m²	i_L, A/m²	*i_H, A/m²	CR, gmd	CR, mpy	$N_{Fe} \times 10^5$ mol/m².s	$N_{O_2} \times 10^5$ mol/m².s	$k \times 10^5$ m/s	$\delta \times 10^5$ m
0	0	Static	8.813	2.39	6.43	220.36	403.39	4.567	0.62	2.75	10.4
500	0.655	9774	15.41	6	9.41	385.27	702.28	4.985	1.55	6.89	4.15
1000	1.309	19534	23.47	13.31	10.16	586.83	1074.24	12.16	3.45	14.89	1.92
1500	1.963	29294	30.51	14.84	15.67	762.84	1396.44	15.81	3.84	14.81	1.19
2000	2.618	39068	61.16	47.49	13.66	1529	2799	31.69	12.3	43.92	0.651

*The value of i_H taken from Table 4-2 because the addition of air bubbles effect on i_L only. So the value of i_L with addition of air bubbles calculated by

diminution the value of corrosion current i_{corr} in Table 4-3 from i_{H} that taken from Table 4-2.

Form these tables it is clear in Table 4-3 that the values of i_{L} increased with increasing the flow velocity at each solution concentrations. The values of measured oxygen solubility in ppm (mg/L) are listed in Tables 4-4 to 4-7 for different temperatures and solutions concentrations.

Figures 4-1 to 4-3 show the cathodic polarization curves of carbon steel in 0.2 M Na_2SO_4 at 32, 42, and 52 °C respectively at different flow velocities. From these figures it clears that increasing the flow velocity leads to increase the corrosion rate that represented by the limiting current density and have complex trend with temperature.

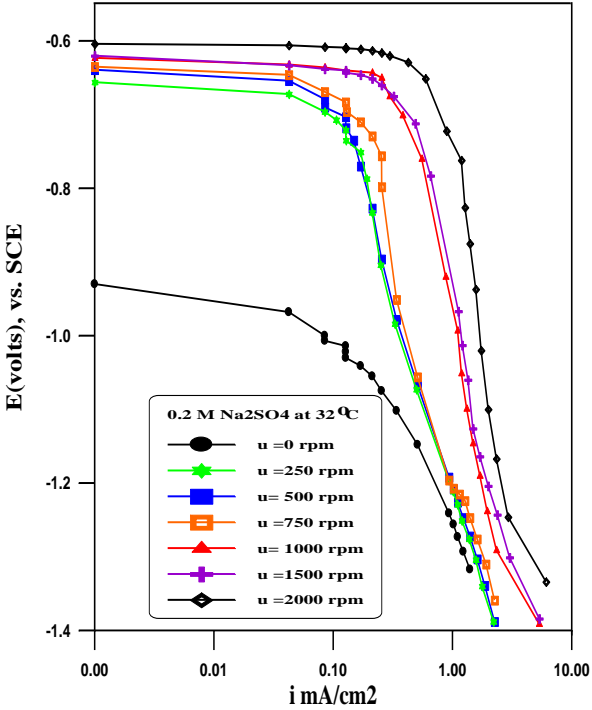


Figure 4-1 Cathodic polarization curves in 0.2 M Na_2SO_4 at 32 °C

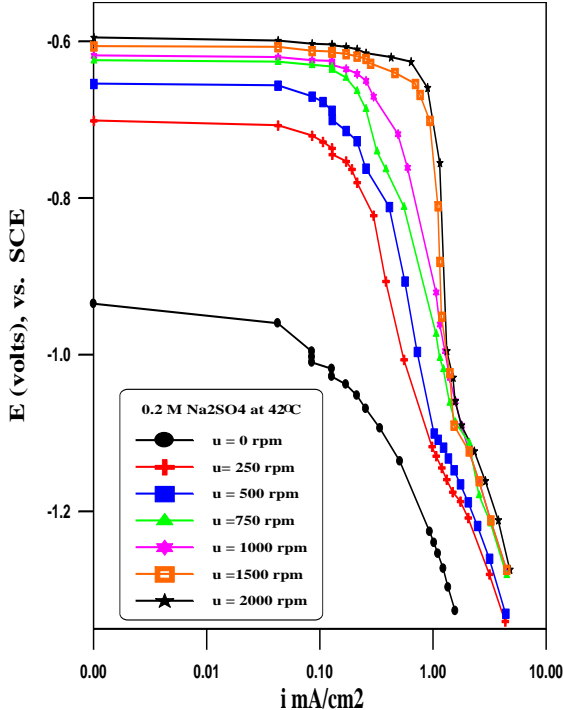


Figure 4-2 Cathodic polarization curves in 0.2 M Na_2SO_4 at 42 °C

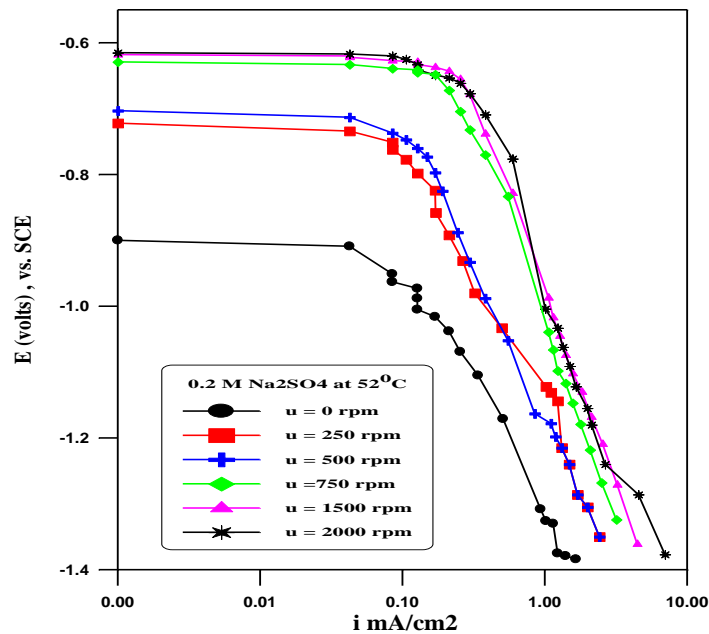


Figure 4-3 Cathodic polarization curves in 0.2 M Na₂SO₄ at 52 °C

Figures 4-4 to 4-6 shows the cathodic polarization curves of carbon steel in 0.2 M Na₂SO₄ with addition of air bubbles at 32, 42, and 52 °C respectively at different flow velocities.

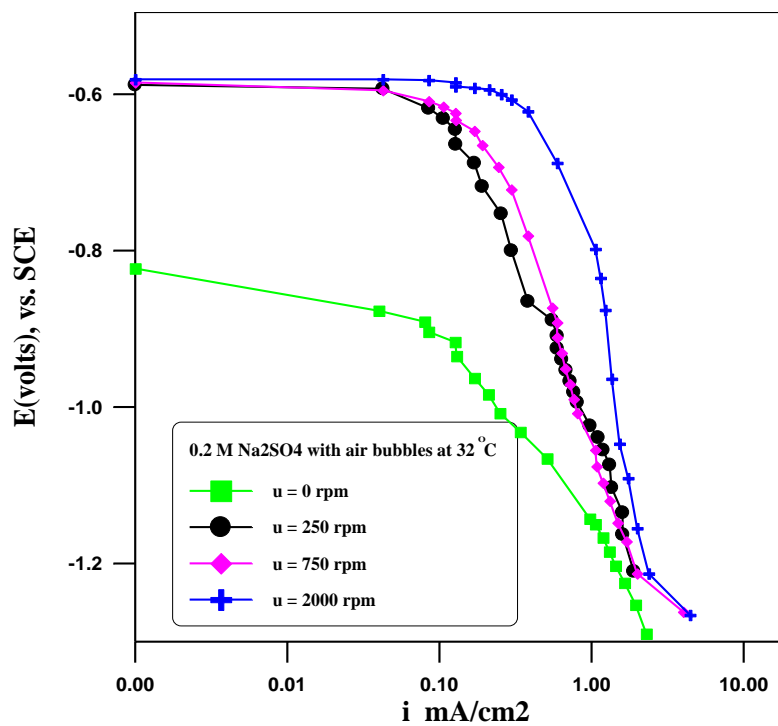


Figure 4-4 Cathodic polarization curves in 0.2 M Na₂SO₄ with air bubbles at 32 °C

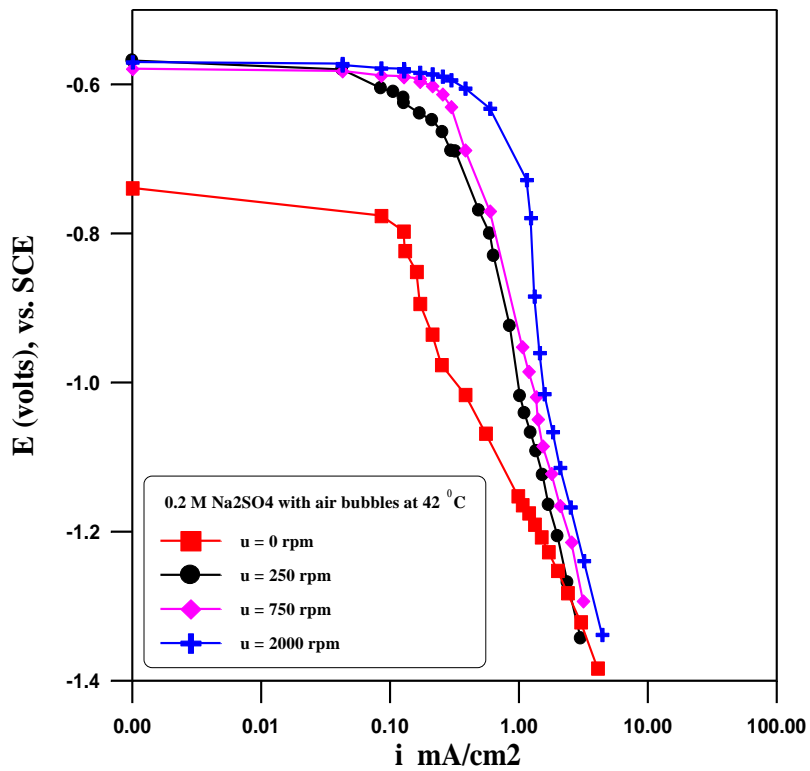


Figure 4-5 Cathodic polarization curves in 0.2 M Na₂SO₄ with air bubbles at 42 °C

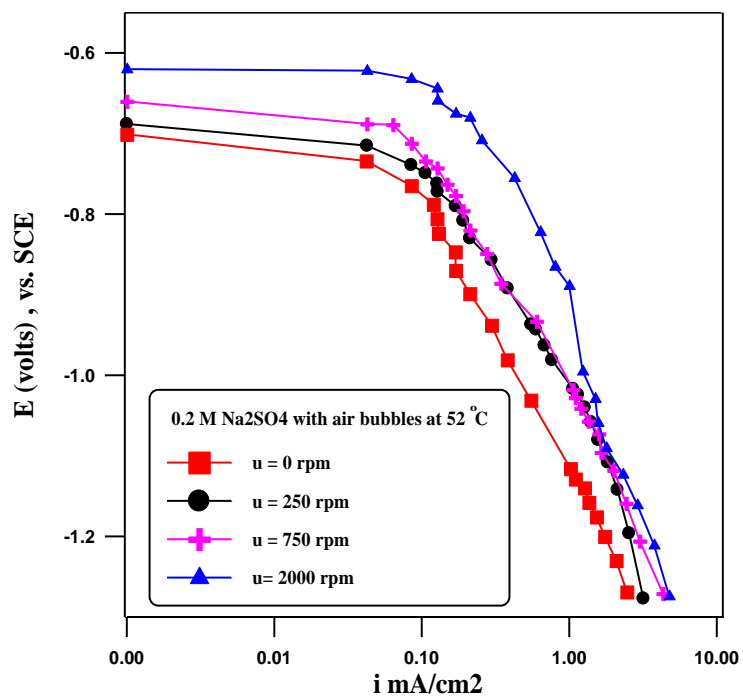


Figure 4-6 Cathodic polarization curves in 0.2 M Na₂SO₄ with air bubbles at 52 °C

Figures 4-7 to 4-9 show cathodic polarization curves of carbon steel in 0.2 M Na_2SO_4 at 250 rpm at different time intervals for temperatures of 32, 42, and 52 °C respectively.

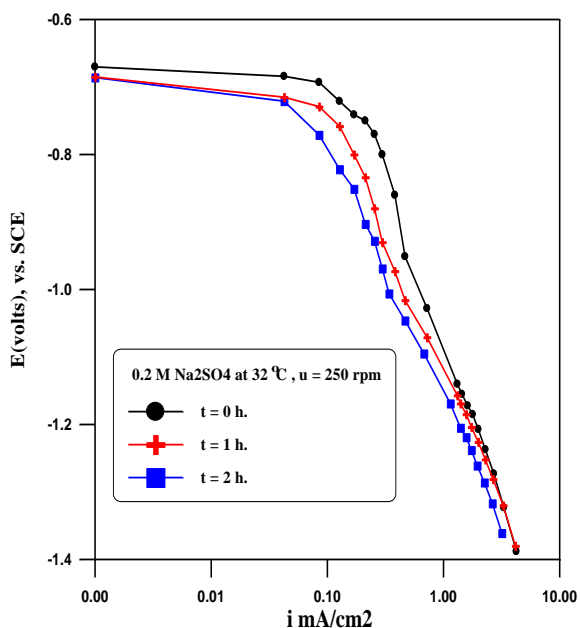


Figure 4-7 Cathodic polarization curves in 0.2 M Na_2SO_4 at 250 rpm at 32 °C for 2h

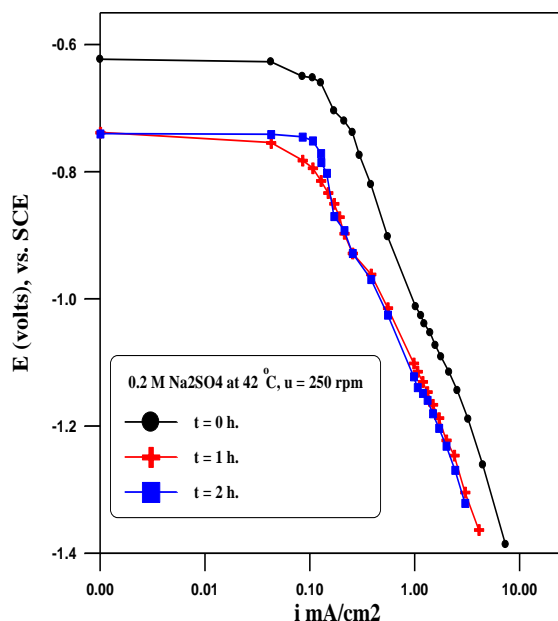


Figure 4-8 Cathodic polarization curves in 0.2 M Na_2SO_4 at 250 rpm at 42 °C for 2h

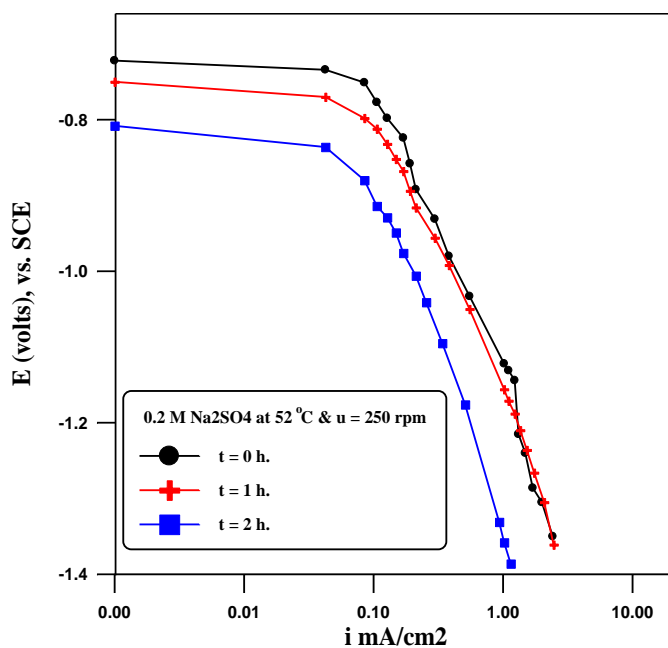


Figure 4-9 Cathodic polarization curves in 0.2 M Na_2SO_4 at 250 rpm at 52 °C for 2h

From these figures it clears that increasing the immersion time leads to decrease the corrosion rate at all temperatures range. Figures 4- 10 and 4-11 shows cathodic polarization curves of carbon steel in 0.2 M Na₂SO₄ at different immersion time intervals and temperature of 32 °C for different velocity of 1000 and 2000 rpm.

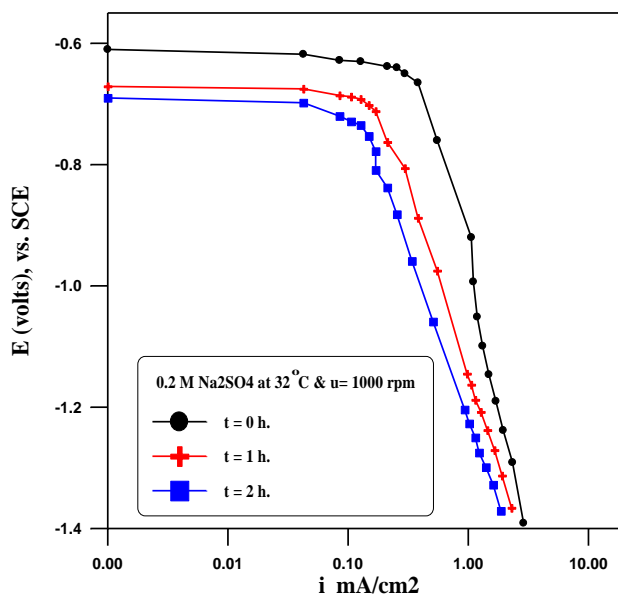


Figure 4- 10 Cathodic polarization curves in 0.2 M Na₂SO₄ at 32 °C for 1000 rpm & 2h

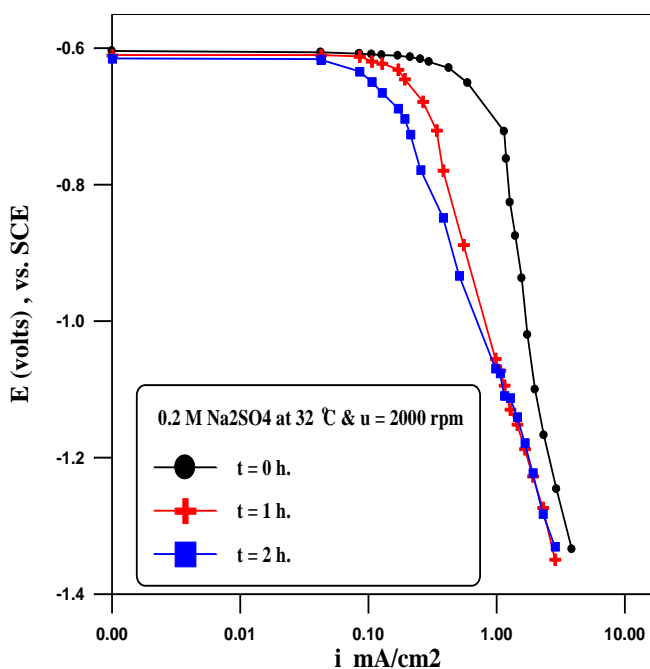


Figure 4- 11 Cathodic polarization curves in 0.2 M Na₂SO₄ at 32 °C for 2000 rpm & 2h

Figures 4-12 to 4-14 show cathodic polarization curves of carbon steel in 0.2 M Na_2SO_4 with addition of air bubbles at 250 rpm at different time intervals for temperatures of 32, 42, and 52 °C respectively.

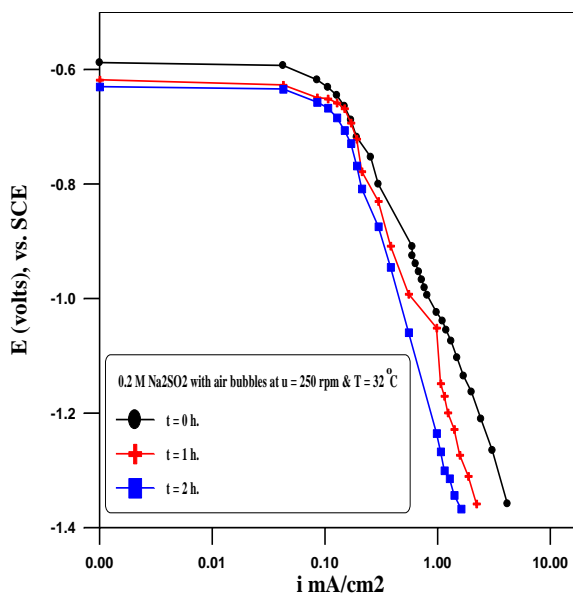


Figure 4-12 Cathodic polarization curves in 0.2 M Na_2SO_4 with air bubbles at 250 rpm, 32 °C and 2h

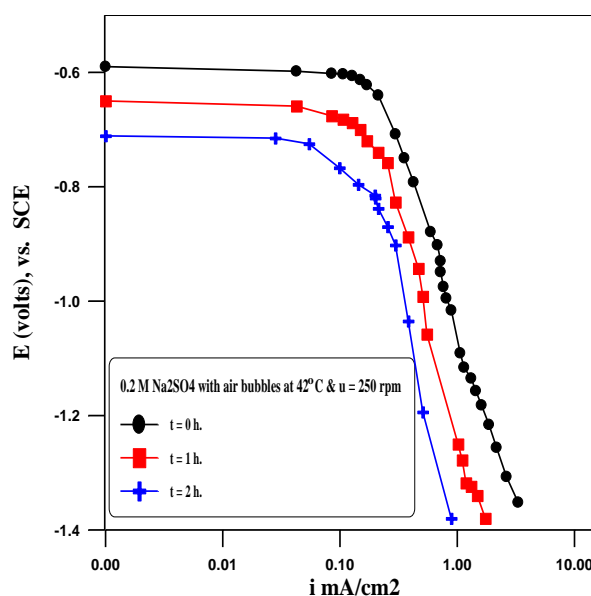


Figure 4-13 Cathodic polarization curves in 0.2 M Na_2SO_4 with air bubbles at 250 rpm, 42 °C and 2h

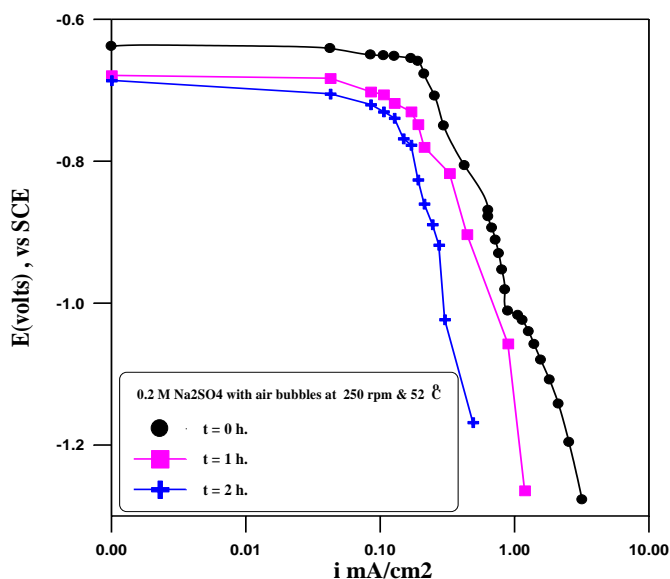


Figure 4-14 Cathodic polarization curves in 0.2 M Na_2SO_4 with air bubbles at 250 rpm, 52 °C and 2h

Figures 4-15 and 4-16 show cathodic polarization curves of carbon steel in 0.2 M Na₂SO₄ with addition of air bubbles at different immersion time intervals and temperature of 32 °C for different velocity of 750 and 2000 rpm respectively.

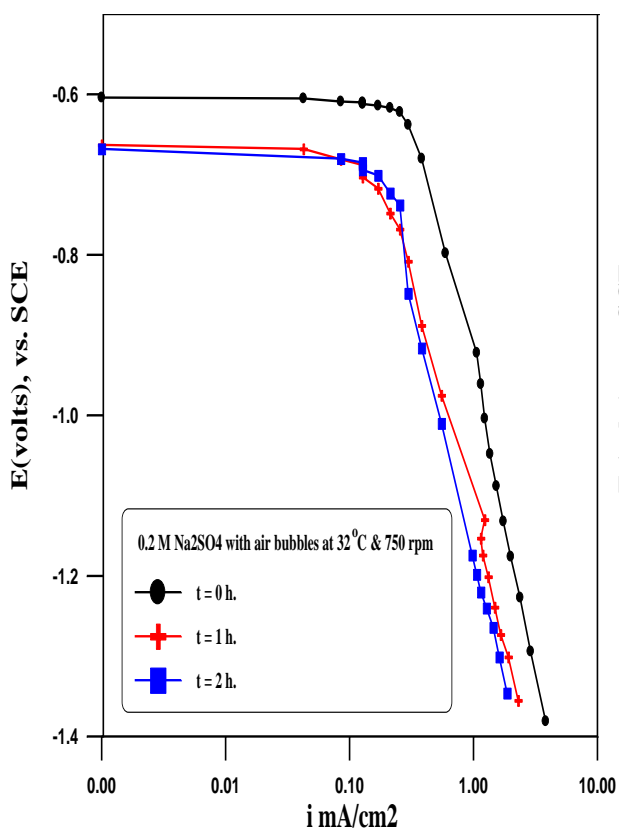


Figure 4-15 Cathodic polarization curves in 0.2 M Na₂SO₄ with air bubbles at 32 °C for 750 rpm and 2h

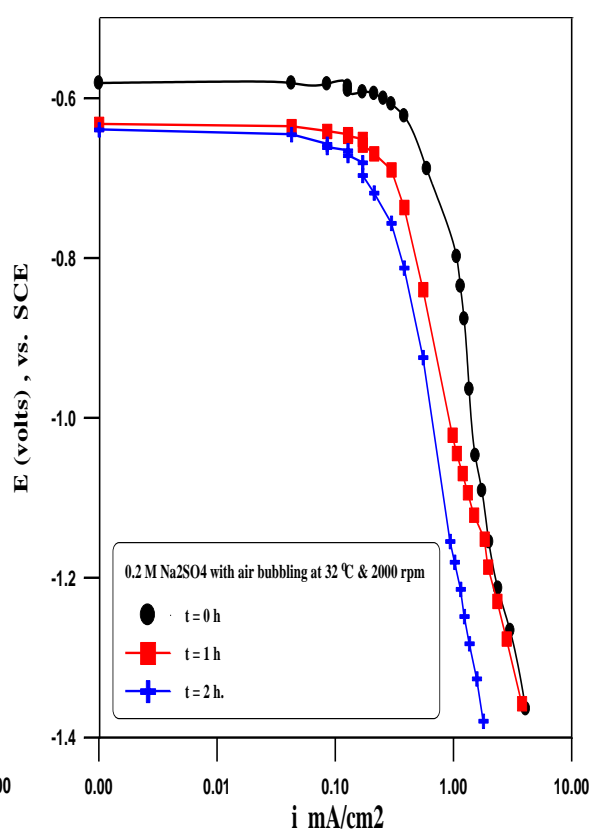


Figure 4-16 Cathodic polarization curves in 0.2 M Na₂SO₄ with air bubbles at 32 °C for 2000 rpm and 2h

Figures 4-17 to 4-21 show the cathodic polarization curves in 0.01, 0.025, 0.05, 0.1, and 0.4 M Na₂SO₄ respectively at constant velocity of 750 rpm and different temperatures of 32, 42, and 52 °C. The results show that the corrosion rate has unstable trend with salt concentrations at specific temperature.

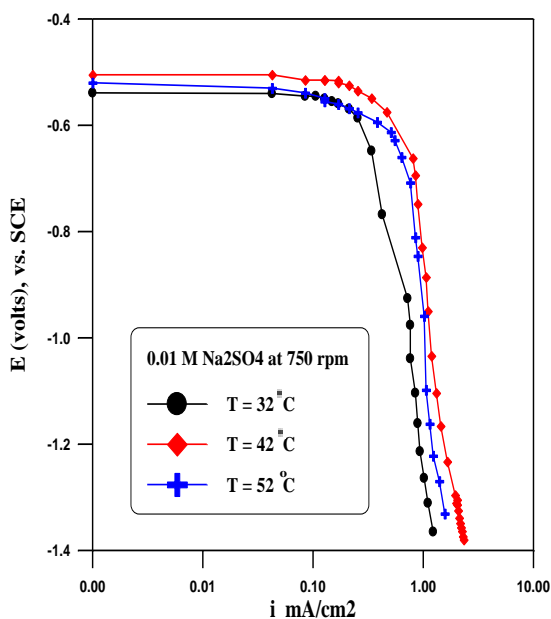


Figure 4-17 Cathodic polarization curves in 0.01 M Na₂SO₄ at 750 rpm

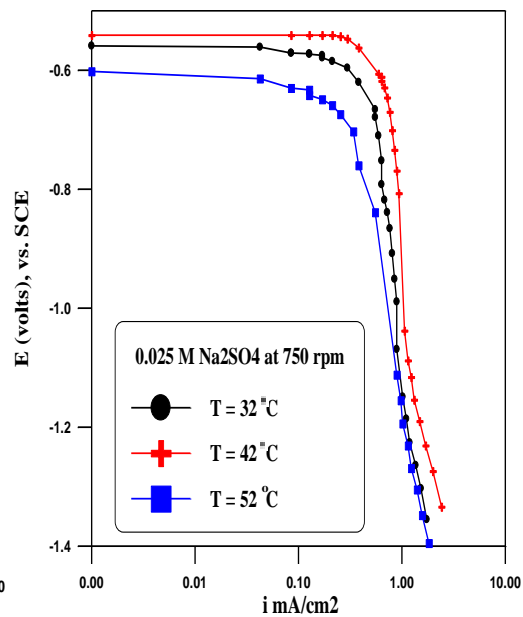


Figure 4-18 Cathodic polarization curves in 0.025 M Na₂SO₄ at 750 rpm

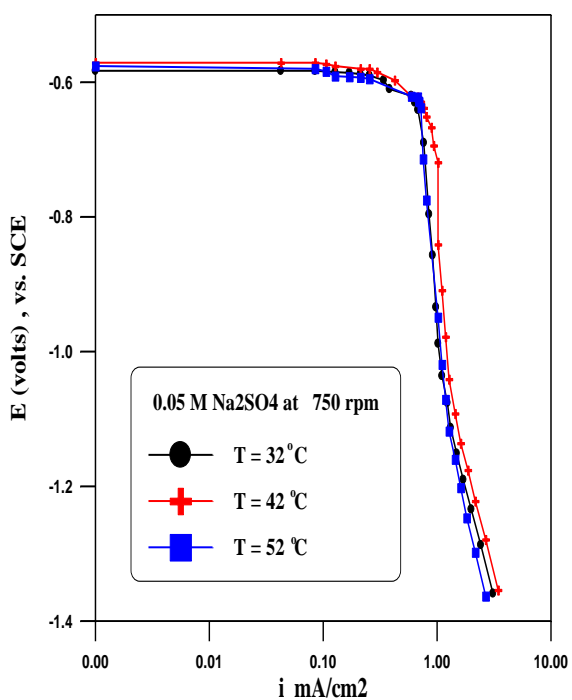


Figure 4-19 Cathodic polarization curves in 0.05 M Na₂SO₄ at 750 rpm

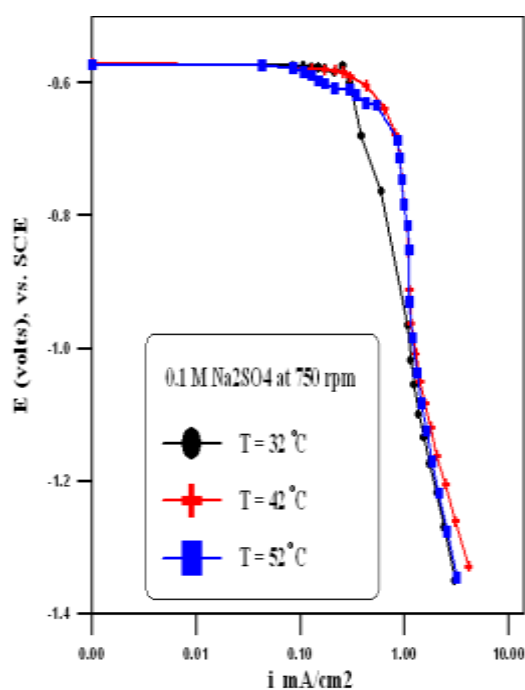


Figure 4-20 Cathodic polarization curves in 0.1 M Na₂SO₄ at 750 rpm

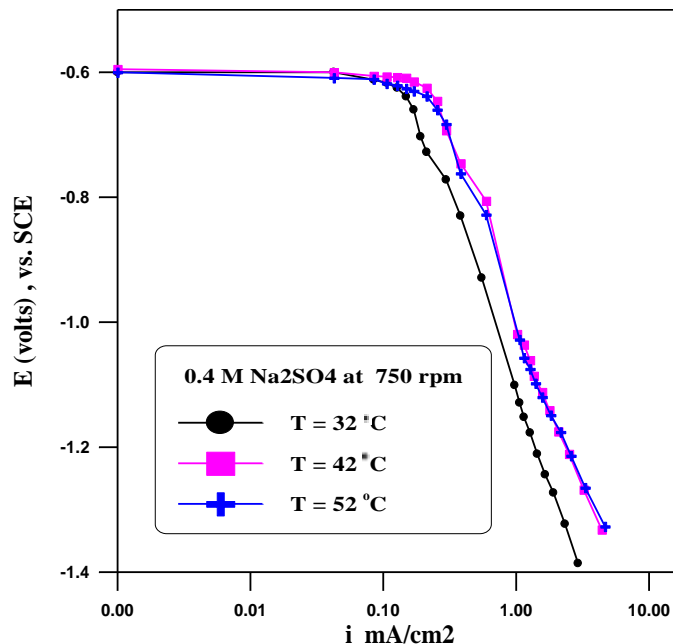


Figure 4-21 Cathodic polarization curves in 0.4 M Na₂SO₄ at 750 rpm

From figure 4-1 to 4-21 the measured values of limiting current density, i_{lim} , k , δ etc. were tabled in Appendix A.

Both anodic and cathodic polarization curves were applied in salt-acid solutions to measure the corrosion current i_{corr} . Fig. 4-22 shows anodic and cathodic polarization curves in 0.01 M Na₂SO₄ with 1 % HCl at 32 °C and different flow velocities it is clear that from Fig. 4-22 increasing velocity leads to increase the corrosion rate.

Figure 4-23 shows anodic and cathodic polarization curves in 0.01 M Na₂SO₄ with 1 % HCl at 250 rpm and different temperatures of 32, 42 and 52 °C. The result reveals that increasing temperatures have a great effect on corrosion rate especially in acid solutions.

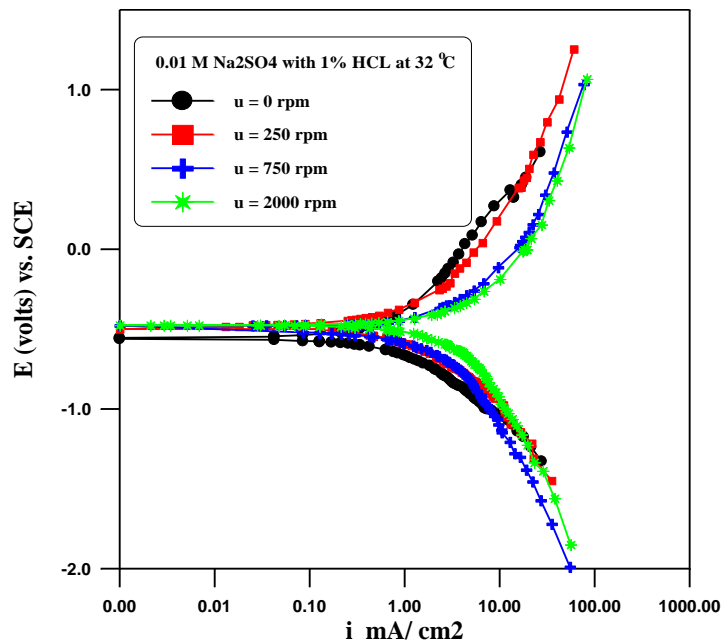


Figure 4-22 Anodic and cathodic polarization curves in 0.01 M Na₂SO₄ with 1 % HCl at 32 °C and different velocities

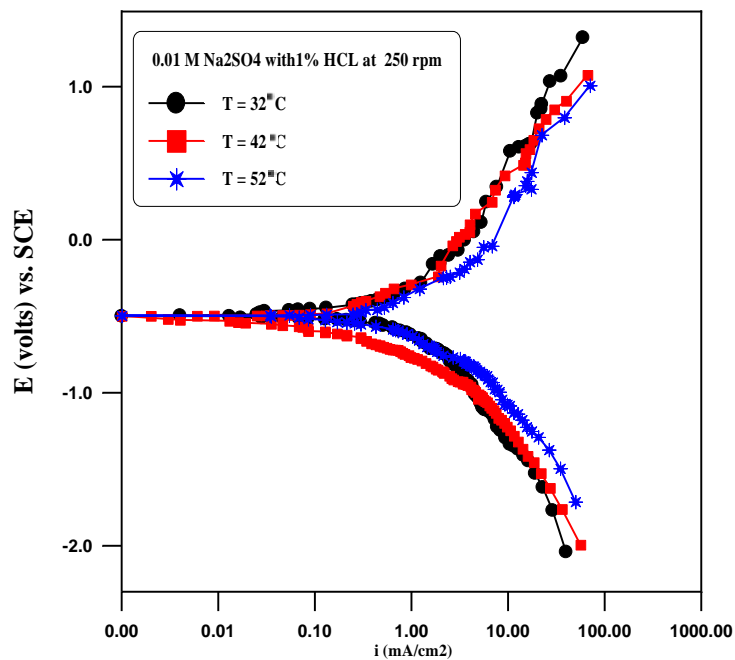


Figure 4-23 Anodic and cathodic polarization curves in 0.01 M Na₂SO₄ with 1 % HCl at 250 rpm and different temperatures

Figures 4-24 to 4-27 shows the anodic and cathodic polarization curves at temperatures of 32, 42, and 52 °C with rotation velocity of 250 rpm in solution having concentrations of 0.05 M Na₂SO₄ + 1 % HCl, 0.2 M Na₂SO₄ + 1 % HCl, 0.2 M Na₂SO₄ + 0.5 % HCl, and 0.2 M Na₂SO₄ + 3 % HCl respectively.

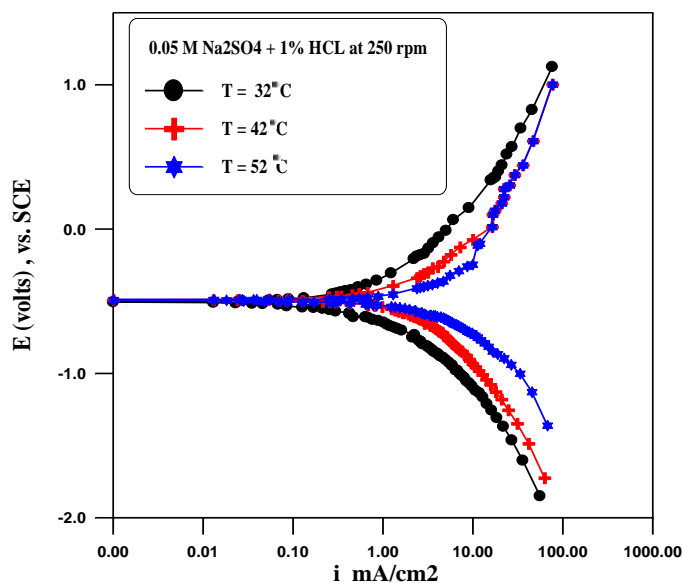


Figure 4-24 Polarization curves at 250 rpm in 0.05 M Na₂SO₄ + 1 % HCl

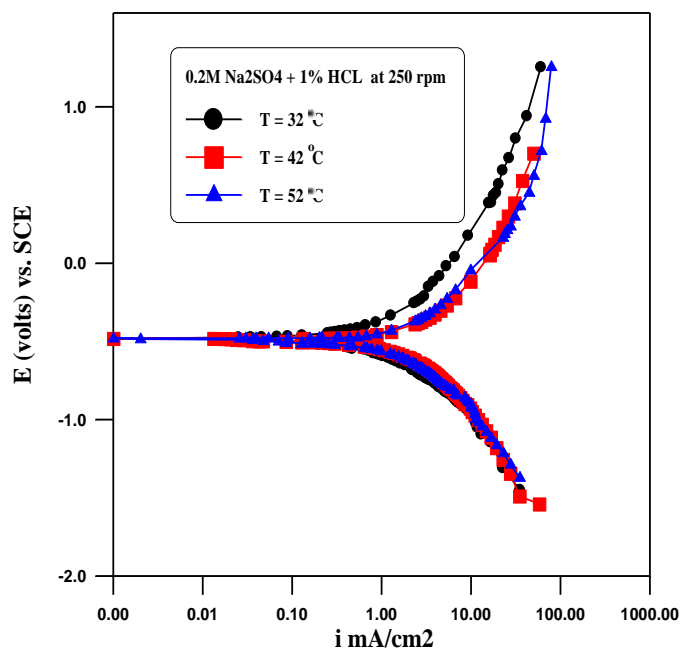


Figure 4-25 Polarization curves at 250 rpm in 0.2 M Na₂SO₄ + 1 % HCl

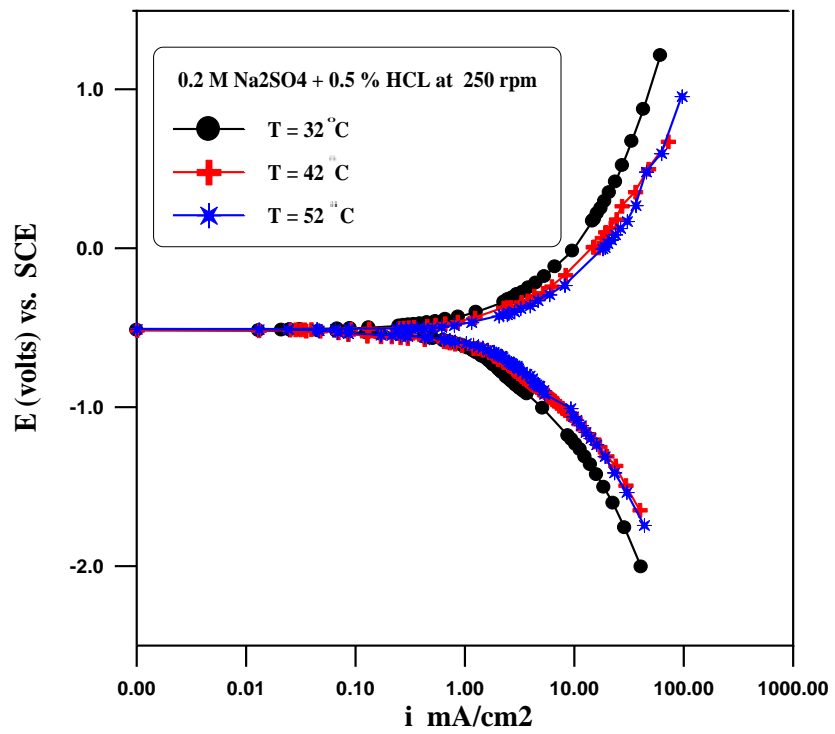


Figure 4-26 Polarization curves at 250 rpm in 0.2 M Na₂SO₄ + 0.5 % HCl

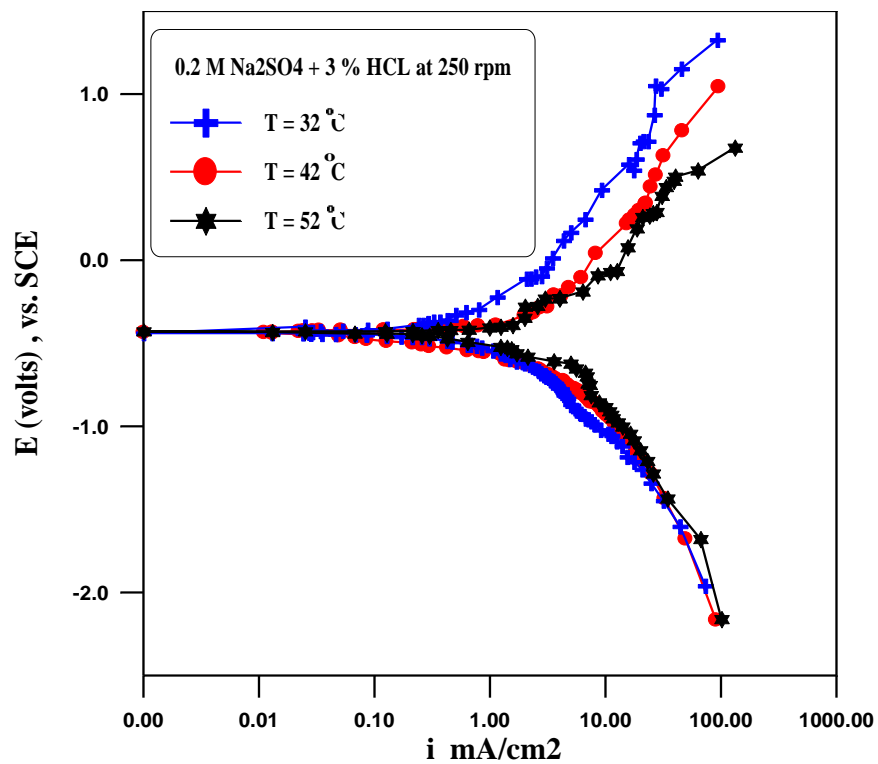


Figure 4-27 Polarization curves at 250 rpm in 0.2 M Na₂SO₄ + 3 % HCl

Figure 4-28 shows polarization curves for carbon steel in 0.2 M Na₂SO₄ + 1 % HCl with addition of air bubbles at 32 °C for different rotational velocities. It clear that addition of air bubbles lead to an increase in the corrosion current also the increase in flow velocity leads to an increase in the corrosion rates.

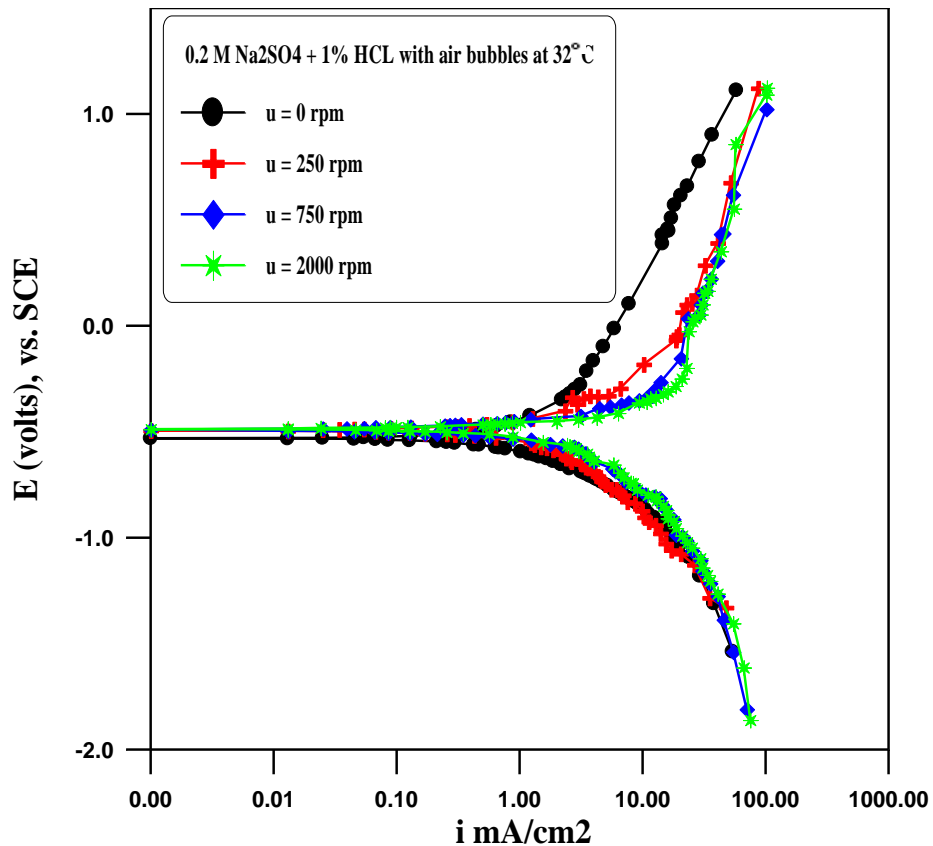


Figure 4-28 Polarization curves at 32 °C and different u in 0.2 M Na₂SO₄ + 1 % HCl with air bubbles

Figure 4-29 shows polarization curves for carbon steel pipe corrosion in 0.2 M Na₂SO₄ + 1 % HCl with addition of air bubbles at 32, 42, and 52 °C and constant velocity of 250 rpm. It clears that increase the solution temperature lead to increase the corrosion rate that here represents by corrosion current i_{corr} .

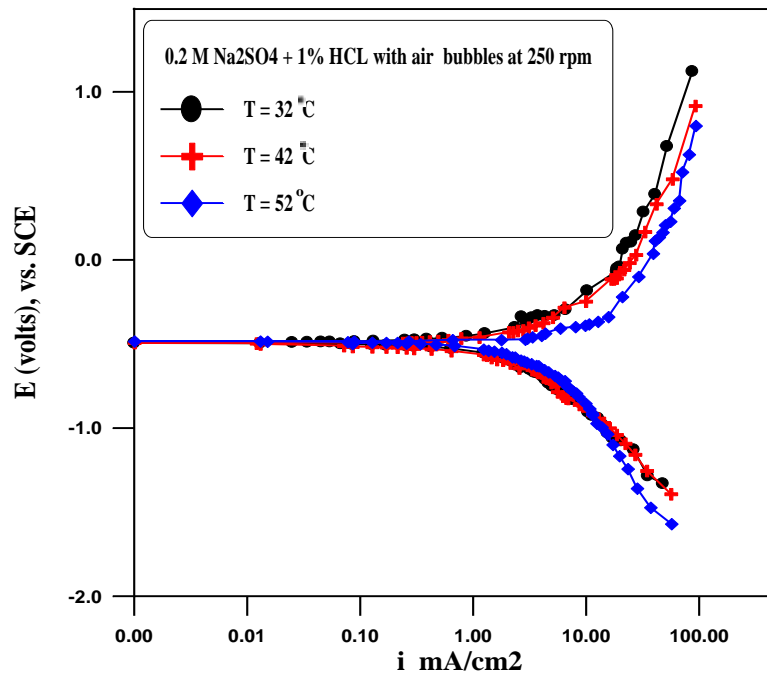


Figure 4-29 Polarization curves at 250 rpm and different T in 0.2 M Na₂SO₄ + 1 % HCl with air bubbles

From figure 4-22 to 4-29, the measured values of corrosion current density, gmd, mpy, and Tafel slopes are presented in Tables in Appendix B.

Table 4-4 Measured oxygen solubility at different sodium sulphate concentrations and temperatures.

Na ₂ SO ₄ concentrations in M	C _b , ppm		
	32 °C	42 °C	52 °C
0.4	5.9	5.08	4.72
0.2	6.2	5.32	4.94
0.1	6.51	5.58	5.17
0.05	6.85	5.84	5.41
0.025	7.19	6.12	5.67
0.01	7.56	6.41	5.93

Table 4-5 Measured oxygen solubility in 0.2 M Na₂SO₄ with addition of air bubbles.

u, rpm T, °C	C_b, ppm		
	32 °C	42 °C	52 °C
0	7.34	6.54	5.97
250	9.01	8.05	6.21
750	10.5	8.21	6.58
2000	12	8.89	6.95

Table 4-6 Measured oxygen solubility in different acid salt mixture at different temperatures.

Solutions concentration	C_b, ppm		
	32 °C	42 °C	52 °C
0.01 M Na ₂ SO ₄ + 1 % HCl	7.34	6.29	5.68
0.05 M Na ₂ SO ₄ + 1 % HCl	6.64	5.71	5.29
0.2 M Na ₂ SO ₄ + 1 % HCl	6.13	5.32	4.97
0.2 M Na ₂ SO ₄ + 0.5 % HCl	6.21	5.37	5.03
0.2 M Na ₂ SO ₄ + 3 % HCl	6.15	5.27	4.88
0.2 M Na ₂ SO ₄ + 5 % HCl	6.00

Table 4-7 Measured oxygen solubility in 0.2 M Na₂SO₄ + 5 % HCl with addition of air bubbles at different velocities and at 32 °C.

u, rpm	0	500	1000	1500	2000
C_b, ppm	7.204	7.22	7.408	8.305	8.965

Table 4-8 Measured oxygen solubility in 0.2 M Na₂SO₄ + 1 % HCl with addition of air bubbles at different velocities and temperatures.

u, rpm \ T, °C	C _b , ppm		
	32 °C	42 °C	52 °C
0	7.33
250	7.90	7.01	6.66
750	8.01
2000	9.16

Table 4-9 Measured pH values for different salt and acid salt mixtures at different concentrations.

Solutions concentration	pH
0.01 M Na ₂ SO ₄	6.94
0.025 M Na ₂ SO ₄	6.84
0.05 M Na ₂ SO ₄	6.83
0.1 M Na ₂ SO ₄	6.78
0.2 M Na ₂ SO ₄	6.74
0.4 M Na ₂ SO ₄	6.7
0.01 M Na ₂ SO ₄ + 1 % HCl	0.05
0.05 M Na ₂ SO ₄ + 1 % HCl	0.05
0.2 M Na ₂ SO ₄ + 1 % HCl	0.05
0.2 M Na ₂ SO ₄ + 0.5 % HCl	0.32
0.2 M Na ₂ SO ₄ + 3 % HCl	-0.4
0.2 M Na ₂ SO ₄ + 5 % HCl	-0.6

Table 4-10 Measured conductivity values of different Na₂SO₄ concentrations at different temperatures.

Solution T, °C	Conductivity, mS		
	32 °C	42 °C	52 °C
0.01	1.985	2.119	2.165
0.025	5.57	5.72	6.21
0.05	8.02	9.32	9.45
0.1	16.2	16.82	17.25
0.2	29.11	30.06	31.2
0.4	41.4	45.7	48.00

Corrosion inhibition of carbon steel pipe in 0.1M Na₂SO₄ + 1 %HCl was carried out using weight loss method for immersion time of 2 h by 1.7×10⁻³ M, 3.4×10⁻³ M indole and 2.74×10⁻³ M CTAB under different flow condition and temperatures. The results obtained from these experiments are shown in Tables 4-11 to 4-14.

Table 4-11 Corrosion of carbon steel pipe in 0.1M Na₂SO₄ + 1 % HCl (uninhibited solution) for 2h immersion time by using weight loss method.

T, °C	u, rpm	u, m/s	Δw, gm	CR, gmd	CR, mpy	N _{Fe} , ×10 ⁵ mol/m ² .s	i _{corr} , A/m ²
32	0	0	0.0604	307.64	563.16	6.38	12.31
	250	0.327	0.0610	310.69	568.74	6.44	12.43
	750	0.982	0.0629	320.37	586.46	6.64	12.81
	1000	1.309	0.0668	340.24	622.84	7.1	13.7
	2000	2.618	0.0695	353.99	648.01	7.34	14.16
42	0	0	0.0620	315.79	578.08	6.54	12.62
52	0	0	0.0653	332.59	608.8	6.89	13.29

Table 4-12 Corrosion of carbon steel pipe in 0.1M Na₂SO₄ + 1 % HCl with 1.7×10⁻³ M indole for 2h immersion time by using weight loss method.

T, °C	u, rpm	u, m/s	Δw, gm	CR, gmd	CR, mpy	N_{Fe},×10⁵ mol/m².s	i_{corr}, A/m²	IE %
32	0	0	0.0081	41.56	76.08	0.861	1.66	86.589
	250	0.327	0.0237	120.713	220.97	2.5	4.82	61.15
	750	0.982	0.0416	211.88	387.86	4.39	8.47	33.86
	1000	1.309	0.0484	246.52	451.28	5.1	9.86	27.54
	2000	2.618	0.0549	279.63	511.89	5.79	11.173	21.01
42	0	0	0.007613	38.78	70.99	8.04	1.55	87.72
52	0	0	0.00743	37.85	69.29	7.84	1.51	88.618

Table 4-13 Corrosion of carbon steel pipe in 0.1M Na₂SO₄ + 1 % HCl with 3.4×10⁻³ M indole at 32 °C for 2h immersion time by using weight loss method.

u, rpm	u, m/s	Δw, gm	CR, gmd	CR, mpy	N_{Fe},×10⁵ mol/m².s	i_{corr}, A/m²	IE %
0	0	0.0072	36.67	67.13	0.759	1.46	88.08
250	0.327	0.016	81.49	149.17	1.69	3.26	73.77
750	0.982	0.02516	128.15	234.59	2.66	5.13	60
1000	1.309	0.0287	146.18	267.59	3.03	5.85	57.04
2000	2.618	0.04	204	373	4.222	8.15	36.41

Table 4-14 Corrosion of carbon steel pipe in 0.1M Na₂SO₄ + 1 % HCl with 2.74×10⁻³ M CTAB for 2h immersion time by using weight loss method.

T, °C	u, rpm	u, m/s	Δw, gm	CR, gmd	CR, mpy	N_{Fe}×10⁵ mol/m².s	i_{corr}, A/m²	IE %
32	0	0	0.0115	58.57	107.23	1.2	2.32	80.96
	250	0.327	0.0287	146.18	267.59	3.03	5.85	52.951
	750	0.982	0.0329	167.57	306.75	3.47	6.69	47.69
	1000	1.309	0.0494	251.6	460.57	5.2	10.03	26.05
	2000	2.618	0.0579	294.91	539.86	6.11	11.79	13.32
42	0	0	0.0128	65.19	119.34	1.35	2.61	79.35
52	0	0	0.0176	89.64	164.09	1.86	3.59	73.05

The pH value of the tested solution (i.e. 0.1M Na₂SO₄ + 1 %HCl) will not changed by the addition of these inhibitors.

A sample of data for polarization experiments results were tabled in Appendix D (in Table D-1 and D-2).

Chapter Five

Discussions

This chapter presents the discussions of experimental results for the whole investigated ranges of salt and acid concentrations, rotational velocities, temperature, oxygen concentration, time, and inhibitor concentration because the influence of these variables on the experimental data needs to be interpreted and understood.

5.1 Effect of Velocity on the Corrosion rate

In weight loss experiments, the solutions were composed of salt and acid salt solutions were investigated under isothermal and flow conditions. Fig. 5-1 illustrates the variation of corrosion rate of commercial carbon steel (CS) pipe that expressed in gmd with flow velocity for a 4 h of immersion time in different electrolytic solutions.

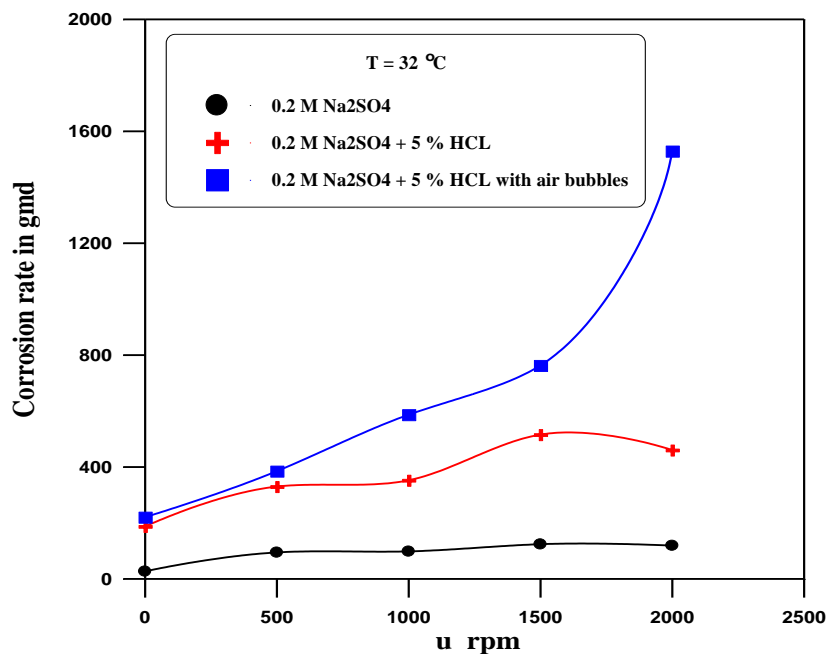


Figure 5-1 Variation of corrosion rate with velocity at 32 °C and 4 h immersion time

From this figure it is clear that increasing the flow velocity leads to an increase in the corrosion rate that represented. This can be attributed to the increase in the concentration of oxygen close to the metal surface by eddy transport. The rate of oxygen reduction reaction is generally limited by the speed at which oxygen can reach the surface of the metal. Previous studies [Foroulis, 1979; Seheers, 1992; Shreir et.al, 2000, Slaiman and Hasan, 2010] indicated that the greater turbulence due to high velocities results in more uniform O_2 concentration near the surface.

Figure 5-1 reveals that the corrosion rate of CS in 0.2 M Na_2SO_4 increased about 340 % when the rotational velocity increased from 0 to 2000 rpm for the other two solutions the increasing was 146 % and 594 % for 0.2M Na_2SO_4 + 5 % HCl and 0.2M Na_2SO_4 + 5 % HCl+ air bubbling respectively.

Previous studies of Alwash et.al [1987] and Turkee [2009] stated that the corrosion rate in aerated acidic solutions increases as the flow increases.

Also according to the observation of the experimental results in Tables 4-2, 4-3 is possible to say that the measured cathodic current is affected by flow and this current can be associated to the H^+ diffusing through the corrosion products layer, where they are reduced to H_2 gas. For that reason, the H^+ reduction is flow dependent [Poulson, 1993; Ross et.al, 1966].

The addition of acid to the salt solution makes the process under mixed control, i.e. mass transfer and activation control, so that the corrosion rate in 0.2M Na_2SO_4 + 5 % HCl was more than in 0.2 M Na_2SO_4 for example, the corrosion rate increase was 621 %, 249 % 259 % 317 %, and 288 % at 0, 500, 1000, 1500, 2000 rpm respectively when acid was added. The increased corrosion rate of iron as pH decreases (i.e. the pH of 0.2 M Na_2SO_4 is 6.74 and it decreases to become -0.6 in 0.2M Na_2SO_4 + 5 % HCl solution) is caused by

increased hydrogen evolution reaction that leads to greater accessibility of oxygen to the metal surface on dissolution of the surface oxide favors oxygen depolarization.

The studied of Osarolube et. al. [2008] stated that the corrosion of mild steels in HCl solutions was attributed to the presence of water, air (oxygen), and H^+ which accelerated the corrosion process.

The addition of air bubbles to 0.2M Na_2SO_4 + 5 % HCl will increase the corrosion rate about 18 % for static condition (0 rpm) and 232 % for 2000 rpm. This is due to increase the solubility of oxygen C_b in the bulk of solution. The increase in C_b is 20 %, 20.3 %, 24 %, 38 %, and 49 % for 0, 500, 1000, 1500, 2000 rpm respectively (as shown in Table 4-7). This leads to a conclusion that increasing velocity leads to an increase in the C_b when pumping the air in the solution because the velocity will increase the turbulence by eddy diffusion and increase the distribution of bubbles within the solution and hence more O_2 transfer to the solution.

5.2 Effect of Velocity and Temperature on Limiting Current Density

Polarization technique was also used to measure the corrosion rate by plotting cathodic polarization curves which obtained from determining the limiting current density (LCD) i_L .

Figure 5-2 shows the effect of velocity on i_L in 0.2M Na_2SO_4 at temperatures of 32, 42, and 52 °C. The values of i_L is obtained from cathodic polarization curve that illustrated in Figs.4-1 to 4-3.

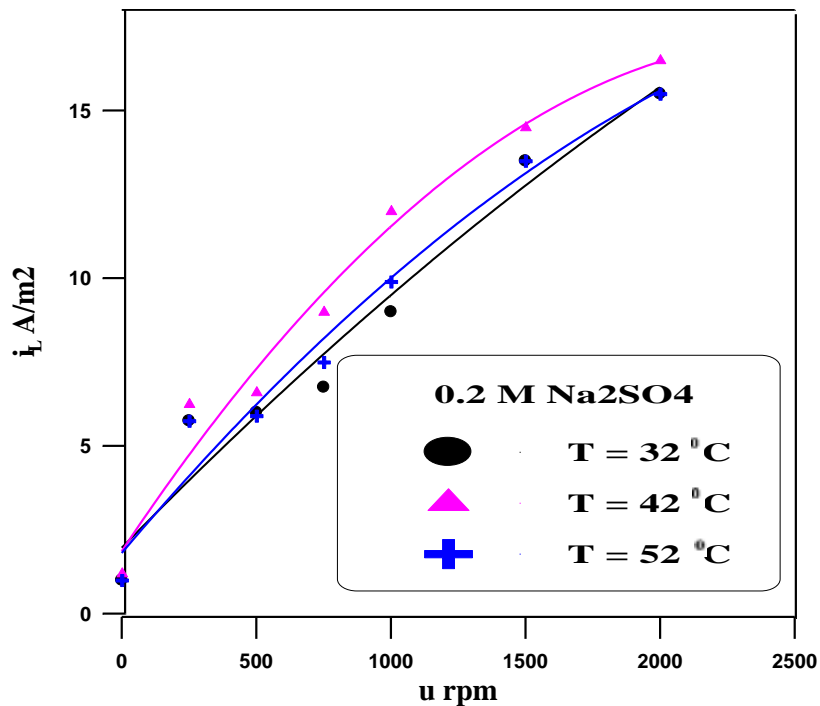


Figure 5-2 Variation velocity and temperature on i_L in 0.2 M Na₂SO₄

It is clear that increasing the velocity leads to an increase in the limiting current. The average increase in the i_L with the velocity for the three temperatures is about 171% for a velocity range from 250 rpm to 2000 rpm. The increase in the i_L is due to the increase in the transport of oxygen to word the metal surface [Foroulis, 1979]. From this figure, it can be seen that the corrosion rate at 42°C is higher than at 32 °C and 52 °C; also, the corrosion rate at 52 °C is higher than at 32 °C. The effect of temperature on the corrosion rate for mass transfer control systems is represented by changing two parameters affecting the corrosion rate in conflicting ways that are the O₂ solubility and diffusivity.

Increasing the temperature will increase the rate of oxygen diffusion to the metal surface by decreasing the viscosity of water and enhancing the corrosion rate. On the other hand, increasing temperature decreases the oxygen solubility the factor that restrains the corrosion [Mahato et.al, 1980].

Figure 5-3 shows the effect of rotational velocity on the limiting current density in presence of air bubbling in 0.2M Na₂SO₄ solution at different temperature.

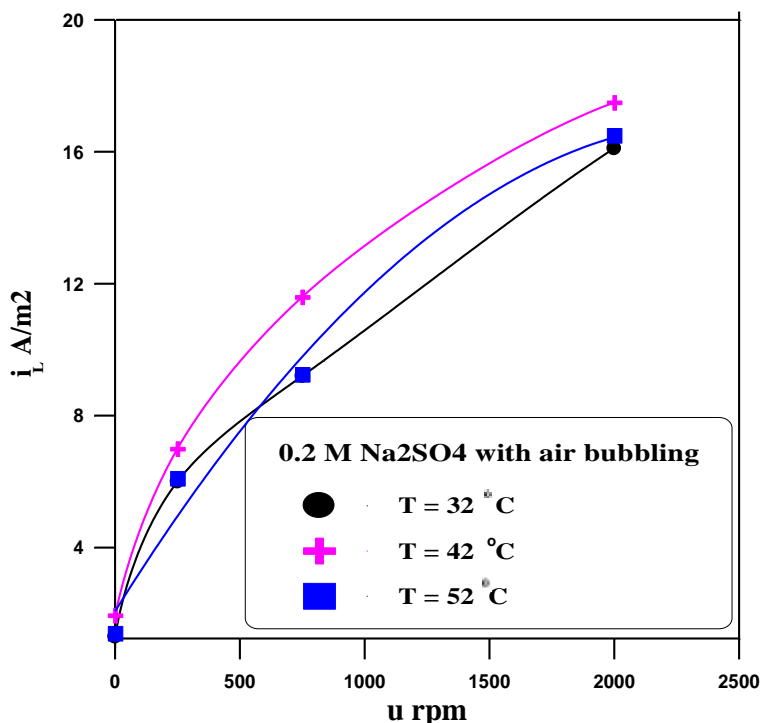


Figure 5-3 Variation of i_L with velocity at different temperatures in 0.2 M Na₂SO₄ with addition of air bubbles.

It is clear that adding air bubbles to the electrolytic solution leads to an increase in the i_L for certain temperature and velocity due to the increased O₂ concentration (as shown in Table 4-5). For mass controlled process, an increase in concentration of the diffusing species in the bulk of the environment increases the concentration gradient at the metal interface. The concentration gradient provides the driving force for the diffusion process. Thus the maximum rate at which oxygen can be diffused to the surface would be essentially directly proportional to the concentration in solution [Stern, 1957]. Comparing the values of i_L in Fig.5-2 (no O₂ bubbling) with this figure indicates that that the increase

in i_L with addition of air bubbles is 30 % for velocity of 0 rpm and 0.625 % for 2000 rpm at 32 °C and 63 % for velocity of 0 rpm, 6 % for 2000 rpm at 42 °C and 40 % for velocity of 0 rpm, 6.5 % for 2000 rpm at 52 °C. The increase in corrosion rate when the velocity increased from 250 rpm to 2000 rpm in presence of air bubbles is 168 % at 32 °C, 150 % at 42 °C, and 154 % at 52 °C.

Figure 5-3 reveals also that, for all velocities, i_L at 42 °C is higher than that at 32 °C and 52 °C for example as temperature increase from 32 to 42 °C the i_L increased by 50 % and about 39 % decrease in i_L when the temperature raised from 42 °C to 52 °C. Also i_L at 52 °C is higher than 32 °C. This behavior of corrosion rates indicates that the combined effect of O₂ solubility and molecular diffusivity is highest at 42 °C followed by 52 °C and 32 °C i.e. at 42 °C the effect of these two parameters on the corrosion rate is maximum.

It is clear that the current reaches the limiting value when the potential approaches the H₂ evolution potential. In addition, the higher the velocity is the higher the i_L will be. It should be noted from Figs. 4-1 to 4-6 that the limiting current density region is not clear for the case of zero rotational velocity (static conditions), where, the polarization curve is not too steep and hence the limiting current cannot be obtained, i.e. the polarization experiments failed to determine the corrosion rate. This behavior can be reasoned to the fact that for stationary conditions the corrosion potential is relatively low, therefore the limiting current occurs near the hydrogen evolution region. Hence, no oxygen limiting current appears due to the generation of other reduction reactions currents such as the hydrogen reduction currents. In such cases, the weight loss method or Tafel extrapolation method can be adopted to measure the corrosion current i_{corr} (i.e. because the process was under diffusion control the i_{corr} will be equal to i_L). The

anodic and cathodic polarization curves for static condition in 0.2 M Na₂SO₄ with and without air bubbling were shown in Appendix C in Figs. C-1 to C-6

Figures 5-4 and 5-5 illustrate the effect of velocity and temperature on the corrosion potential (E_{corr}) in 0.2M Na₂SO₄ with and without air bubbles respectively.

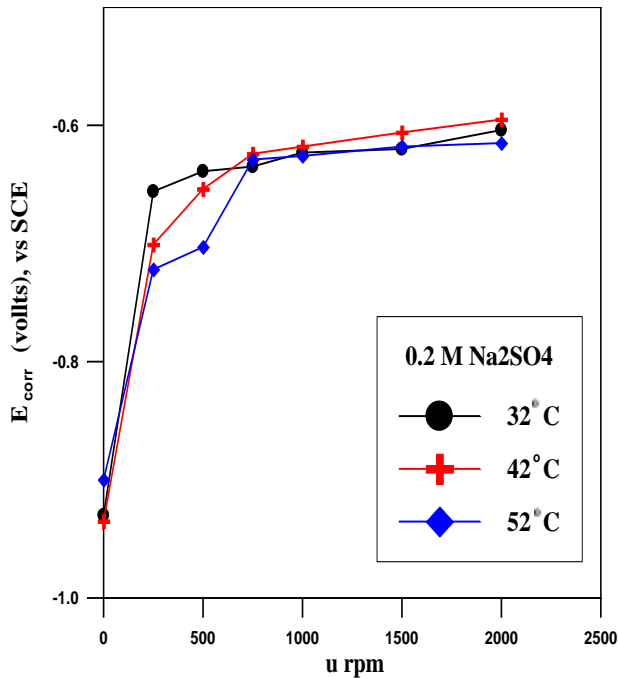


Figure 5-4 E_{corr} vs. u in 0.2 M Na₂SO₄

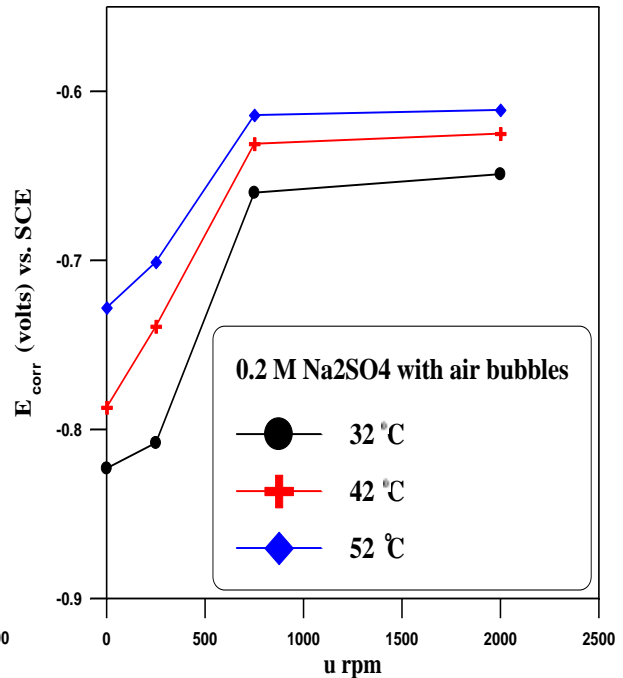


Figure 5-5 E_{corr} vs. u in 0.2 M Na₂SO₄ with air bubbles.

It is clear that corrosion potential is shifted to more positive values with increasing rotation velocity. From Fig. 5-4 it is clear that the effect of temperature on E_{corr} is negligible, while Figure 5-5 indicates considerable increase in E_c with the temperature. This indicates that the high concentration of O₂ leads to an increase in the effect of temperature on E_{corr} . Therefore, the corrosion potential in aerated and oxygen-saturated solutions is flow dependent since the cathodic process, i.e., oxygen reduction reaction, is mass transfer controlled. This behavior is in agreement with previous findings [Hubbard and

Lightfoot, 1966; Nesic et.al, 1995; Chin and Nobe, 1977; Ross et.al, 1996]. Ross et. al. [1996] stated that the increase in E_{corr} with velocity is due to the increase in oxygen transport to the metal surface and when the system is free from oxygen, velocity has no effect on E_{corr} . The corrosion potential decreases with time generally the corrosion potential becomes more negative with time depending on the solutions velocity and temperatures. The variation of E_{corr} with velocity, temperature and time are presented in figures C-7 to C-14 in Appendix C.

5.3 Effect of Corrosion Product Formation on Limiting Current Density (LCD)

In general, as the corrosion proceeds, the process becomes more complex due to building up of corrosion products which restrain the oxygen transport to the surface, growth of the surface roughness which increases the momentum and mass transport between surface and solution, changing physico-chemical properties of the corrosion products; and changing mechanics of flow. The formation of corrosion product layer has a noticeable effect on the corrosion rate of the metal depending on the solution nature and on the temperature and hydrodynamics [Brodkey and Hershey, 1989; Hasan, 2003; Slaiman and Hasan, 2010, Mahato et.al, 1968 b]. Fig. 5-6 illustrates the variation of i_L with time in 0.2 M Na_2SO_4 for 2 h run's time at different temperatures of 32, 42, and 52 °C and constant flow velocity of 250 rpm.

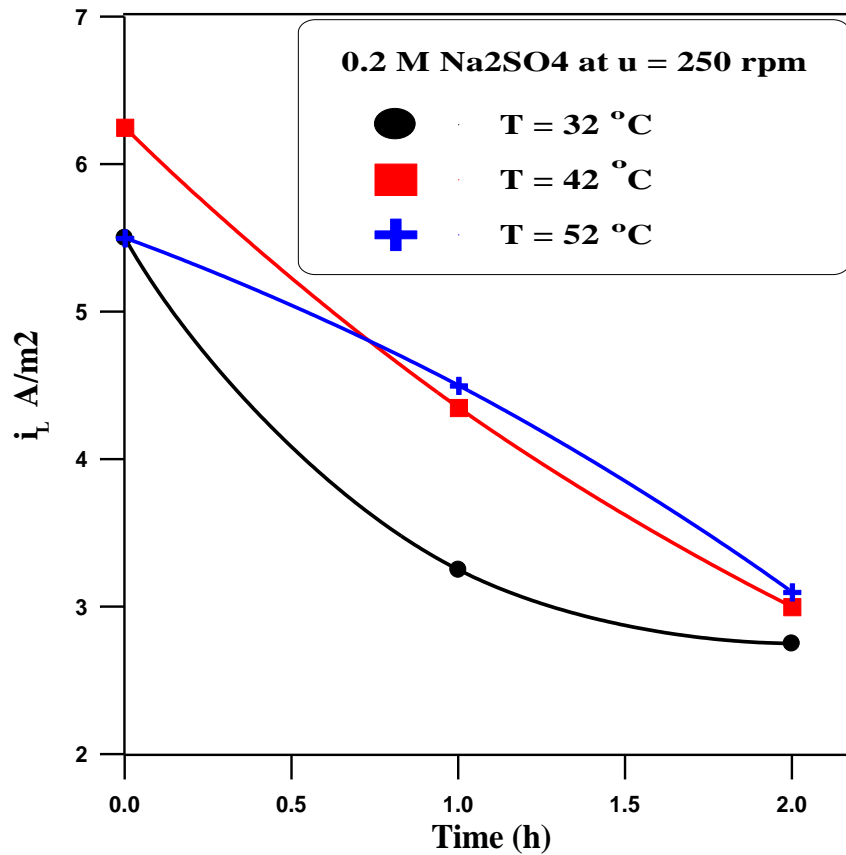


Figure 5-6 Variation of i_L with time in 0.2 M Na₂SO₄ at 250 rpm

The i_L decreases with time due to the continuous growth of the corrosion product layer (fouling layer) which decreases the arrival of O₂ to metal surface and the activity of the surface and hence the corrosion rate [Mahato et.al, 1968 b]. It can be seen from this figure that increasing time results in a decrease in the i_L and this is valid for the three time intervals. The highest decrease in i_L is for temperature of 42 °C. The decrease in i_L for 32 °C and 52 °C is lower which is up to 52 % after 2 h of exposure time for 42 °C and 50 % and 44 % for 32 °C and 52 °C respectively.

When no corrosion products are found i.e. at 0 h, the corrosion rate recorded the highest value at 42 °C, while, the corrosion rates are comparable at 32 °C and 52 °C.

When the layer of corrosion product formed at times of 1 h and 2 h, the value of i_L for 32 °C still lower than values at 42 °C and 52 °C where they are comparable. Also, the rise in temperature contributes to increase the porosity (or decrease the density) of corrosion products layer and that facilitates the passage of O_2 toward the surface [Mahato et.al, 1968a, b; Slaiman and Hasan, 2010]. That is why the effect of corrosion products to decrease the corrosion rate at 32 °C and 42 °C is higher than in 52 °C.

Figure 5-7 shows the variation of i_L with time in 0.2 M Na_2SO_4 at temperature of 32 °C and different velocities, i.e. 250, 1000, and 2000 rpm. Examining this Fig., shows that i_L values decrease with the formation of corrosion products with time for all values of velocity. Also this figure indicates that the i_L has slight decrease with time at low velocity value. But for high velocity the decrease in i_L with time becomes higher at first time interval but after 2 h the decrease is slight. The decreases are 50 %, 42 %, and 56 % in the i_L with time for velocity of 250 rpm, 1000 rpm and 2000 rpm respectively. Hence, the higher the velocity is the higher the decrease in the corrosion rate due to high amount of corrosion products formed which in turn restrains the arrival of dissolved O_2 to the surface. This indicates the important inhibitive effect of this fouling layer to decrease the corrosion.

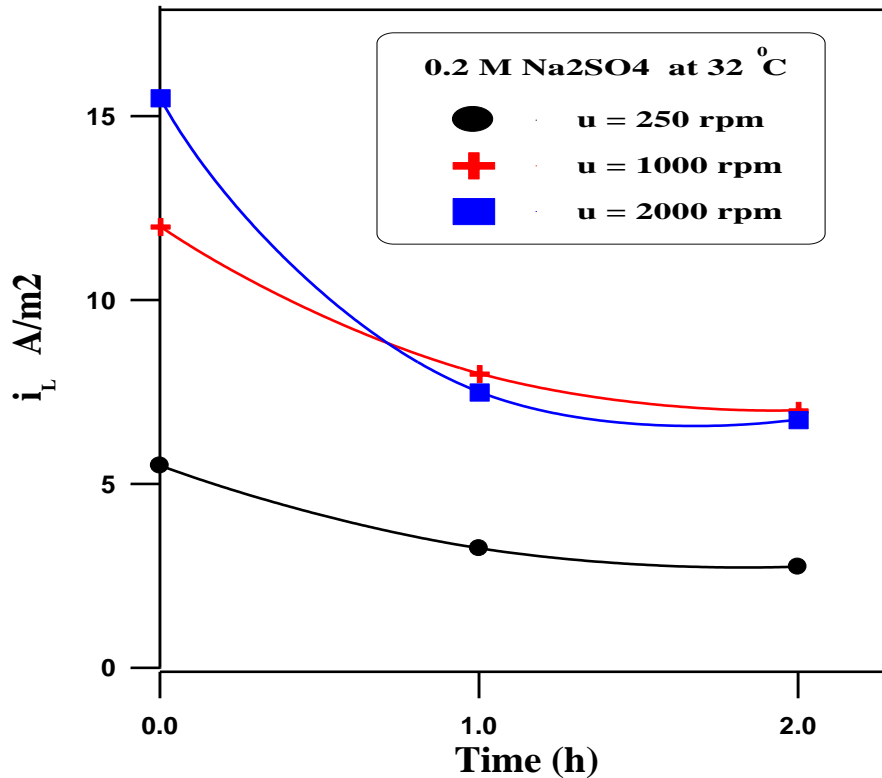


Figure 5-7 Variation of i_L with time at 32 °C and different velocities in 0.2 M Na₂SO₄

These results agree with the studies of Mahato et. al, [1968 a, b; 1980] for pipe flow that have indicated that the corrosion rate always decreases with time. Also, Slaiman and Hasan [2010] for pipe flow noticed that at low temperatures, the formation of corrosion product leads to a decrease in the corrosion rates even at high velocities, but at high temperature and high flow velocities, the formation of corrosion product leads to an increase in the corrosion rate.

Figure 5-8 illustrates the variation of i_L with time in 0.2 M Na₂SO₄ with addition of air bubbles at constant velocity of 250 rpm and different temperatures of 32, 42, 52 °C. It's clear that at time zero, the corrosion rate at 42, 52 °C is higher than at 32 °C. The reason is discussed before. The figure reveals that at 32 °C, i_L decreases with time due to the formation of corrosion product. While for high temperature 42 °C and 52 °C, i_L steeply decreases at first hour then it has

slight decrease with time because of the corrosion rate is higher at first hour than second hour . The highest decrease in i_L was noticed with temperature of 42 °C the decrease of i_L at 32 °C and 52 °C is lower which is up to 50 % after 2 h of exposure time for 42 °C and 29 % and 46 % for 32 °C and 52 °C respectively.

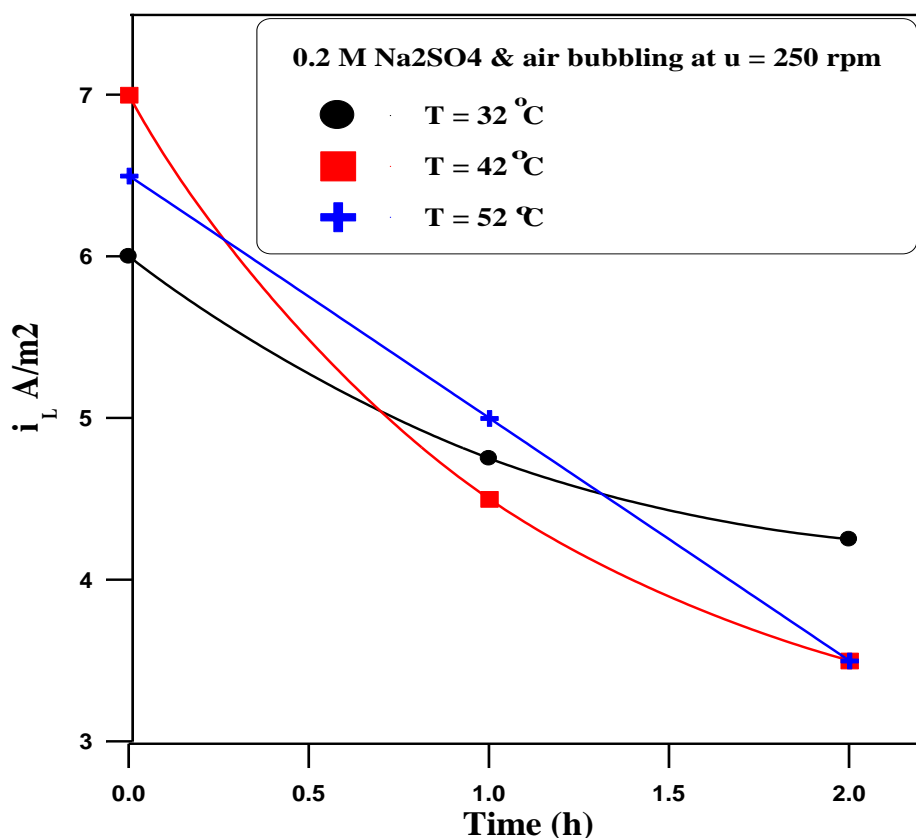


Figure 5-8 Variation of i_L with time in 0.2 M Na₂SO₄ with addition of air bubbles at 250 rpm and different temperatures.

Figure 5-9 shows the effect of time on the i_L at the three velocities of 250, 750, 2000 rpm at temperature of 32 °C in 0.2 M Na₂SO₄ in presence of air bubbles. Figure 5-9 shows the same behavior of i_L with time at different velocities as in Fig. 5-7 but with a significant increase in the limiting current density due to the increase in O₂ concentration accompanying the air bubbling.

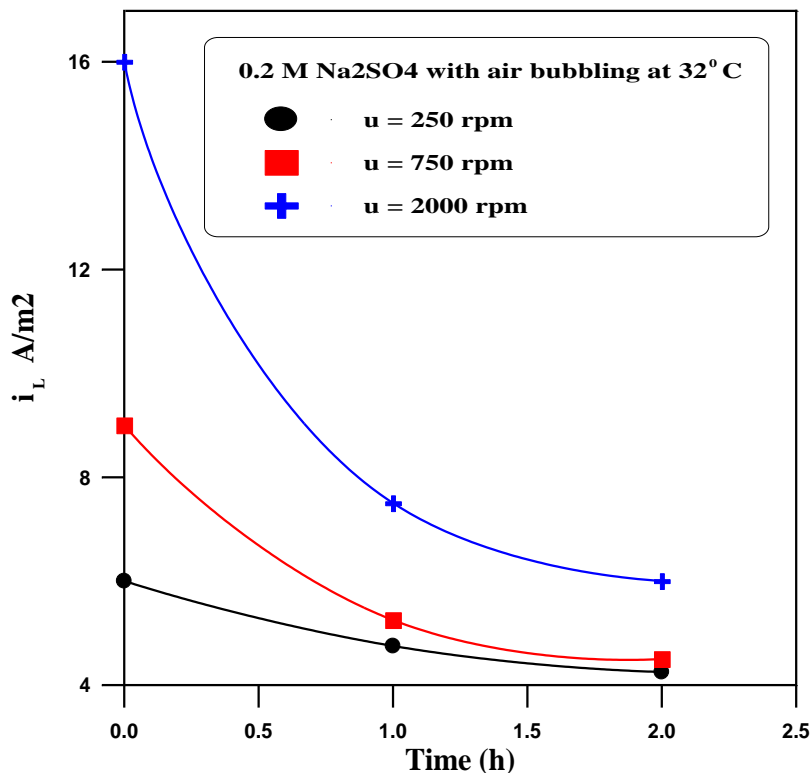


Figure 5-9 Effect of time on the i_L at the three velocities and 32 °C in 0.2 M Na₂SO₄ in presence of air bubbles.

5.4 Effect of Salt Concentration on LCD

Figure 5-10 shows the effect of sodium sulphate concentrations on the i_L at 750 rpm. It is clear that increasing Na₂SO₄ concentration from 0.01 to 0.1 M leads to an increase in i_L from 5.75 to 7.5 A/m² (30 %) at 32 °C, from 9 to 12 A/m² (34 %) at 42 °C, and from 7.75 to 11 A/m² (42 %) at 52 °C. Beyond this concentration, the i_L shows a considerable decrease at all temperatures. This behavior can be attributed to the increased electro-conductivity because of the increased salt content, until the salt concentration is great enough to cause an appreciable decrease in the oxygen solubility, resulting in a decrease in the rate of depolarization. The same trend was noticed in previous works for corrosion in NaCl solution [Revie and Uhlig, 2008]. Peralta et al. [2002] stated that the

mechanism of corrosion attack in sulphate solutions occurring on the surface of the mild steel after a certain exposure as mentioned before in chapter one.

Figure 5-11 shows the experimentally measured electrical conductivity of the solution for different salt concentrations at various temperatures using digital electrical conductivity meter. It is clear that increasing salt concentration leads to an increase in the conductivity of the solution at constant temperature. Also, the conductivity increased with temperature rise.

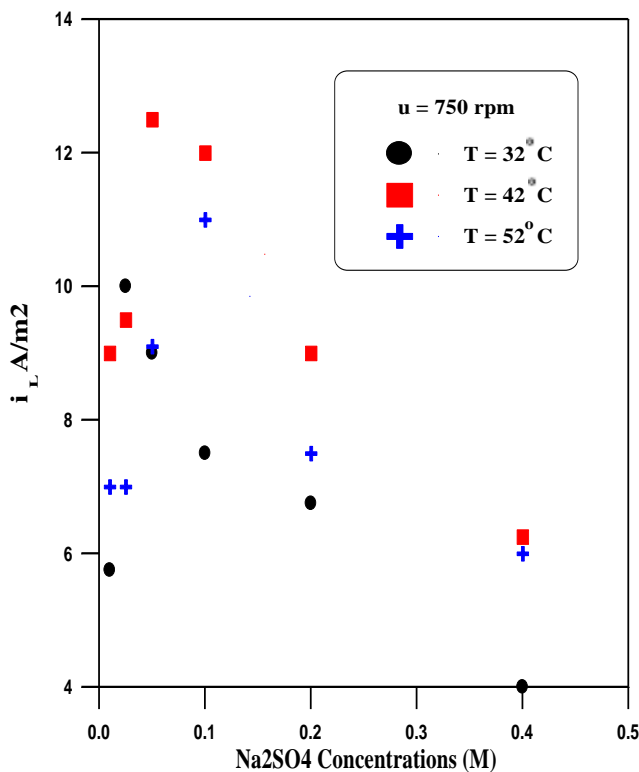


Figure 5-10 Effect of sodium sulphate concentrations on the i_L at 750 rpm

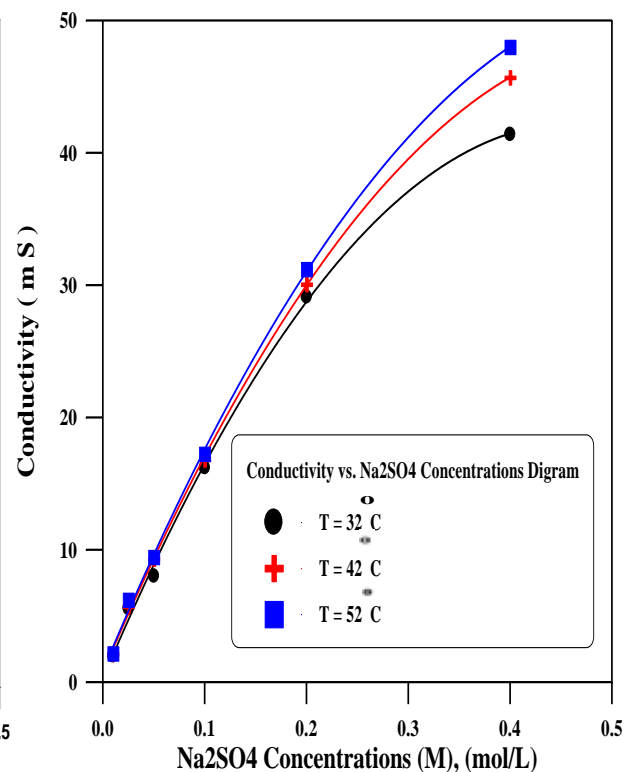


Figure 5-11 Conductivity versus Na₂SO₄ concentrations.

5.5 Comparison of Corrosion Rate in Presence and Absence of Air Bubbling

Figures 5-12 to 5-14 illustrate a comparison of the variation of i_L with time in presence and absence of air bubbling. It is evident that the bubbling has noticeable effect on the corrosion rate (i_L) for all temperatures. The i_L at 32 °C increases with air bubbling from 9 % at time zero to 55 % at time 2 h, while it ranges from 12 % to 17 % for 42 °C and 18 % to 13 % for 52 °C. This indicates that the high temperatures give lower increase in the corrosion rate with addition of air bubbles. The behavior can be interpreted in reference to Tables 4-4 and 4-5 where the increase in O_2 solubility with air bubbling is highest for 42 °C causing highest increase in the corrosion rate. Table 4-4 shows the experimentally measured solubility of oxygen (C_b) in ppm by using oxygen meter at various sodium sulphate concentrations. From the table, it is clear that at a given temperature, increasing the dissolved salt concentration leads to a decrease in the O_2 concentration. Also, the temperature has an effect on the solubility of oxygen at constant salt concentration, that is, increasing the temperature leads to a significant decrease in the O_2 concentration. Table 4-5 shows C_b in 0.2 M Na_2SO_4 solution with air bubbling under different conditions. It is clear that adding air bubbles leads to an increase in the O_2 concentration at constant salt concentration and temperature. However, increasing velocity leads to an increase in the C_b when pumping the air in the solution because the velocity will increase the turbulence by eddy diffusion and increase the distribution of bubbles within the solution and hence more O_2 transfer to the solution. Also increasing the temperature for a constant salt concentration and velocity leads to a decrease in C_b because the escape of O_2 from the solution to atmosphere.

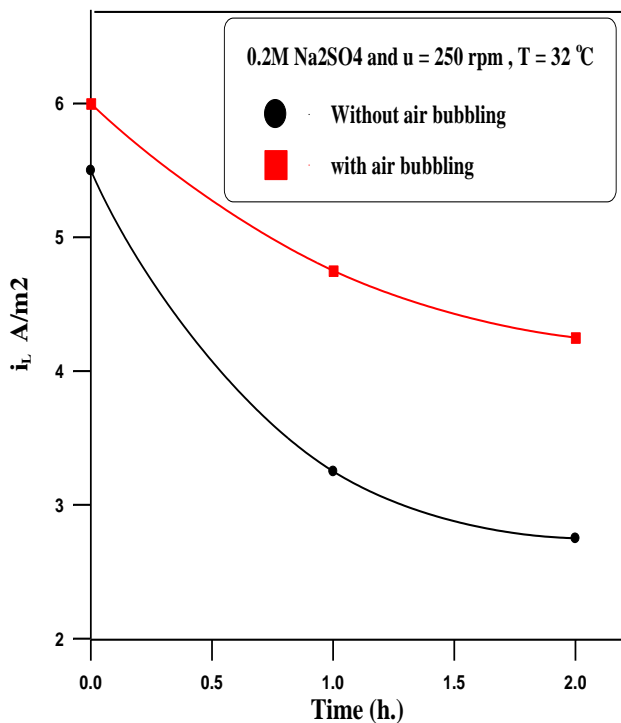


Figure 5-12 i_L vs. time with and without using air bubbles at 32 °C and 250 rpm.

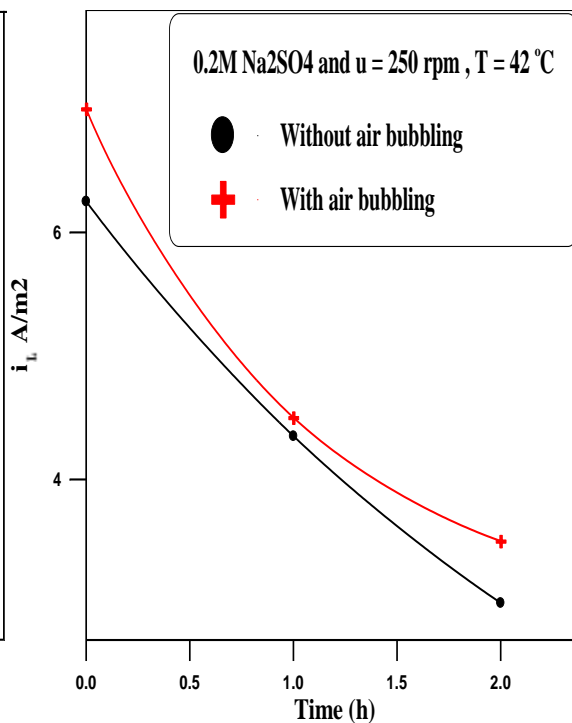


Figure 5-13 i_L vs. time with and without using air bubbles at 42 °C and 250 rpm.

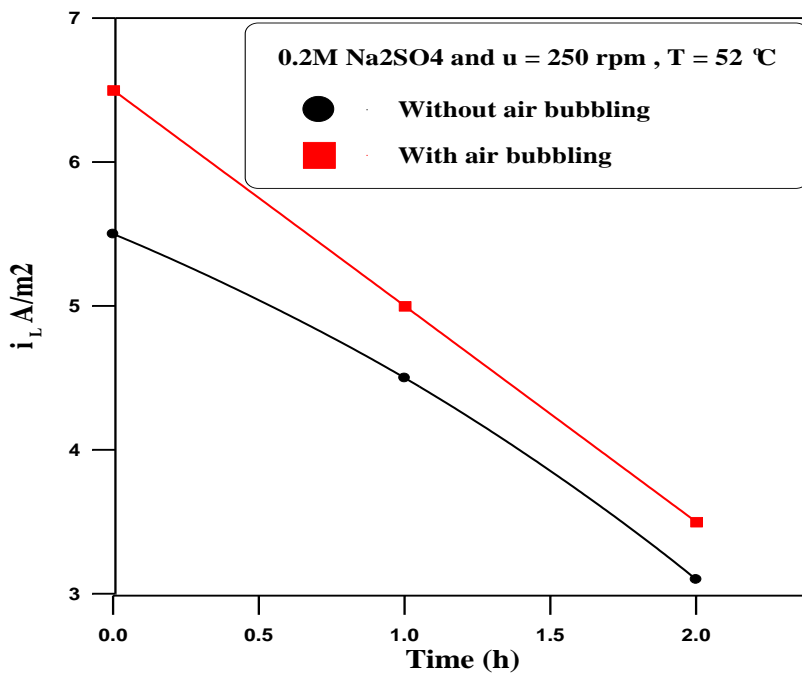


Figure 5-14 i_L vs. time with and without air bubbling at 52 °C and 250 rpm

5.6 Effect of Parameters on Mass Transfer Coefficient (k) and Diffusion Layer Thickness (δ)

Figures 5-15 to 5-30 illustrated the variation of k and δ with velocity, temperature, and time in different solutions. In general from these Figures it is clear that increasing the flow velocities leads to an increase in the mass transfer coefficient k m/s due to increasing the molar flux of oxygen by forced convection mass transport from bulk to the surface. The dependency of k on velocity is high when the corrosion process is under mass transfer control. Many studies [Poulson, 1983; Hasan, 2003; Mahato et.al, 1980; Mahato, 1968a, b] have shown that for such system the corrosion rate obeys the mass transfer theories depending on the geometry and solution nature. Also, these studies revealed that the mass transfer theory can be employed successfully to estimate the corrosion rate. Generally in neutral solutions the cathodic corrosion process is usually the reduction of oxygen. The kinetics of this cathodic process is controlled by the rate at which oxygen can diffuse to the surface of metal, which is slower than the rate of consumption of oxygen by the cathodic reaction. Thus, the rate of this reaction remains constant unless the rate of supply of oxygen to the surface of metal is increased by increasing fluid flow rate.

It is clear that increasing velocity decreases the diffusion layer (δ), The decrease in the thickness of diffusion layer is due to the fact that when velocity increases, the eddy diffusion increases leading to enhance the transport of O_2 from the bulk to the surface and hence the eddies penetrate the diffusion layer decreasing its thickness.

The effect of temperature on the k and δ for mass transfer control systems is represented by changing two parameters affecting the corrosion rate in

conflicting ways that are the O_2 solubility and diffusivity. So increasing temperature has complex trend on k and δ it increases the mass transfer coefficient due to the increase of the diffusivity of certain solution and flow velocity and decrease the diffusion layer due to decrease the oxygen solubility.

It evident that with increasing exposure time leads to a decrease in the mass transfer coefficient at specific temperature and velocity this fact was due to reduce of oxygen transport to electrode surface because of formation and growth of corrosion product layer that lead to increase the resistance to mass transfer [Mahato, 1968a]. Because the corrosion rate decreases with time, δ is increased.

In addition there is considerable increase of k and decrease of δ at certain temperature and velocity in solutions when air is bubbled due to increase the oxygen concentration.

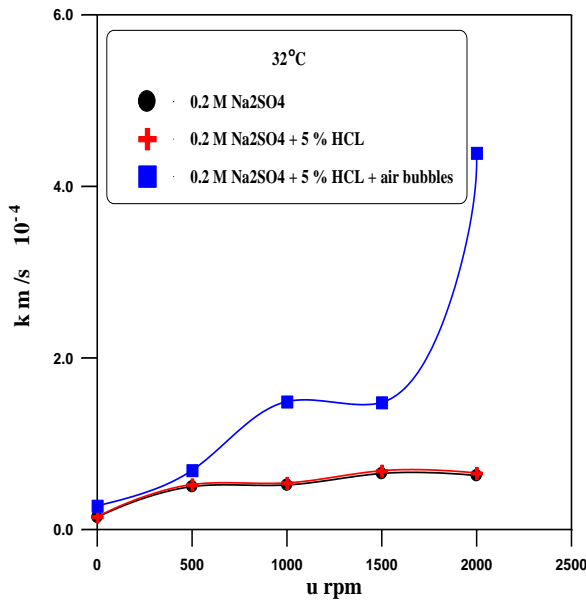


Figure 5-15 Variation of k with u at $32\text{ }^\circ\text{C}$ by using W.L. method

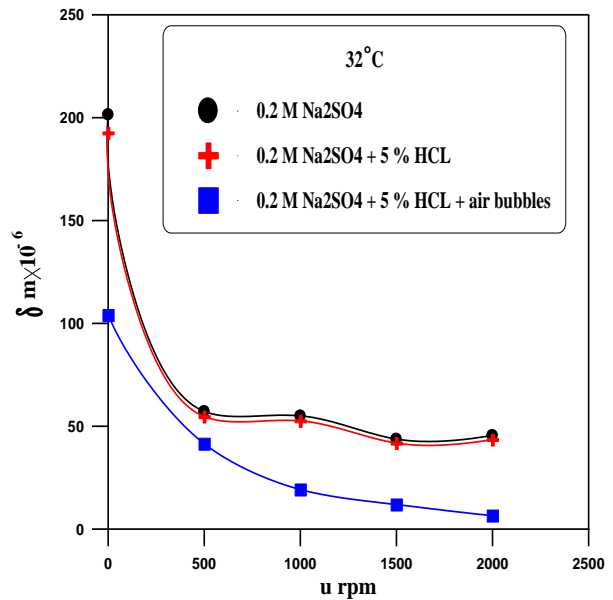


Figure 5-16 Variation of δ with u at $32\text{ }^\circ\text{C}$ by using W.L. method

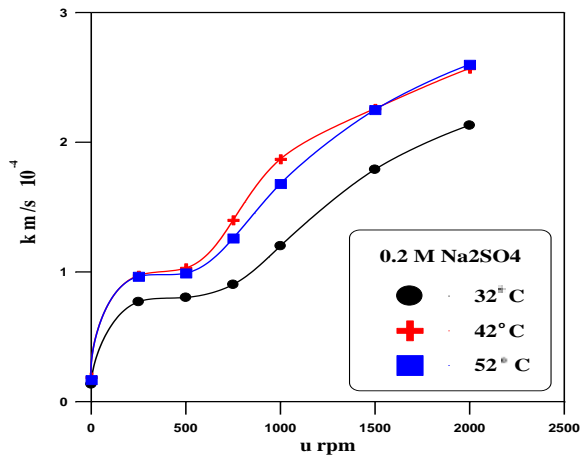


Figure 5-17 Variation of K with u in $0.2 \text{ M Na}_2\text{SO}_4$

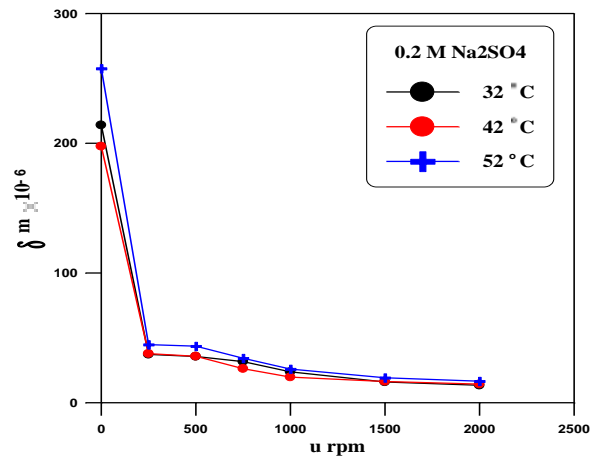


Figure 5-18 Variation of δ with u in $0.2 \text{ M Na}_2\text{SO}_4$

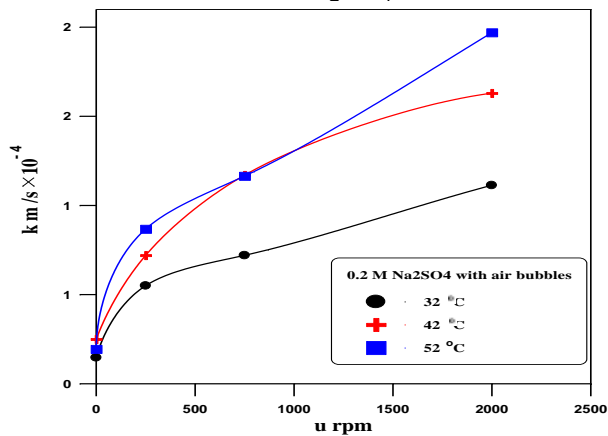


Figure 5-19 Variation of K with u in $0.2 \text{ M Na}_2\text{SO}_4$ with air bubbles

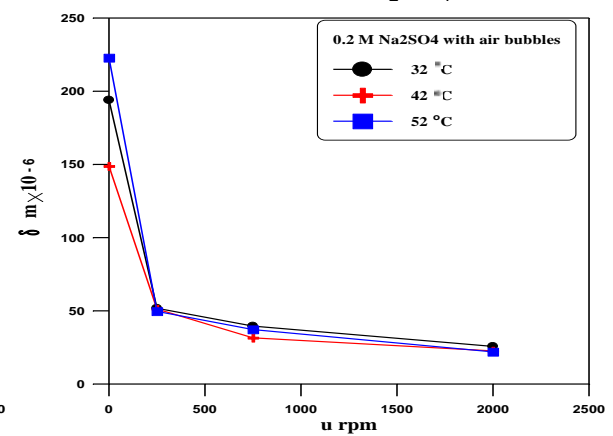


Figure 5-20 Variation of δ with u in $0.2 \text{ M Na}_2\text{SO}_4$ with air bubbles

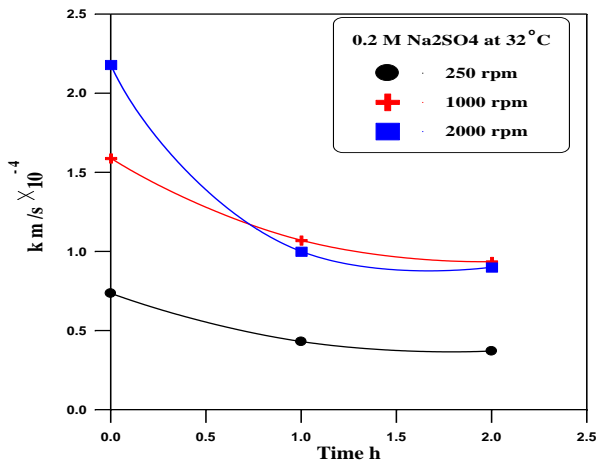


Figure 5-21 Variation of K with t at 32°C

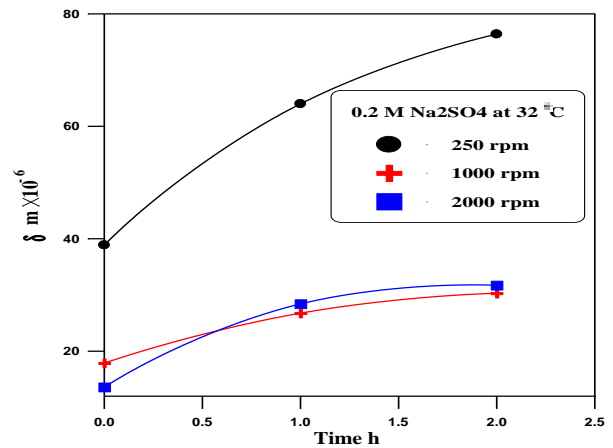


Figure 5-22 Variation of δ with t at 32°C

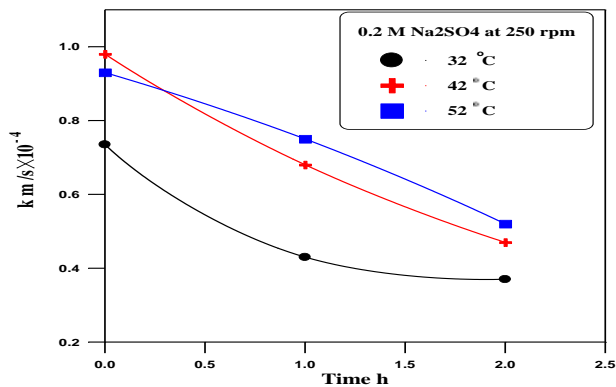


Figure 5-23 Variation of K with t at 250 rpm

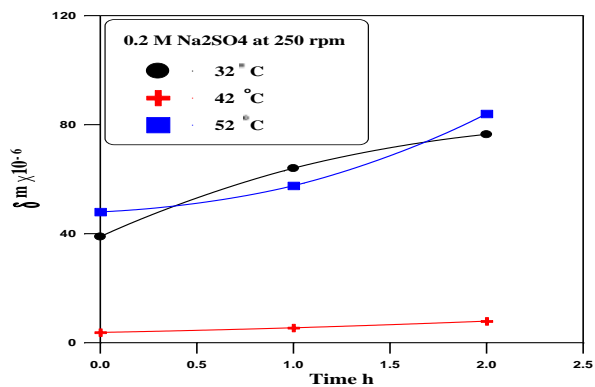


Figure 5-24 Variation of δ with t at 250 rpm

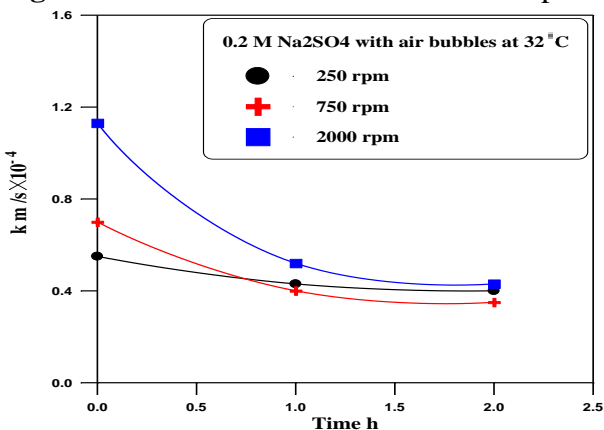


Figure 5-25 Variation of K with t at 250 rpm in 0.2 M Na_2SO_4 with air bubbles

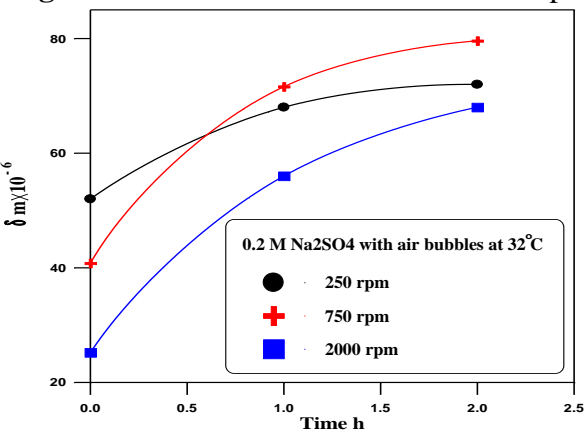


Figure 5-26 Variation of δ with t at 250 rpm in 0.2 M Na_2SO_4 with air bubbles

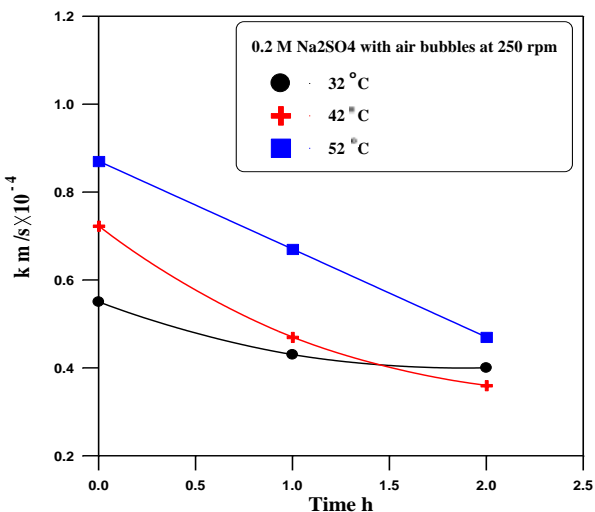


Figure 5-27 Variation of K with t at 32 °C in 0.2 M Na_2SO_4 with air bubbles

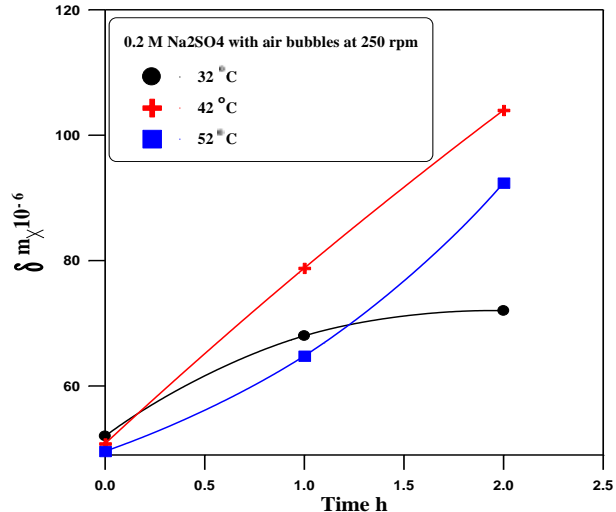


Figure 5-28 Variation of δ with t at 32 °C in 0.2 M Na_2SO_4 with air bubbles

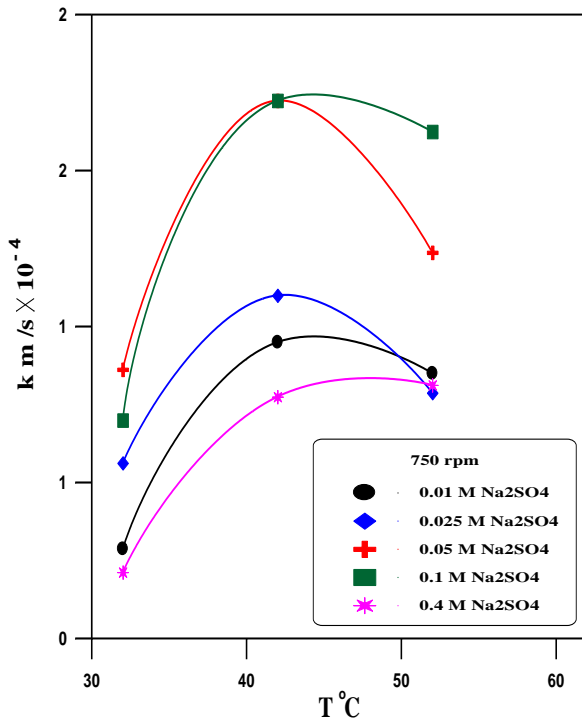


Figure 5-29 Variation of K with T at different salt concentration

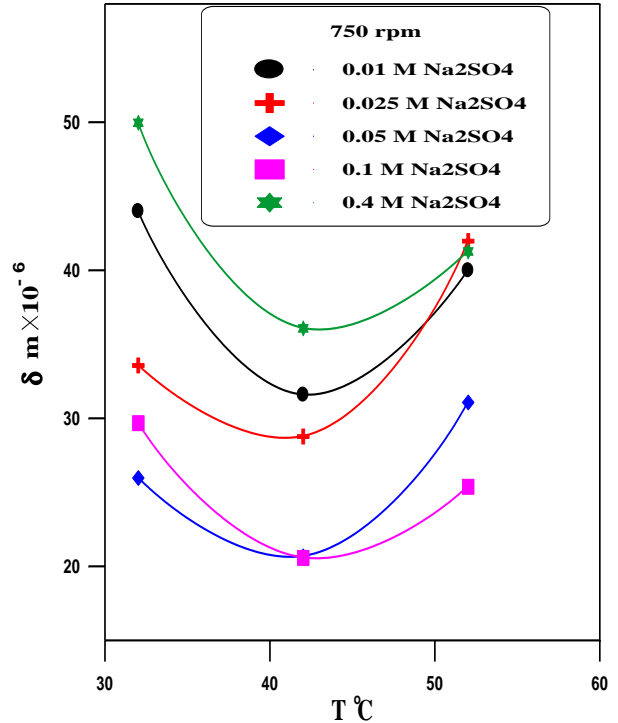


Figure 5-30 Variation of δ with T at different salt concentration

Using statistical analysis (User-specified regression) for the results of polarization the following correlation is obtained for the whole range of velocity, temperatures, salt concentration, and immersion time.

$$CR = 1.200104 \times u^{0.506106} \times T^{0.296961} \times t^{-0.206527} \times C_{salt}^{0.02493} \times C_b^{0.180802} \quad (6.1)$$

Where: CR in gmd ($\text{g}/\text{m}^2 \cdot \text{day}$), u in rpm, T in $^{\circ}\text{C}$, t in h., C_{salt} is salt concentration in M (mole/L), C_b in ppm (mg/L). This equation with coefficient of determination (R^2) of 92.670 % and mean errors of 20 %

In general, this empirical equation indicates that increasing the flow velocity, temperature, salt concentration, and oxygen concentration (C_b) leads to an increase in the corrosion rate of carbon steel pipes. The flow velocity gives

highest dependence of 0.506 [Mahato 1968 b]. Because the system was under diffusion (mass transfer) control, so the velocity has great effect on the corrosion rate. The dependence of time is -0.206. This means that the time has negative effect on the corrosion rate, i.e. it decreases the corrosion rate where the previous studies [Mahato et al., 1968a, b, 1980] indicated that the corrosion rate always decreases with time. The corrosion rate had unstable trend with the salt concentrations so that C_{salt} having scarce increasing effect on the corrosion rate with dependence of 0.024 that represented the mean value for the range of salt concentration used. The dependence of temperature is 0.2969 [Hasan, 2011; Poulson, 1983] which means that temperature have increasing effect on the corrosion rate depending on diffusivity and solubility.

5.7 Acid-Salt Solution

5.7.1 Effect of Velocity on Corrosion Current (i_{corr})

Figure 5-31 illustrated the variation of velocity with corrosion current in acid salt solution mixture consist of 0.01M Na_2SO_4 + 1% HCl at constant temperature of 32 °C. It is clear that increasing the flow velocity from 0 to 2000 rpm lead to increase the i_{corr} increase about 525 %. This increasing was due to increase the oxygen transport to metal surface with increase the flow velocity. This agrees with previous studied that found increases the corrosion rate of iron in oxygen saturated acid solutions, with increasing velocity of the solution [Ross et.al, 1966]. However, it is well known that, in the presence of oxygen in acid solutions, two cathodic reactions take place which are hydrogen evolution reaction (HER) and oxygen reduction reaction. The first reaction, i.e., HER, is an activation controlled process. It was stated earlier, that oxygen transfer to the

cathodic area is often rate controlling, i.e., a mass transfer controlled process. Therefore, the effect of flow on the limiting current density of the oxygen reduction reaction in acid solutions is to increase i_L as the flow increases [Alwash et.al, 1987]. Corrosion current show high increase in its value in salt acid solution when comparing with solution containing salt only for example i_{corr} increased about 491 % when comparing 0.01M Na_2SO_4 with 0.01M Na_2SO_4 +1 % HCl at 750 rpm.

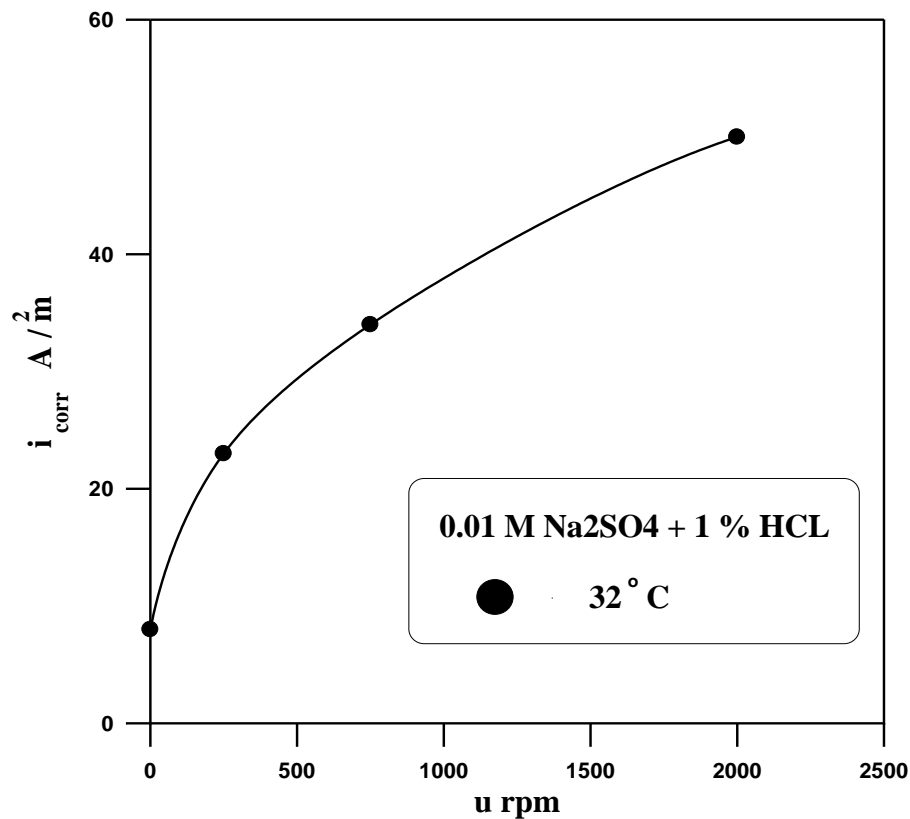


Figure 5-31 Variation of i_{corr} with velocity at 32 °C in 0.01M Na_2SO_4 +1 % HCl

Figure 5-32 shows the variation of i_{corr} with velocity at 32 °C in 0.2 M Na_2SO_4 +1 % HCl with addition of air bubbles and in 0.2 M Na_2SO_4 with addition of air bubbles.

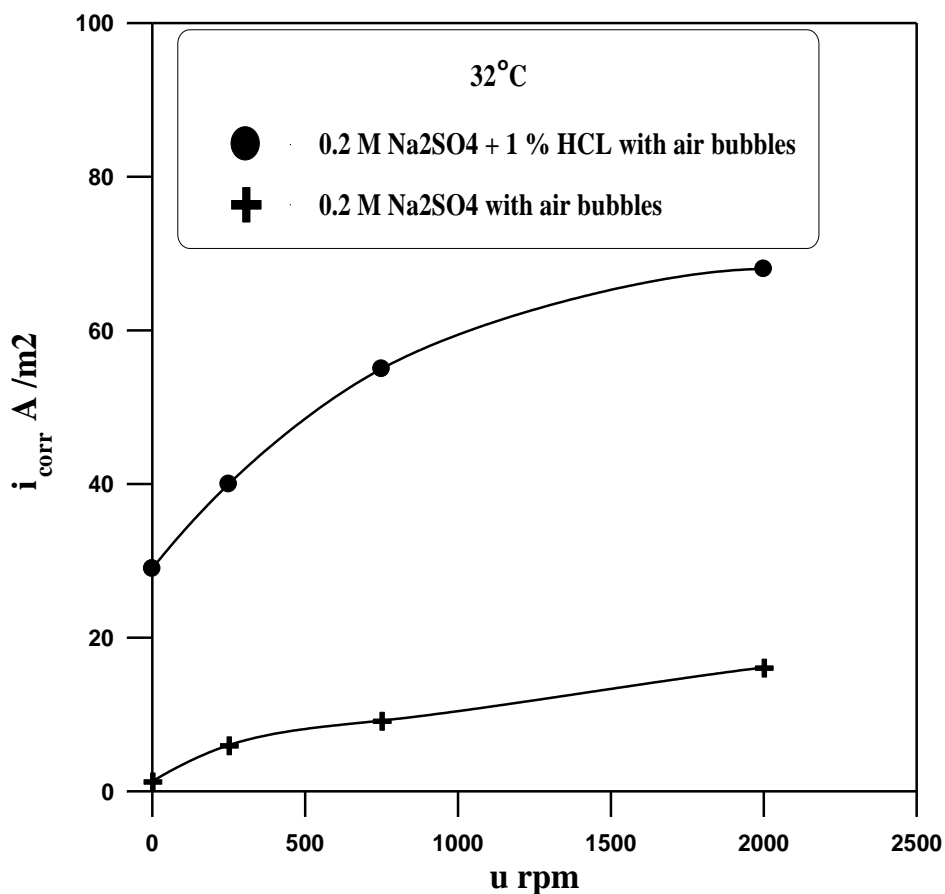


Figure 5-32 Variation of i_{corr} with velocity at 32 °C in 0.2 M Na₂SO₄ +1 % HCl and in 0.2 M Na₂SO₄ both with addition of air bubbles.

It is clear that addition of acid to the solution lead to increase the corrosion current about 879 % as average for the studied velocity range. Also it is notice that the corrosion current increased about 134 % as the velocity increase from 0 to 2000 rpm for acid solution i.e. in 0.2 M Na₂SO₄ +1 % HCl with addition of air bubbles. These air bubbles lead to increase the corrosion current due to increase the solubility of oxygen about 32 % as average for example i_{corr} at velocity of 250 rpm increased about 43 % when air was bubbled in 0.2 M Na₂SO₄ +1 % HCl.

5.7.2 Effect of Temperature and Concentration

Figures 5-33 and 5-34 illustrate the variation of corrosion current i_{corr} with temperature in different acid salt solution mixtures at constant velocity of 250 rpm. It is clear that increasing the temperature leads to an increase in the i_{corr} . This is true for all range of solution concentrations that have been investigated. An increase in temperature of oxygen saturated acid solutions can affect the corrosion behavior of materials in different ways: (i) The rate of chemical reaction is increased with temperature. This issue is here very effective because the system was under activation control because of the presence of acid [Khadom et.al, 2009], (ii) The solubility of some of the reaction products may change resulting in different corrosion reaction products,(iii) The solubility of gases in solution is decreased because the system is open leading to a decrease in the CR [Fontana, 1986; Revie and Uhlig, 2008], (iiii) Viscosity is decreased leading to an increase in the diffusion coefficient [Bird et.al, 2002; Brodkey and Hershey 1989] .

In general, as temperature rises, diffusion increases, and both overvoltage and viscosity decrease. Increased diffusion enables more dissolved oxygen to reach a cathodic surface, thereby depolarizing the corrosion cell. Overvoltage decreases causing depolarization by hydrogen evolution. A decrease in viscosity aids both depolarization mechanisms because it favors solution of atmospheric oxygen and enhances hydrogen evolution. In general if the diffusion rates are doubled for certain increase in temperature, activation process may be increased by 10 - 100 times depending on the magnitude of activation energy [Shreir et.al, 2000; Yaro et. al, 2010]. In Fig.5-33 increasing the temperature from 32 to 52 °C leads to increase i_c about 400 %, 82 % and 75 % in 0.01 M Na_2SO_4 + 1 % HCl, 0.05 M Na_2SO_4 + 1 % HCl, and 0.2 M Na_2SO_4 + 1 % HCl respectively. While in

Fig.5-34 the increase is 100 %, 75 %, and 65 % in 0.2 M Na₂SO₄ + 0.5 % HCl, 0.2 M Na₂SO₄ + 1 % HCl, 0.2 M Na₂SO₄ + 3 % HCl.

Also from Fig. 5-33 it can be noticed the same behavior of salt as before in section 5-4 where the increase in i_{corr} with increased salt content from 0.01 to 0.05 M at constant acid concentration (1%) then the decrease in 0.2 M Na₂SO₄ + 1 % HCl still higher than the values of i_{corr} in 0.01 M Na₂SO₄ + 1 % HCl. This is true for all range of temperature.

From Fig. 5-34 it is evident that increasing acid concentration leads to an increase in the corrosion current for all temperatures. This observation is attributable to the fact that the corrosion reaction like almost all chemical reactions, normally as the concentration of corrosive acid media is increased the corrosion rate likewise increases. This primarily due to the fact that the amounts of hydrogen ions, which are the active species, are increased as acid concentration is increased. This agree with the studied of Ita and Offiong, [1997]; Onuchukwu and Trasatti, [1994]. Also it was found that the at low pH values the evolution of hydrogen tends to eliminate the possibility of protective films formation so that steel continues to corrode [Noor et.al, 2008]. The increase in i_{corr} was 70 % (for 32 °C), 45 % (for 42 °C), and 40 % (for 52 °C) for increasing the acid solution from 0.5 % to 3 % with addition of constant amount of salt (i.e. 0.2 M Na₂SO₄).

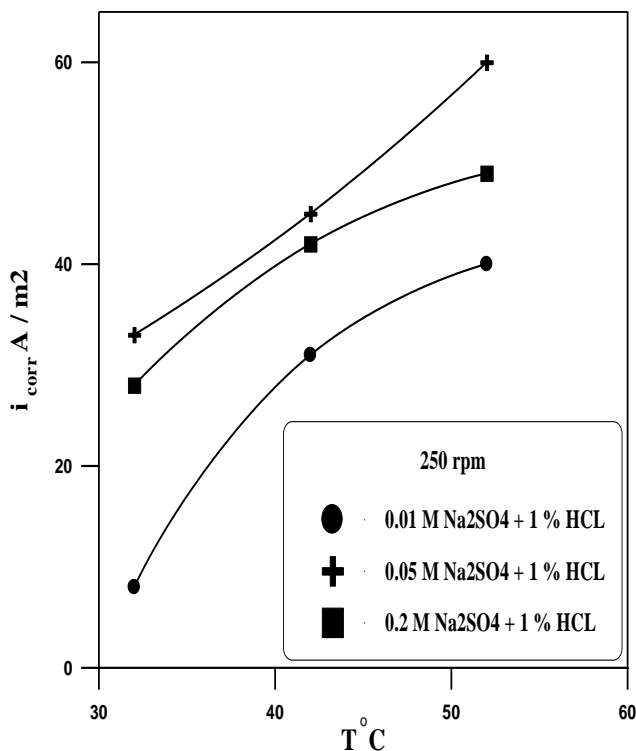


Figure 5-33 Variation of i_{corr} with T at 250 rpm in 1% HCl with different salt concentrations

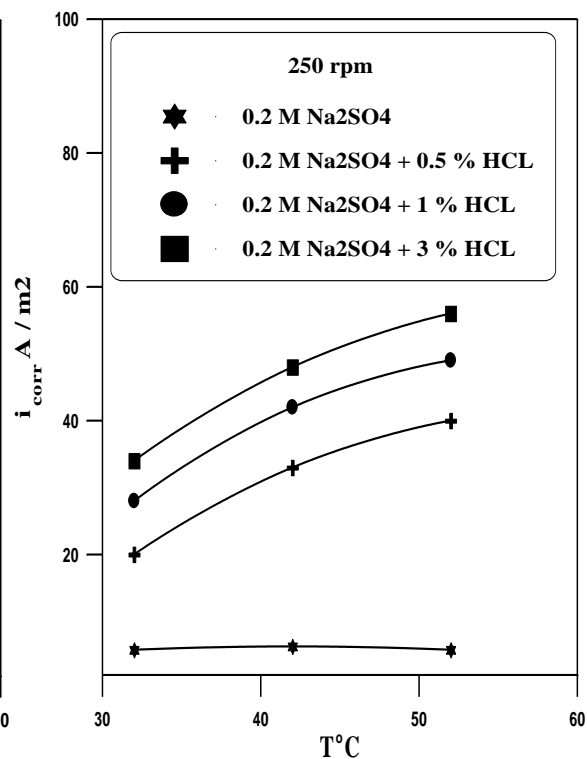


Figure 5-34 Variation of i_{corr} with T in 0.2 M Na₂SO₄ with different acid concentrations at 250 rpm

Figure 5-35 illustrated the variation of i_{corr} with temperature at 250 rpm in 0.2 M Na₂SO₄ + 1% HCl with and without addition of air bubbles. It is clear that increasing the temperature leads to increase the i_{corr} for both solutions. The increase is about 73 % and 75 % for 0.2 M Na₂SO₄ + 1% HCl with and without addition of air bubbles respectively. Also it can be noticed that addition of air bubbles leads to an increase in the corrosion current by about 43 %, 38 %, and 41 % for temperatures of 32, 42, and 52 °C. This is due to an increase in the oxygen concentration in the solution by about 29 %, 32 %, and 34 % for temperatures of 32, 42, and 52 °C respectively as shown in Table 4-8.

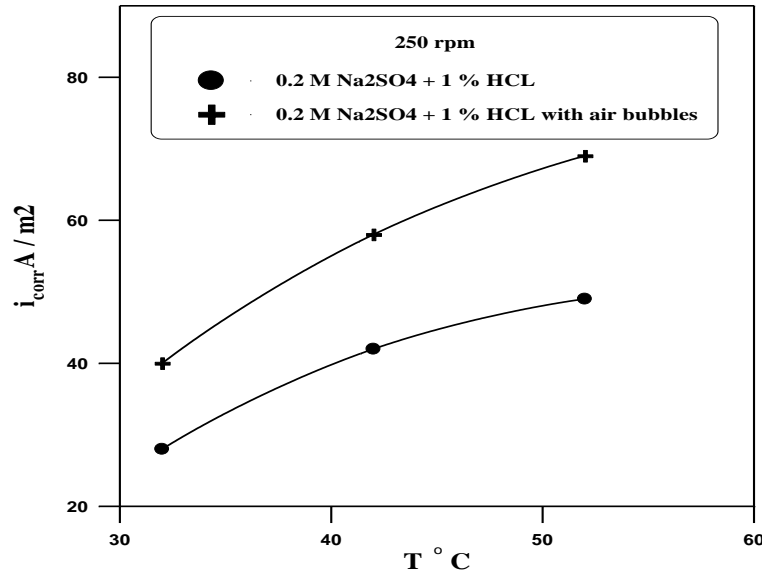


Figure 5-35 Variation of i_{corr} with T at 250 rpm in 0.2 M Na_2SO_4 + 1% HCL with and without addition of air bubbles.

Also it is noticed that the corrosion potential E_{corr} increased with increasing velocity and temperature as shown in Appendix C in Figures C-12 to C-14.

Using statistical analysis the following correlation in acidic salt solutions mixture is obtained for the whole range of velocity, temperature, salt concentration, and acid concentration.

$$CR = 0.162482 \times u^{0.216304} \times T^{1.562532} \times C_{\text{salt}}^{0.079978} \times C_b^{1.08665} \times C_H^{0.208651} \quad (6.2)$$

With coefficient of determination (R^2) of 85.349 % and mean error of 14 %, where C_H is acid concentration (i.e. hydrogen concentration) in M (mole / L). Because the process under activation control, the temperature has greater effect on corrosion rate and higher dependence (1.562532) [Shreir et.al, 2000; Yaro et. al, 2010; Osarolube et.al, 2008, Popova 2007]. By comparing Eq.(6.1) with

Eq.(6.2), it can be noticed that the temperature dependence in Eq.(6.2) is higher than that in Eq.(6.1) while velocity dependence in Eq.(6.1) is higher than that in Eq.(6.2). this means that in acid solutions the temperature is most important factor effect corrosion rate while in salt solutions (diffusion control process) velocity is the most important factor [Shreir et.al, 2000]. According to the dependences increasing the oxygen solubility, salt concentration, and acid concentration leads to increase the corrosion as discussed previously. Also the dependence of C_b in Eq.(6.2) is higher than that in Eq.(6.1) indicating that the effect of O_2 concentration on the corrosion rate is higher in case of acids.

In general corrosion rates obtained from polarization measurement are in good agreement with the weight loss measurements. The corrosion rates in both methods shows that increase the flow velocity leads to increase the corrosion rate. Also the data obtained from weight loss measurements are lower than that obtained via polarization technique for clean surface because of the effect of time.

5.8 Addition of Inhibitors

The effect of inhibitor was investigated in solution of 0.1 M Na_2SO_4 + 1% HCl with addition of different amounts of indole in concentrations of 1.7×10^{-3} M and 3.4×10^{-3} M (200 ppm and 400 ppm). Also addition of 2.74×10^{-3} M (1000 ppm) cetyl trimethyl ammonium bromides inhibitor (CTAB) under different solution temperature of 32, 42, and 52 °C and velocities of 0, 250, 750, 1000, 2000 rpm. By using weight loss method for 2 h immersion time.

5.8.1 Indole

5.8.1.1 Effect of Velocity on IE

Figure 5-36 shows the variation of corrosion rate with velocity at constant temperature of 32 °C in 0.1 M Na₂SO₄ + 1% HCl with and without addition of 1.7×10⁻³ M and 3.4 ×10⁻³ M (200 ppm and 400 ppm) indole.

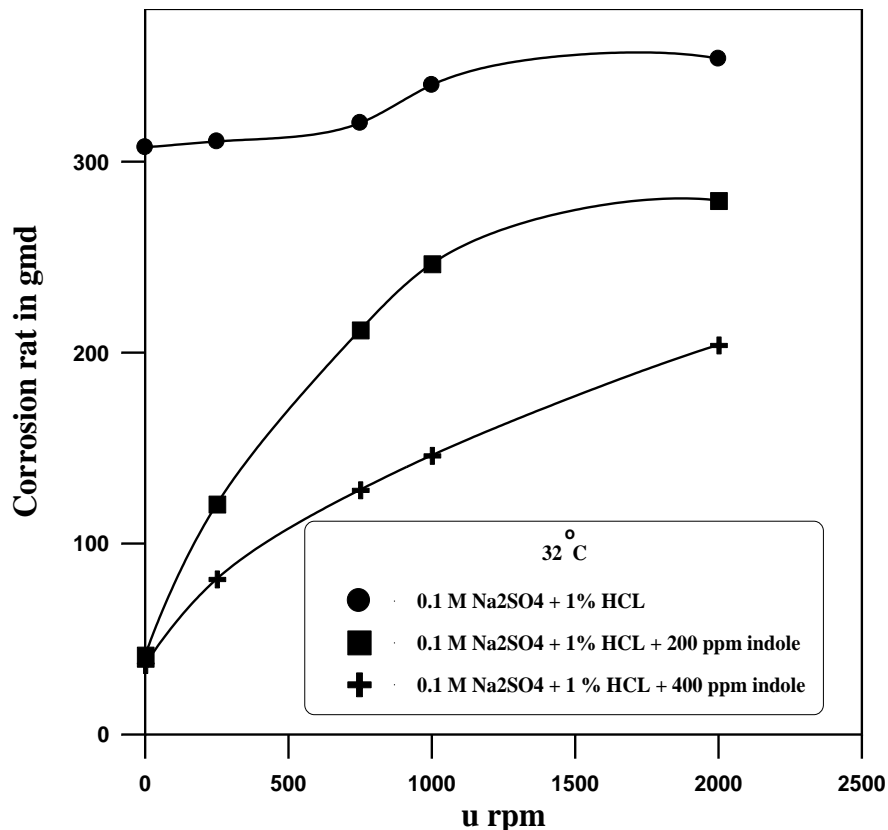


Figure 5-36 Variation of CR with velocity in presence of indole.

It is clear from these figures that increasing the velocity leads to an increase the corrosion rate (gmd) for all solutions (i.e. with and without addition of indole inhibitor). The increase is 151% in 0.1 M Na₂SO₄ + 1% HCl for velocity increase from 0 to 2000 rpm, 456 % with addition of 3.4 ×10⁻³ M (400 ppm) indole for velocity increase from 0 to 2000 rpm, and 573 % with addition 1.7×10⁻³ M (200 ppm) indole for velocity increase from 0 to 2000 rpm.

Figure 5-37 illustrates the variation of inhibition efficiency with u at 32 °C.

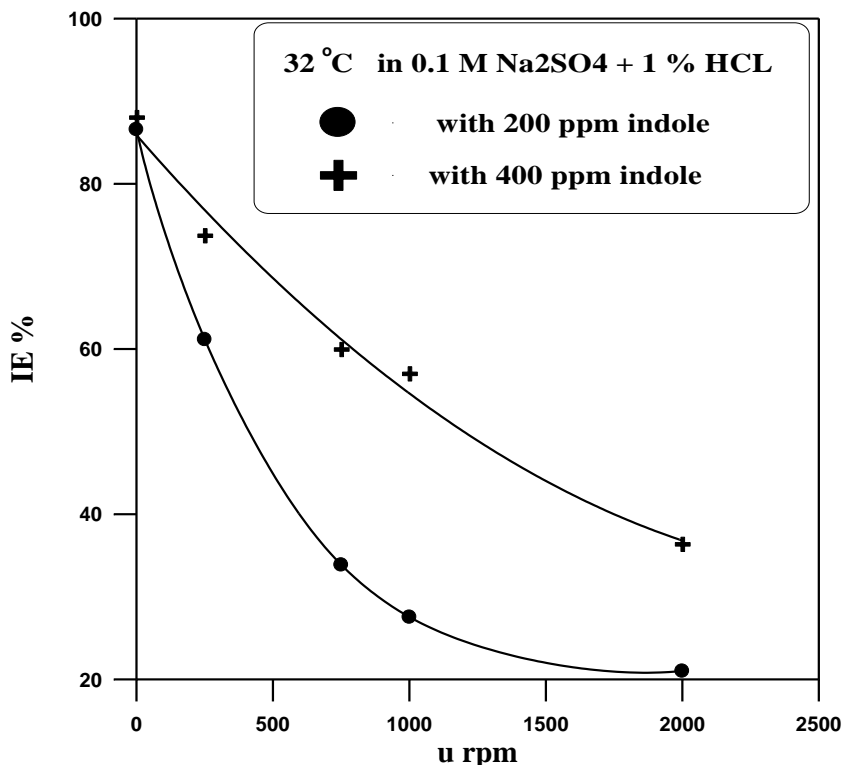


Figure 5-37 Variation of IE % with u at 32 °C

It is clear that increasing the inhibitor concentration leads to an increase in the inhibition efficiency at constant velocity and temperature. For example, as indole concentration increased from 1.7×10^{-3} M to 3.4×10^{-3} M (200 to 400 ppm) in the solution the inhibition efficiency increased from 86.589 % to 88.08 %, 61.15 % to 73.77 %, 33.86 % to 60 %, 27.54 % to 57.04 % and from 21.01 % to 36.41 % for velocity of 0, 250, 750, 1000, and 2000 rpm respectively. The previous studies of Ismail et.al [2000]; El Maghraby and Soror [2010a, b]; Mobin et.al [2011] agree with this results which stated that increasing inhibitor concentration leads to increase inhibition efficiency.

Also it is clear that increasing u from 0 to 2000 rpm leads to a considerable decrease in the IE by 76 % in 1.7×10^{-3} M (200 ppm) indole and about 59 % in 3.4×10^{-3} M (400 ppm) indole for u range from 0 to 2000 rpm. The

hydrodynamic factor had two opposite effects on inhibition performances. On the one hand, it increased mass transport of inhibitor molecules to the electrode surface which was beneficial to improving inhibition efficiency. On the other hand, high shear stress resulted from high flow velocity would also remove inhibitor films from metal surface which was harmful to inhibition efficiency [Slaiman et. al., 2008; Musa et.al, 2009; Musa et.al, 2010; Ortega-Toledo et.al, 2011]. The highest IE is at zero velocity and it is about 86.589 % and 88.08 % for 1.7×10^{-3} M and 3.4×10^{-3} M (200 and 400 ppm) indole respectively. The very good inhibiting properties of indole, especially in HCl, can be explained by the substance polymerization in an acidic medium forming intermediate cation. The adsorbed inhibitor molecules and/or ions block significantly some of the active sites on the metal surface, which is energetically inhomogeneous [Popova, 2007]. The chemical structure of indole that formed from addition of benzene ring to pyrrole this addition had much influence on the inhibiting properties of indole. The increase in inhibition efficiency of inhibitor was due to the mobile electrons in benzene ring that can interact with d-orbital of Fe atoms of metal surface [Sanad et.al, 2000].

The best inhibitive properties of indole could be due to similar processes if one supposes that the dimers block more efficiently the metal surface. The presence of a lone electron pair is necessary for appearance of inhibitive properties, because it acts as a reaction centre of the molecule for the adsorption. The aromatic π -electron system facilitates the planar orientation of the molecule in the adsorption state. Also the adsorption of indole in the presence of SO_4^{-2} is lower than in the medium containing Cl^- , which is justified by the indole action as a weak acid, because it has only a single pair of electrons, which is displaced and takes part in the π -electron aromatic system [Popova et.al, 2007].

5.8.1.2 Effect of Temperature on IE

From Table 4-11 it is evident that increasing the temperature leads to an increase in the corrosion rate for uninhibited solution. Fig. 5-38 illustrates the variation of IE with temperature in 0.1 M Na₂SO₄ + 1 % HCl + 1.7×10⁻³ M (200 ppm) indole at constant velocity of 0 rpm. This figure shows high inhibition efficiency in the presence of 1.7×10⁻³ M (200 ppm) indole. This can be interpreted on the nearly constant activation energy for the range of temperature that has been used (32-52 °C) that will not affect the adsorption of inhibitor on metal surface [Sanad et.al, 2000].

As well as raising the temperature from 32 to 52 °C, the IE exhibits slight increase in very small amount i.e. at 32 °C the IE was 86.589 % while for 52 °C it was 88.618 %. The increase of IE with temperature at constant concentration of the inhibitor is explained with the change in the adsorption character – it is physical at a low temperature and transforms into chemical with its increase [Popova, 2007]. Riggs and Hurd [1967] considered the rate of metal dissolution in presence of an inhibitor as a sum of two rates: the first one is connected with the process taking place on the surface free from an inhibitor, while the second one – with that proceeding on the surface occupied by the inhibitor. At high concentrations the first rate is insignificantly small and the corrosion mechanism includes a direct reaction of the inhibitor molecules with the surface of the metal. Then the activation energy (E_a) of the inhibited metal dissolution can be higher as well as lower than that of the uninhibited reaction in case of a high degree of surface coverage.

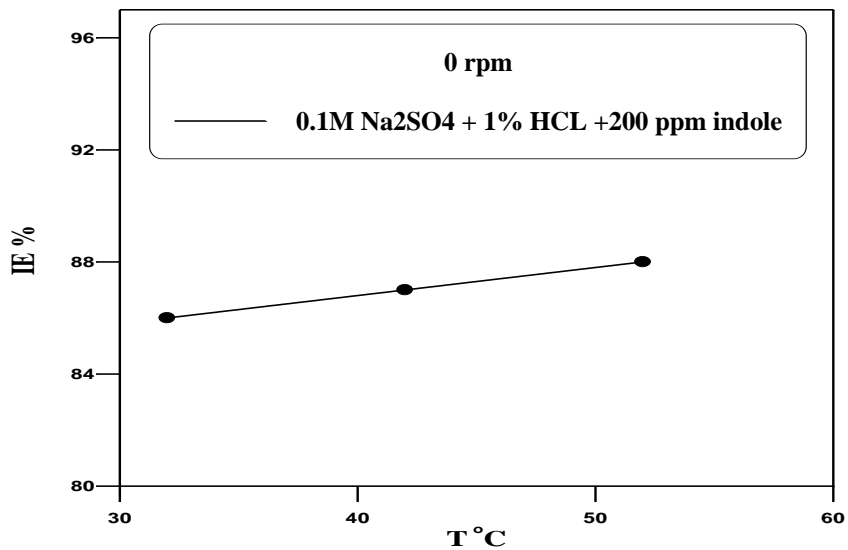


Figure 5-38 Variation of IE with T at 0 rpm in 0.1 M Na₂SO₄ + 1 % HCl + 1.7×10^{-3} (200 ppm) indole

5.8.2 Cetyl Trimethyl Ammonium Bromides Inhibitor (CTAB)

5.8.2.1 Effect of Velocity on IE of CTAB

Figure 5-39 shows the variation of IE with velocity at 32 °C in 0.1 M Na₂SO₄ + 1 % HCl + 2.74×10^{-3} M (1000 ppm) CTAB.

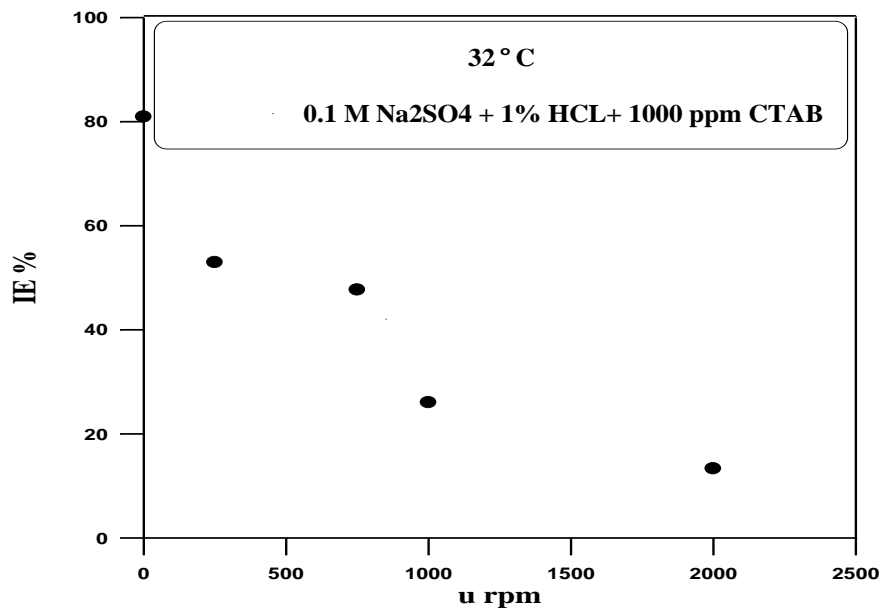


Figure 5-39 Variation of IE with u at 32 °C in CTAB solution

This figure shows that the maximum IE was 80.96 % at zero velocity then with increasing u the IE drops to 13.32 % at 2000 rpm. Thus, this behavior reveals that changing the velocity from 0 (static) to 2000 rpm causes the inhibition efficiency to decrease by 84 %. The decrease in the IE with velocity is due to the increased shear force as stated above. The good inhibition efficiency that given by CTAB in fact is due to the large molecular weight of CTAB, thus CTAB can relatively easily adsorb on the carbon steel surface by Van der Waals force. In addition, the main hydrophilic part $N^+ (CH_3)_3$ of CTAB may attack the C-steel surface while the main hydrophobic part $CH_3 (CH_2)_{15}$ may extend to the solution face. Furthermore CTAB may chemisorb at steel / solution interface via chemical bond between positively charged nitrogen atoms and negatively charged carbon steel surface as follows: in strong acidic solution, CTAB as a cationic surfactant, ionizes and carry a positive charge. Steel surface is positively charged in presence of acidic medium because of $E_c - E_{q=0}$ (zero charge potential) >0 , while bromide ion is negatively charged. As a result, the specific adsorption of bromide ion occurs onto carbon steel surface, ionized CTAB easily reaches carbon steel surface, and the dipoles of the surface compound are oriented with their negative ends towards solution, preventing acid solution attach directly to carbon steel surface. So, bromide ion acts as an adsorption mediator of an adsorption composite film in which bromide ion are sandwiched between metal and positively charged part of the inhibitor. This film acts as a barrier facing corrosion process [El Maghraby and Soror, 2010a, b].

5.8.2.2 Effect of Temperature on IE of CTAB

The effect of temperature on the inhibiting process is of a great importance in industry. Figure 5-40 show the variation of inhibition efficiency with temperature at

constant velocity of 0 rpm in 0.1 M Na₂SO₄ + 1% HCl + 2.74×10⁻³ M (1000 ppm) CTAB at temperatures range from 32 °C to 52 °C.

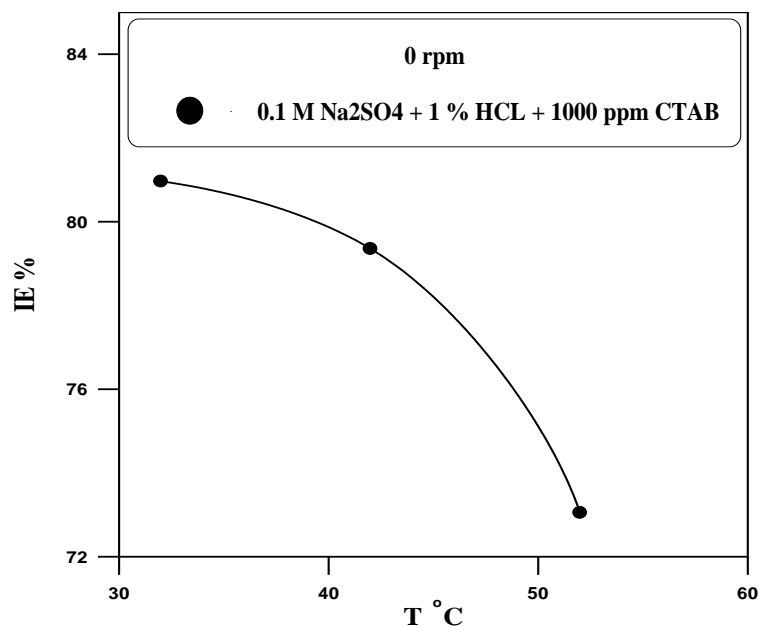


Figure 5-40 Variation of IE with T at 0 rpm in 0.1 M Na₂SO₄ + 1% HCl + 2.74×10⁻³ M (1000 ppm) CTAB

It is clear from this figure that increasing the temperature leads to an increase in the corrosion rate for inhibited and uninhibited solution and subsequently decreasing of the inhibition efficiency. As temperature increases from 32 to 52 °C the inhibition efficiency decreased from 80.96 % to 73.05 % indicating that the high temperature might result in desorption of the inhibitor molecules from the carbon steel surface and this agree with previous study that reported by Li et al. [2008], which indicated that the higher temperatures might cause desorption of CTAB from the carbon steel surface. When comparing the result in Table 4-14 it is clearly indicating that the presence of inhibitor causes a marked decrease in the corrosion rate, i.e. this may be ascribed to adsorption of inhibitor over the corroded surface and the maximum inhibition corresponds to

the formation of a monolayer of the additive on the active sites of the metal surface [El Maghraby and Soror, 2010b].

Whereas comparing the result with addition of 2.74×10^{-3} M (1000 ppm) CTAB and addition of 1.7×10^{-3} M and 3.4×10^{-3} M (200 and 400 ppm) indole to the acidic solution that consists of 0.1 M Na_2SO_4 + 1% HCl it can be conclude that the addition of these small amount to the corrosive solution leads to a decrease in the corrosion rate (gmd) and given good inhibition efficiency. Also the order of increasing the inhibition efficiency of inhibitors that used in 0.1 M Na_2SO_4 + 1% HCl as follows: Indole > CTAB. This is because indole reveals excellent inhibition efficiency for high temperature and in small amount (i.e. low concentration).

Chapter Six

Conclusions and Suggestions for Future Work

6.1 Conclusions

For present system the following conclusions can be drawn:

1. The CR in salt solutions increases with increasing rotation velocity and has complex trend with temperature and oxygen concentration. The CR increases three times as u increases from 0 to 2000 rpm. In acid-salt solution the CR or i_{corr} higher than in salt solution and increases with increasing both T and u
2. When air is bubbled in Na_2SO_4 solution, the O_2 concentration increases slightly causing an appreciable increase in the CR ranging from 10 % to 50 % depending on u and T . In addition, the increase in the O_2 concentration shifts E_{corr} considerably to more positive direction. The corrosion rate at 42 °C is higher than that at 32 °C and 52 °C in presence and absence of air bubbles.
3. With increasing Na_2SO_4 concentrations up to 0.1 M the CR increases by 40 % to 55 % and then the CR decreases mainly due to the decrease in O_2 concentration with further increase in Na_2SO_4 concentration. While increasing the acid concentration from 0.5 % to 3 % at constant salt concentration leads to an increase in the corrosion rate by 52 % (as an average) for three temperatures.
4. The time has a noticeable effect on the corrosion rate due to the formation of corrosion product layer. The formation of this layer causes reduction in corrosion rate by 40 % to 55 % depending on the temperature and rotational velocity.

5. Increasing the velocity from 0 to 2000 rpm and temperature from 32 to 52 °C leads to a decrease in the IE for CTAB inhibitor by 84 % and by 10 % respectively as temperature increased.
6. Increasing the temperature and inhibitor concentration leads to an increase in the inhibition efficiency for indole by 56 % when inhibitor concentration increased, and by 2.3 % as temperature increase from 32 to 52 °C, while increasing the velocity leads to a decrease in the IE by 56 %.
7. Because indole reveals excellent inhibition efficiency (about 88.618 %) for high temperature and in low concentration this indicates that indole is better than CTAB inhibitor.

6.2 Suggestions for Future Work

1. Measuring the corrosion rate in new corrosive solution by using different acid and salt solutions such as Na_2SO_3 , KCl , H_2SO_4 and comparing between the results.
2. Studying the effect of higher temperatures on the corrosion rate and used inhibitor efficiency under static and dynamic conditions.
3. Studying the effect of long exposure time.
4. Using electrochemical impedance spectroscopy (EIS) and electrochemical noise (EN) analysis in order to determine the corrosion mechanism and to obtain representative corrosion rates of the system.
5. Studying the effect of air bubbles on the IE.

References

- Abboud Y., A. Abourriche, T.Saffaj, M. Berrada, M. Charrouf, A. Bennamara, and H. Hannache, "A Novel Azodye, 8- Quinolinol – 5- Azo Anti- Pyrine as Corrosion Inhibitor for Mild Steel in Acidic Media", *Desalination*, vol.237, pp.175- 189, 2009.
- Ahamad, I., R.Prasad, and M.A. Quraishi, "Thermodynamic, Electrochemical and Quantum Chemical Investigation of Some Schiff Bases as Corrosion Inhibitors for Mild Steel in Hydrochloric Acid Solutions", *Corrosion Science*, vol.52, pp.933- 942, 2010.
- Ali J.M, S. A. Sameh and Q. M. Abbas "The Corrosion of (Fe, Zn Cu) Metals in 3.5%NaCl Solution Under Different Flow Conditions", *Eng. and Tech. journal*, No. 15, vol.27 , pp.2792- 2805, 2009.
- Al-Sawaad H. Z.M., A.S.K. Al-Mubarak, and A.M. Haddad, "The Inhibition Effects of Dimethylol-5-Methyl Hydantoin and its Derivatives on Carbon Steel Alloy", *J. Mater. Environ. Sci.*, No. 4, vol. 1, pp. 227-238, 2010.
- Al-Sehaibani H., "Evaluation of extracts of Henna leaves as environmentally friendly corrosion inhibitors for metals", vol. 31, pp.1060–1063, 2000.
- Alwash S.H., V. Ashworth, M. Shirkhazadeh, and G.E Thompson, "an Investigation of the Reduction of Oxygen at a Rotating Disk Electrode with Heat Transfer Facilities", *Corrosion Science*, vol. 27, pp. 1301-1311, 1987.
- Amin M. A., M. A. Ahmed, H. A. Arida, T. Arslan, M. Saracoglu, and F. Kandemirli, "Monitoring Corrosion and Corrosion Control of Iron in HCl by Nonionic Surfactants of the TRITON-X Series Part II Temperature Effect, Activation Energies and Thermodynamics of Adsorption", *Corrosion Science*, vol. 53, pp. 540–548, 2011.
- Amin M.A., S.S. Abd El-Rehim, E.E.F. El-Sherbini, and R.S. Bayoumi, "The Inhibition of Low Carbon Steel Corrosion in Hydrochloric Acid Solutions by Succinic Acid Part I , Weight Loss, Polarization, EIS, PZC, EDX, and SEM Studies", *Electrochimica. Acta.*, vol. 52, pp. 3588, 2007.
- Andijani I., "Ac Impedance Studies on the Corrosion Behavior of Carbon Steel in Deaerated Chloride Solution", the 6th Saudi Engineering Conference, KFUPM, vol. 5, pp. 43-56, 2002.

- Arab S. T. and E. A. Noor, "Inhibition of Acid Corrosion of Steel by Some S Alkylisothiuronium Iodides", *Corrosion*, vol. 49, pp.122–129, 1993.
- Ashassi-Sorkhabi H., B. Shaabani, and D. Seifzadeh, "Effect of Some Pyrimidine Schiff Bases on the Corrosion of Mild Steel in HCl Solution", *Electrochimica. Acta.*, vol. 50, pp. 3446, 2005.
- Ashassi-Sorkhabi H., D. Seifzadeh, and M. Hosseini, "EN, EIS and Polarization Studies to Evaluate the Inhibition Effect of 3H- phenothiazin- 3one, 7- dimethylamin on Mild Steel Corrosion in 1 M HCl Solution", *Corrosion Science*, vol. 50 pp. 3363-3370, 2008.
- Ashida Y. , L. G. McMillin and G. Taylor, "The Effect of Temperature Oscillation on the Passive Corrosion Proper-ties of Alloy 22", *Electrochemistry Communications*, No. 5, vol. 9, pp.1102-1106, 2007.
- Bagotsky V. S., "Fundamentals of Electrochemistry", Second Edition, John Wiley and Sons, Inc., Hoboken, New Jersey, 2006.
- Bannerjee G. and S.N.Malhotra, "Contribution to the Adsorption of Aromatic Amines on Mild Steel Surfaces from HCl Solutions by Impedance, UV and Raman Spectroscopy", *Corrosion-NACE*, vol. 48, pp.10, 1992.
- Belfilali I., A. Chetouani, B. Hammouti, A. Aouniti, S. Louhibi, and S.S. Al-Deyab , "Synthesis and Application of 1,7- bis (2- Hydroxy Benzamido)-4- Azaheptane Corrosion Inhibitor of Mild Steel in Molar Hydrochloric Acid Medium", *Int. J. Electrochem. Sci.*, vol. 7, pp. 3997 – 4013, 2012.
- Bentiss F., M. Traisnel, and M. Lagrenee, "The Inhibition Action of 3, 6- Bis (2- Methoxyphenyl) - 1, 2 – Dihydro- 1, 2, 4, 5- Tetrazine on the Corrosion of Mild Steel in Acidic Media", *Corrosion Science*, vol. 42, pp.127- 146, 2000.
- Bentiss F., M. Traisnel, and N. Chaibi, "4-Oxadiazoles Used as Corrosion Inhibitors in Acidic Media: Correlation between Inhibition Efficiency and Chemical Structure", *Corrosion Science*, vol. 44, pp. 2271–2289, 2002.
- Bird R.B., W.E. Stewart, and E.N. Lightfoot, "Transport Phenomena", second edition, John Wiley & Sons, New York, 2002.
- Bornstein N. S. and M. A. Decrescente, "The Role of Sodium in the Accelerated Oxidation Phenomenon Termed Sulfidation", *Metall. Trans. No. 10*, vol. 2, pp.2875- 2883, 1971.
- Brodkey, R. S. and H. C. Hershey, "Transport Phenomena", second edition, McGraw Hill, New York, 1989.

- Chauhan L.R., and G. Gunasekaran, "Corrosion Inhibition of Mild Steel by Plant Extract in Dilute HCl Medium", *Corrosion Science*, vol. 49, pp. 1143–1161, 2007.
- Chebabe D., Z.A. Chikh, and N. Hajjaji, "Corrosion Inhibition of Armco Iron in 1m HCl Solution by Alkyltriazoles", *Corros. Sci.*, vol. 45, pp. 309–320, 2003.
- Chin R.J., and K. Nobe, "Electrochemical aspects of Steel Corrosion in Sea Water", *Corrosion J.*, vol.33, pp.364, 1977.
- Ciubotariu A. C., L. Benea, and P. L. Bonora, "Corrosion studies of carbon steel X60 by electrochemical methods" *Journal of Optoelectronics and Advanced Materials*, No. 5, vol. 12, pp. 1170 – 1175, 2010.
- Ebenso E. E., I. B. Obot, and L. C. Murulana, "Quinoline and its Derivatives as Effective Corrosion Inhibitors for Mild Steel in Acidic Medium", *Int. J. Electrochemical. Sci.*, vol.5, pp. 1574 – 1586, 2010.
- Eid N.M.A. "Localized Corrosion at Welds in Structural Steel under Desalination Plant Conditions Part II: Effect of Heat Treatment, Test Temperature and Test Media", *Corrosion Science*, vol. 73, pp. 407-415, 1989.
- El Maghraby A. A. and T. Y. Soror, "Efficient Cationic Surfactant as Corrosion Inhibitor For Carbon Steel in Hydrochloric acid Solutions", *Advances in Applied Science Research*, No. 2, vol. 1, pp. 156-168, 2010a.
- El Maghraby A. A. and T. Y. Soror, "Quaternary Ammonium Salt as Effective Corrosion Inhibitor for Carbon Steel Dissolution in Sulphuric Acid Media", *Advances in Applied Science Research*, No. 2, vol. 1, pp. 143-155, 2010b.
- El Ouali I., B. Hammouti, A. Aouniti, Y. Ramli, M. Azougagh, E.M. Essassi, and M. Bouachrine, "Thermodynamic Characterization of Steel Corrosion in HCl in the Presence of 2- Phenylthieno (3, 2-B) Quinoxaline", *J. Mater. Envir. Sci.*, No. 1, vol. 1, pp.1-8, 2010.
- Elayyachy E., A. El Idrissi, and B. Hammouti, "New Thio-Compounds as Corrosion Inhibitor for Steel in 1M HCl", *Corrosion Science*, vol, 48, pp. 2470– 2479, 2006.
- Elewady G.Y., "Pyrimidine Derivatives as Corrosion Inhibitors for Carbon Steel in 2M Hydrochloric Acid Solution", *Int. J. Electrochemical Sci.*, vol. 3, pp. 1149 – 1161, 2008.

- Fontana M.G., "Corrosion Engineering," third edition, McGraw-Hill Book Company, New York, 1986.
- Foroulis Z. A. "The Influence of Velocity and Dissolved Oxygen on the Initial Corrosion Behavior of Iron in High Purity Water", Corrosion, vol. 35, pp. 340-344, 1979.
- Fouda A.S., G.Y. Elewady and M. N. El-Haddad, "Corrosion Inhibition of Carbon Steel in Acidic Solution Using Some Azodyes" Canadian Journal on Scientific and Industrial Research, No. 1, vol. 2, 2011.
- Frateur I., L. Lartundo-Rojas, C. Méthivier, A. Galtayries, and P. Marcus, "Influence of Bovine Serum Albumin in Sulphuric Acid Aqueous Solution on the Corrosion and the Passivation of An Iron- Chromium Alloy", Electrochimica. Acta., vol. 51, pp. 1550, 2006.
- Gabe D. R., "The Rotating Cylinder Electrode", J. Appl. Electrochemica., vol. 4, pp. 91-108, 1974.
- Gabe D.R. , and F.C. Walsh, "The Rotating Cylinder Electrode: A Review of Development", J. Appl. Electrochemical, No. 1, vol. 13, pp. 3-22, 1983.
- Gabe D.R. and P.A. Makanjoula, EFCF Publication Series No. 15, Electrochemical Eng., AIChE Symposium Series, No. 98, pp.309, 1986.
- Garnica-Rodriguez A., J. Genesca, M. J. Flores, and R. Duran-Romero, "Electrochemical Evaluation of Aminotriazole Corrosion Inhibitor under Flow Conditions", J. Appl. Electrochem., vol.39, pp.1809-1819, 2009.
- Gedeon G, "Corrosion Overview", corrosion, vol. 4 pp. 37- 43, 2000.
- Genesca J. , R. Olalde, A. Garnica, N. Balderas, J. Mendoza, and R. Duran-Romero, "Electrochemical Evaluation of Corrosion Inhibitors in CO₂ Containing Brines", Corrosion, NACE, vol. 00162, pp.23, 2010.
- George K. and S. Nestic, "Electrochemical Investigation and Modeling of Carbon Dioxide Corrosion of Carbon Steel in the Presence of Acetic Acid", Corrosion 2004 NACE, vol. 04379, pp.25, 2004.
- Goebel J. A, F. S. Pettit and G. W. Goward, "Mechanisms for the Hot Corrosion of Nickel-Base Alloys", Metall. Trans., No. 1, vol. 4, pp. 261- 278, 1973.
- Goncalves, R.S., and L.D. Mello, "Electrochemical Investigation of Ascorbic Acid Adsorption on Low Carbon Steel in 0.5 M Na₂SO₄ Solutions", Corrosion Science, vol.43, pp. 457- 470, 2001.

- Guthrie J., B. and C. Gretchen, "Accelerated Corrosion Testing" *Advanced Materials and Processes Technology Quarterly*, No. 3, vol. 6, pp.11, 2002.
- Hamdy A., M.A. Shoeib, A.G. Sa`eh and Y. Barakat, "The Electrochemical Behavior of Mild Steel in Sulfide Polluted NaCl at Different Velocities", *Int. J. Electrochem. Sci.*, vol.3, pp.1142 – 1148, 2008.
- Hasan B. O, "Effect of Salt Content on the Corrosion Rate of Steel Pipe in Turbulently Flowing Solutions", *Nahrain University College of Engineering Journal (NUCEJ)*, No. 1, vol.13, pp. 66-73, 2010.
- Hasan S. K. and P. Sisodia "Paniala (*Flacourtia Jangomas*) Plant Extract as Eco Friendly Inhibitor on the Corrosion of Mild Steel in Acidic Media", *Rasayan J. Chem.* No. 3, vol.4, p.548-553, 2011.
- Hasan, B. O., "Heat, Mass, and Momentum Analogies to Estimate Corrosion Rates under Turbulent Flow Conditions" Ph. D. Thesis Dept. of Chem. Eng., University of AL-Nahrain, Baghdad, 2003.
- Heitz E., "Corrosion of Metals in Organic Solvents", *Advances in Corrosion Science and Technology*, vol. 4, pp. 149, 1974.
- Holman J.P., "Introduction to Heat Transfer", 3rd Edition, New York, Mc-Graw Hill, 1997.
- Hubbard, D. W. and E. N. Lightfoot, "Correlation of Heat and Mass Transfer Data for High Schmidt and Reynolds Numbers", *Ind. Eng. Chem.* vol.5, pp. 370–379, 1966.
- Huijbregts W., "Acid Corrosion Resistance of Boiler Steels." *Materials Performance.* vol. 3, pp. 23-27, 2007.
- Ismail A.A., S.H.Sanad, A.A.El- Meligi, "Inhibition Effect of Indole and Some of Its Derivatives on Corrosion of C- Steel in HCl", *J. Mater. Technol.* , No. 4, vol. 16, pp.397-400, 2000.
- Ita B.A., and O.E. Offiong, "Adsorption Studies on Corrosion Inhibition Properties of 2- acetylpyrole and 2- acetylpyrole- (2- acetylthiosemicarbazone) on Mild Steel in Hydrochloric Acid Medium", *Global J. pure and App. Sci*, vol.5, pp.497-501, 1997.
- Jeyaprabha C., S. Sathiyarayanan, and G. Venkatachari, "Influence of Halide Ions on the Adsorption of Diphenyl Amine on Iron in 0.5 M H₂SO₄ Solutions" *Electrochim. Acta*, vol. 51, pp. 4080- 4088, 2006.

- Khadom A. A., A. S. Yaro, A. H. Kadum, A.S. AlTaie and A. Y. Musa “The Effect of Temperature and Acid Concentration on Corrosion of Low Carbon Steel in Hydrochloric Acid Media”, *American Journal of Applied Sciences*, No. 7, vol. 6, pp. 1403-1409, 2009.
- Khaled K. F., O. A. Elhabib, A. El-mghrabya, O. B. Ibrahima, and M. A. M. Ibrahimd, “Inhibitive Effect of Thiosemicarbazone Derivative on Corrosion of Mild Steel in Hydrochloric Acid Solution”, *J. Mater. Environ. Sci.*, No. 3, vol. 1, pp.139-150, 2010.
- Kustu C., K.C. Emregu, and O. Atakol, “Schiff Bases of Increasing Complexity as Mild Steel Corrosion Inhibitors in 2 M HCl”, *Corrosion Science*, vol. 49, pp. 2800–2814, 2007.
- Laurie S. M. and M. Edwards, “Temperature Effects on Iron Corrosion”, *National Science Foundation*, vol. 4, pp. 66-76, 2000.
- Lebrini M., F. Robert, H. Vezin, and C. Roos, “Electrochemical and Quantum Chemical Studies of Some Indole Derivatives as Corrosion Inhibitors for C38 Steel in Molar Hydrochloric Acid”, *Corrosion Science*, vol. 52, pp. 3367–3376, 2010.
- Lgamri A., H.A. El Makarimb, and A. Guenbour, “Electrochemical Study of the Corrosion Behaviour of Iron in Presence of New Inhibitor in 1M HCl”, *Prog. Org. Coat.*, vol. 48, pp. 63–70, 2003.
- Li X., S. Deng, G. Mu, H. Fu, and F. Yang, "Inhibition Effect of Nonionic Surfactant on the Corrosion of Cold Rolled Steel in Hydrochloric Acid”, *Corrosion Science*, No. 2, vol. 50, pp. 420–430, 2008.
- Liang Y., T. Ji, Y. Zhuang and X. Lin, “Research on Stress Corrosion of Concrete in Sodium Sulphate Solution”, *journal of applied mechanics and materials*, vols. 94-96, pp. 1243-1246, 2011.
- Liu F.G., M. Du, J. Zhang, and M.Qiu, “ Electrochemical Behavior of Q 235 Steel in Salt Water Saturated with Carbon Dioxide Based on New Imidazoline Derivative Inhibitor”, *Corrosion Science*, vol. 51, pp. 102, 2009.
- Loto R. T., C. A. Loto, A. P. I. Popoola, and M. Ranyaoa, “Pyrimidine Derivatives as Environmentally-Friendly Corrosion Inhibitors: A Review” *International Journal of Physical Sciences*. No. 14, vol. 7, pp. 2136 – 2144, 2012.

- Lyon W., “Standard Handbook of Petroleum and Natural Gas Engineering”, vol.1, Gulf Company, Houston, Texas, 1996.
- Mahato B. K., C. Y. Cha and W. Shemlit, “Unsteady State Mass Transfer Coefficients Controlling Steel Pipe Corrosion under Isothermal Flow Conditions”, Corrosion Science, vol.20, pp.421–441, 1980.
- Mahato B. K., F. R. Stewrd and L. W. Shimlit, “Steel Pipe Corrosion under Flow Condition - II Mass Transfer Correlations with Temperature Effects”, Corrosion Science J., vol.8, pp.737–749, 1968a.
- Mahato B. K., S. K. Voora and L. W. Shemilt, “Steel Pipe Corrosion under Flow Condition - an Isothermal Correlation for a Mass Transfer Model” Corrosion science, vol. 8, pp. 173–193, 1968b.
- Martinez R. G, J. M. Flores, R. D. Romero and J. G. Llongueras, “Rotating Cylinder Electrode Study on the Influence of Turbulent Flow, on the Anodic and Cathodic Kinetics of X52 Steel Corrosion, in H₂S Containing Solutions” Afinidad, No. 519, vol.62, pp.448-454, 2005.
- Mobin M., M. Parveen, and M. Alam Khan, “Inhibition of Mild Steel Corrosion Using L-tryptophan and Synergistic Surfactant Additives”, Portugaliae Electrochimica Acta, No. 6, vol. 29, pp. 391- 403, 2011.
- Mora-Mendoza J. L. , J. G. Chacon-Nava, G. Zavala-Olivares, M. A Gonzalez-Nunez, and S. Turgoose, “Influence of Turbulent Flow on the Localized Corrosion Process of Mild Steel with Inhibited Aqueous Carbon Dioxide Systems”, Corrosion, vol.58, pp.608-619, 2002.
- Muralidharan S., K.L.N. Phani, S. Pitchumani, S. Ravichandran, and S.V.K. Iyer, “Polyamino – Quinine Polymer: A New Class of Corrosion Inhibitor for Mild Steel”, J. Electrochemical. Soc., vol. 142, pp. 1478, 1995.
- Musa A. Y., A. A. H. Kadhum, A. B. Mohamad, M. S. Takriff, S. K. Kamarudin, and A. R. Daud, “Determination of Mild Steel Corrosion Rate under Turbulent Flow in Highly Acidic Solution”, journal of applied science, No. 13, vol. 11, pp.2464-2466, 2011.
- Musa A. Y., A. H. Kadhum, A. Mohamad, A. Daud, M. S.Takriff , S. K. Kamarudin, and N. Muhamad”, “Stability of Layer Forming for Corrosion Inhibitor on Mild Steel Surface under Hydrodynamic Conditions”, Int. J. Electrochem. Sci., vol.4, pp.707 – 716, 2009.

- Musa A. Y., A. H. Kadhum, and A. Muhamad, "Corrosion Inhibitor Film Forming in Aerated and Deaerated Solutions", *Int. J. Electrochemical Science*, vol.5, pp.1911 – 1921, 2010.
- Nahl'e A., I. Abu-Abdoun, I. Abdel-Rahman, and M. Al-Khayat, "UAE Neem Extract as a Corrosion Inhibitor for Carbon Steel in HCl Solution", *International Journal of Corrosion*, vol.460154, pp.9, 2010.
- Nesic N., B.F.M. Pots, J. Postlethwaite, and N. Trevenot, "Superposition of Diffusion and Chemical Reaction Controlled Limiting Currents – Application to CO₂ Corrosion", *J. Corrosion Science and Eng.*, vol.1, Paper 3, 1995.
- Nesic S., G. T. Solvi, and J. Enerhaug, "Comparison of the Rotating Cylinder and Pipe Flow Tests for Flow-Sensitive Carbon Dioxide Corrosion", *Corrosion*, No. 10, vol.51, pp.773-787, 1995.
- Nesic S., J. Bienkowski, K. Bremhorst, and K. S. Yang, "Testing for Erosion-Corrosion under Disturbed Flow Conditions Using a Rotating Cylinder with a Stepped Surface", *Corrosion*, vol. 56, pp. 1005-1014, 2000.
- Nessim I .M, A.Hamdy, M.M. Osman and M. N. Shalaby, "Inhibitory Effect of Some Cationic Gemini Surfactants for Carbon Steel in Sea Water", *Journal of American Science*, No. 8, vol. 7, pp.78-90, 2011.
- Noor E. A and A. H. Al-Moubaraki, "Corrosion Behavior of Mild Steel in Hydrochloric Acid Solutions", *Int. J. Electrochemical Science*, vol.3, pp.806 – 818, 2008.
- Nor A. M., M.F. Suhor, M.F. Mohamed, M. Singer and S. Nesic, "Corrosion of Carbon Steel in High CO₂ Environment: Flow Effect" *NACE International, corrosion 2011*, vol. 11242, pp. 18, 2011.
- Obi-Egbedi N.O., K. E. Essine, I. B. Obot and E. E. Ebenso, "1,2-Diaminoanthraquinone as Corrosion Inhibitor for Mild Steel in Hydrochloric Acid: Weight Loss and Quantum Chemical Study" *International Journal of Electrochemical Science*, vol. 6, pp. 913 – 930, 2011.
- Ochoa N., F. Moran, N. Pe'be`re, and B. Tribollet, "Influence of Flow on the Corrosion Inhibition of Carbon Steel by Fatty Amines in Association with Phosphonocarboxylic Acid Salts", *Corrosion Science*, vol. 47, pp. 593–604, 2005.

- Ogunleye I. O., G. J Adeyemi and A.O.V Oyegoke, "Effect of Grape Fruit Juice on the Corrosion Behaviour of Mild Steel in Acidic Medium" *American Journal of Scientific and Industrial Research*, No. 4, vol. 2, pp. 611-615, 2011.
- Oguzie E., "Corrosion Inhibition of Mild Steel in Hydrochloric Acid Solution by Methylene Blue Dye", *Materials Letters*, vol. 59, pp.1076- 1079, 2005.
- Onuchukwu A.L, and S.P. Trasatti, "Corrosion Inhibitive Properties of Tannins from Nigerian Local Plants", *corrosion science*, vol.36, pp.185-189, 1994.
- Ortega-Toledo D.M., J.G. Gonzalez-Rodriguez, M.Casales, A.Caceres and L. Martinez, "Hydrodynamic Effects on the CO₂ Corrosion Inhibition of X-120 Pipeline Steel by Carboxyethyl-imidazoline", *Int. J. Electrochem. Sci.*, vol.6, pp. 778 – 792, 2011.
- Osarolube E., I. O. Owate, and N. C. Oforka, "Corrosion Behaviour of Mild and High Carbon Steels in Various Acidic Media", *Scientific Research and Essay*, No. 6, vol.3, pp. 224-228, 2008.
- Papavinasam S., R.W. Revie, M. Attard, A. Demoz, and K. Michaelian, "Comparison of Laboratory Methodologies to Evaluate Corrosion Inhibitors for Oil and Gas Pipelines", *Corrosion*, vol.59, pp.897-912, 2003.
- Peralta S. A., J. G. Llongueras , M. P. Pardavé and M. R. Romo, "Study of the Electrochemical Behaviour of a Carbon Steel Electrode in Sodium Sulphate Aqueous Solutions Using Electrochemical Impedance Spectroscopy", *Journal of Solid State Electrochemistry Springer-Verlag*, vol. 6, pp. 142, 2002.
- Perez N. "Electrochemistry and Corrosion Science" Kluwer Academic Publishers, USA, 2004.
- Perry R.H, and D.W. Green, "Perry Chemical Engineers Handbook", 7thed, M.C. Graw-Hill, United States, 1997.
- Pickett D. J. and K. L. Ong, "The Influence of Hydrodynamic and Mass Transfer Entrance Effects on the Operation of a Parallel Plate Electrochemical Cell," *Electchimica Acta*, vol. 19, pp. 875–881, 1974.
- Ponce-de-Leo'n C., C. T. J. Low, G. Kear, and F. C. Walsh, "Strategies for the Determination of the Convective-Diffusion Limiting Current from Steady State Linear Sweep Voltammetry", *J. Appl. Electrochem.* , vol. 37, pp. 1261–1270, 2007.

- Popova A., “Temperature Effect on Mild Steel Corrosion in Acid Media in Presence of Azoles”, *Corrosion Science*, vol. 49, pp. 2144–2158, 2007.
- Popova A., M. Christov, A. Zwetanova, “Effect of the Molecular Structure on the Inhibitor Properties of Azoles on Mild Steel Corrosion in 1 M Hydrochloric Acid” *Corrosion Science*, vol. 49, pp.2131–2143, 2007.
- Popova A., M. Christov, S. Raicheva, and et al., “Adsorption and Inhibitive Properties of Benzimidazole Derivatives in Acid Mild Steel Corrosion”, *Corrosion Science*, vol. 46, pp. 1333–1350, 2004.
- Poulson B. , “Advances in Understanding Hydrodynamic Effect on Corrosion”, *Corrosion Science*, No.1- 4, vol.35, pp.655-665, 1993.
- Poulson B., “Electrochemical Measurements in Flowing Solutions”, *Corrosion Science*, vol. 23, pp.391–408, 1983.
- Quraishi M.A., and H.K. Sharma, “4-Amino-3-Butyl-5-Mercapto- L, 2, 4-Triazole: a New Corrosion Inhibitor for Mild Steel in Sulphuric Acid”, *Mater. Chem. Phys.*, vol. 78, pp. 18–21, 2002.
- Rajappa S., R. Zhang, and M. Gopal, “Corrosion in Multiphase Systems Center”, *Corrosion 98 NACE*, vol.26, pp.2-26, 1998.
- Raspi I. A, “Influence of Sodium Salts of Organic Acids as Additives on Localized Corrosion of Aluminum and its Alloys”, *Nickel Corros*, vol. 49, pp. 821, 1993.
- Revie R.W. and H. H. Uhlig, “Corrosion and Corrosion Control an Introduction to Corrosion Science and Engineering” fourth edition, John Wiley & Sons, Inc., Hoboken New Jersey, 2008.
- Riggs O.L., and R.M. Hurd, "Temperature Coefficient of Corrosion Inhibition" *Corrosion*, vol. 23, pp.252-258, 1967.
- Roberge P. R. “Handbook of Corrosion Engineering” McGraw-Hill Companies, United States of America, 2000.
- Robert G., Kelly and J. R. Scully, D. W. Shoesmith, and R. G. Buchheit “Electrochemical Techniques in Corrosion Science and Engineering”, Marcel Dekker, Inc. New York, 2003.
- Ross T. K., G. C. Wood, & I. Mahmud, “The Anodic behaviour of Iron-Carbon Alloys in Moving Acid Media”, *J. Electrochem. Soc.*, vol. 113, pp. 334-345, 1966.

- Samide A., “N-(2-Hydroxybenzilidene) Thiosemicarbazide Surfactant as An Effective Inhibitor for Corrosion of Carbon Steel in Diluted Acidic Solutions. Part I”, *Optoelectronics and Advanced Materials – Rapid Communications*, No. 6, vol. 4, p. 884 – 887, 2010.
- Sanad S.H., A.A. Ismail, and A.A.El- Meligi, “Indole and its Derivatives as Corrosion Inhibitors for C- Steel during Pickling”, *J. Mater. Technol.* , No. 3, vol. 16, pp.291-296, 2000.
- Sanyal B., “Organic Compounds as Corrosion Inhibitors in Different Environments – a Review”, *Prog. Org. Coat.*, vol. 9, pp. 165–236, 1981.
- Scheers P.V., “The Effects of Flow Velocity and PH on the Corrosion Rate of Mild Steel in a Synthetic Mine Water”, *J. S. Afr. Inst. Min. Metall.*, No. 10, vol. 92, pp. 275-281, 1992.
- Shreir L.L., R.A. Jarman and G.T. Burstein,” *Corrosion Metal / Environment Reactions*” third edition, Butterworth-Heinemann Volume I, Great Britain, 2000.
- Singh D.D.N., and A.K. Singh, “Synergistic Effects of Inorganic and Organic Cations on Inhibitive Performance of Propargyl Alcohol on Steel Dissolution in Boiling Hydrochloric Acid Solution”, *Corrosion*, vol. 49, pp.594–600 , 1993.
- Slaiman Q. J. M. and B. O. Hasan “Study on Corrosion Rate of Carbon Steel Pipe under Turbulent Flow Conditions” *The Canadian Journal of Chemical Engineering*, vol. 88, pp. 1114- 1120, 2010.
- Slaiman Q. J. M., B. O. Hasan and H. A. Mahmood, “Corrosion Inhibition of Carbon Steel under Two-Phase Flow (Water–Petroleum) Simulated by Turbulently Agitated System”, *the Canadian Journal of Chemical Engineering*, vol. 86, pp.240 – 248, 2008.
- Stern M., “Fundamentals Electrode Processes in Corrosion,” *Corrosion-NACE*, vol. 13, pp. 97–104 1957.
- Stringer J., “Hot Corrosion in Gas Turbines”, *ASM International, High Temperature Corrosion and Materials Application*, vol. 9, pp. 249-258, 2007.
- Subramanian R., “Effect of Adsorption of Some Azoles on Copper Passivation in Alkaline Medium”, *Corrosion Science*, vol. 44, pp. 535-554, 2002.

- Sun Y., K. George, and S. Nestic, "The Effect of Cl⁻ and Acetic Acid on Localized CO₂ Corrosion in Wet Gas Flow", Corrosion 2003 NACE, vol. 03327, pp.28, 2003.
- Syed S. "Atmospheric Corrosion of Materials" Emirates Journal for Engineering Research, No. 1, vol. 11, pp.1-24, 2006.
- Talbot D.E.J. and J.D.R. Talbot, "Corrosion Science and Technology", by CRC Press LLC, U.S.A., 1998.
- Touhami, F., A. Aouniti, S. Kertit, Y. Abed, B. Hammouti, A. Ramdani, and K. Elkacemi, "Application of Argania Plant Extract as Green Corrosion Inhibition for Steel in 1 M HCl", Corrosion Science, vol. 42, pp. 929, 2000.
- Turkee H. M., "Investigation of the Performance of Some Corrosion Inhibitors in Aerated Acid Solutions" M.Sc. Thesis Dept. of Chem. Eng., University of AL-Nahrain, Baghdad, 2009.
- Wan N. W.B., A. Ahmad, R. Rosliza, Y. Prawoto and F. Zulkifli, "The Study of Temperature Effect on Mild Steel Coated with Aerosol Paint", International Journal of Engineering Science and Technology, No. 9, vol. 3, pp.7175-7179, 2011.
- Yaro A. S., R. K. Wael, and A. A. Khadom, "Reaction Kinetics of Corrosion of Mild Steel in Phosphoric Acid", Journal of the University of Chemical Technology and Metallurgy, No. 4, vol. 45, pp. 443-448, 2010.
- Zerga B., R. Saddik, B. Hammouti, M. Taleb, M. Sfaira, M. Ebn Touhami, S.S. Al-Deyab, and N. Benchat, "Effect of New Synthesised Pyridazine Derivatives on the Electrochemical Behaviour of Mild Steel in 1M HCl Solution: Part-1", Int. J. Electrochem. Sci., vol.7, pp. 631 – 642, 2012.
- Zhang F., J. Pan, and P. M. Claesson, "Electrochemical and AFM Studies of Mussel Adhesive Protein (Mefp-1) as Corrosion Inhibitor for Carbon Steel", Electrochimica. Acta. , vol.56, pp. 1636–1645, 2011.
- Zvandasara T., "Influence of Hydrodynamics on Carbon Steel Erosion Corrosion and Inhibitor Efficiency in Simulated Oil Field Brines", PhD thesis 2009.

Appendix -A-

Table A-1 Measured density of the solutions used in experiments

Density (kg / m³)				
Solution concentration	T	32 °C	42 °C	52 °C
0.01 M Na ₂ SO ₄		1006.9	1007.8	1003.27
0.025 M Na ₂ SO ₄		1009.86	1004.54	1005.19
0.05 M Na ₂ SO ₄		1014.32	1012.14	1010.49
0.1 M Na ₂ SO ₄		1026.5	1009.23	1014.36
0.2 M Na ₂ SO ₄		1035.14	1029.56	1023.91
0.4 M Na ₂ SO ₄		1055.86	1051.71	984.45
0.01 M Na ₂ SO ₄ + 1 % HCl		1021.06	1009.26	1000.02
0.05 M Na ₂ SO ₄ + 1 % HCl		1019.73	1015.2	1017.13
0.2 M Na ₂ SO ₄ + 1 % HCl		1015.71	1013.97	1010.07
0.2 M Na ₂ SO ₄ + 0.5 % HCl		1034.79	1032.23	1029.93
0.2 M Na ₂ SO ₄ + 3 % HCl		1045.76	1045.49	1033.53
0.1 M Na ₂ SO ₄ + 1 % HCl + 200 ppm indole		1024.88	1023.86	1014.92
0.1 M Na ₂ SO ₄ + 1 % HCl + 1000 ppm CTBA		1029.48	1016.26	1014.79
0.1 M Na ₂ SO ₄ + 1 % HCl + 400 ppm indole		1030.14	1028.88	1016.23

Table A-2 Viscosity of the pure water [Holman, 1997]

T (°C)	32	42	52
μ (pa. s) × 10³	1.79	1.502	1.272

Table A-3 Diffusivity of oxygen in pure water [Hasan, 2003]

T (°C)	32	42	52
D_o (m ² /s) ×10 ⁹	2.857	3.68	4.32

Table A- 4 Corrosion of carbon steel in 0.2 M Na₂SO₄ and 32 °C

u, rpm	u, m/s	Re	$i_L=i_{corr}$, A/m ²	CR, gmd	CR, mpy	$N_{O_2} \times 10^5$ mol/m ² .s	$N_{Fe} \times 10^5$ mol/m ² .s	$K \times 10^4$ m/s	$\delta \times 10^6$ m	E_{corr} , V
0	0	Static	1	25	45.8	0.259	0.518	0.134	214	-0.93
250	0.327	4698	5.75	143.8	236	1.49	2.98	0.77	37.24	-0.656
500	0.655	9409	6	150	275	1.55	3.109	0.803	35.64	-0.639
750	0.982	14107	6.75	168.8	309	1.749	3.498	0.903	31.68	-0.635
1000	1.309	18804	9	224.9	412	2.33	4.66	1.2	23.8	-0.623
1500	1.963	28199	13.5	336.3	616	3.49	6.97	1.79	15.96	-0.62
2000	2.618	37609	16	399.9	732	4.15	8.29	2.13	13.44	-0.604

Table A- 5 Corrosion of carbon steel in 0.2 M Na₂SO₄ and 42 °C

u, rpm	u, m/s	Re	$i_L=i_{corr}$, A/m ²	CR, gmd	CR, mpy	$N_{O_2} \times 10^5$ mol/m ² .s	$N_{Fe} \times 10^5$ mol/m ² .s	$K \times 10^4$ m/s	$\delta \times 10^6$ m	E_{corr} , V
0	0	Static	1.2	30	55	0.311	0.622	0.188	197.6	-0.935
250	0.327	5609	6.25	156	286	1.62	3.24	0.973	37.84	-0.701
500	0.655	11225	6.6	165	302	1.71	3.421	1.03	35.8	-0.654
750	0.982	16829	9	225	412	2.34	4.67	1.4	26.2	-0.624
1000	1.309	22433	12	300	549	3.11	6.22	1.87	19.72	-0.618
1500	1.963	33640	14.5	363	664	3.76	7.52	2.26	16.32	-0.606
2000	2.618	44865	16.5	413	755	4.275	8.55	2.57	14.32	-0.595

Table A- 6 Corrosion of carbon steel in 0.2 M Na₂SO₄ and 52 °C

u, rpm	u, m/s	Re	i_L=i_{corr}, A/m²	CR, gmd	CR, mpy	N_{O₂},×10⁵ mol/m².s	N_{Fe},×10⁵ mol/m².s	K,×10⁴ m/s	δ,×10⁶ m	E_{corr}, V
0	0	Static	1	25	45.8	0.259	0.518	0.168	257.6	-0.9
250	0.327	6581	5.75	144	263	1.489	2.98	0.965	44.8	-0.722
500	0.655	13181	5.9	148	270	1.53	3.06	0.99	43.6	-0.703
750	0.982	19762	7.5	188	344	1.94	3.89	1.26	34.28	-0.629
1000	1.309	26342	9.9	248	453	2.57	5.13	1.68	25.92	-0.626
1500	1.963	39503	13.5	337	618	3.49	6.99	2.25	19.2	-0.618
2000	2.618	52685	15.5	387	709	4.02	8.03	2.6	16.56	-0.615

Table A- 7 Corrosion of carbon steel in 0.2 M Na₂SO₄ with addition of air bubbles and 32 °C

u, rpm	u, m/s	Re	i_L=i_{corr}, A/m²	CR, gmd	CR, mpy	N_{O₂},×10⁵ mol/m².s	N_{Fe},×10⁵ mol/m².s	K,×10⁴ m/s	δ,×10⁶ m	E_{corr}, V
0	0	Static	1.3	33	59.5	0.337	0.674	0.147	194	-0.823
250	0.327	4698	6	150	275	1.55	3.109	0.55	51.72	-0.808
750	0.982	14107	9.2	230	421	2.39	4.77	0.72	39.56	-0.66
2000	2.618	37609	16.1	402	737	4.17	8.34	1.113	25.68	-0.649

Table A- 8 Corrosion of carbon steel in 0.2 M Na₂SO₄ with addition of air bubbles and 42 °C

u, rpm	u, m/s	Re	i_L=i_{corr}, A/m²	CR, gmd	CR, mpy	N_{O₂},×10⁵ mol/m².s	N_{Fe},×10⁵ mol/m².s	K,×10⁴ m/s	δ,×10⁶ m	E_{corr}, V
0	0	Static	1.95	48.8	89.3	0.51	1.01	0.25	148.8	-0.787
250	0.327	5604	7	175	320	1.82	3.63	0.72	51.2	-0.739
750	0.982	16829	11.6	290	531	3.01	6.01	1.17	31.52	-0.631
2000	2.618	44865	17.5	438	801	4.53	9.069	1.63	22.6	-0.625

Table A- 9 Corrosion of carbon steel in 0.2 M Na₂SO₄ with addition of air bubbles and 52 °C

u, rpm	u, m/s	Re	i_L=i_{corr}, A/m²	CR, gmd	CR, mpy	N_{O2},×10⁵ mol/m².s	N_{Fe},×10⁵ mol/m².s	K,×10⁴ m/s	δ,×10⁶ m	E_{corr}, V
0	0	Static	1.4	35	64.1	0.36	0.725	0.194	222.8	-0.728
250	0.327	6581	6.5	163	298	1.69	3.37	0.868	49.6	-0.701
750	0.982	19762	9.25	231	423	2.395	4.79	1.165	37.2	-0.614
2000	2.618	52685	16.5	413	755	4.28	8.55	1.97	21.92	-0.611

Table A- 10 Corrosion of carbon steel in 0.2 M Na₂SO₄ at 32 °C for immersion time of 2 h and velocity of 250 rpm

Time, h	i_L=i_{corr}, A/m²	CR, gmd	CR, mpy	N_{O2},×10⁵ mol/m².s	N_{Fe},×10⁵ mol/m².s	K,×10⁴ m/s	δ,×10⁶ m	E_{corr}, V
0	5.5	138	251.72	1.42	2.83	0.735	38.88	-0.67
1	3.25	81.06	148.4	0.84	1.68	0.43	64	-0.685
2	2.75	68.99	126.3	0.72	1.43	0.37	76.4	-0.686

Table A- 11 Corrosion of carbon steel in 0.2 M Na₂SO₄ at 32°C for immersion time of 2 h and velocity of 1000 rpm

Time, h	i_L=i_{corr}, A/m²	CR, gmd	CR, mpy	N_{O2},×10⁵ mol/m².s	N_{Fe},×10⁵ mol/m².s	K,×10⁴ m/s	δ,×10⁶ m	E_{corr}, V
0	12	299.2	547.7	3.1	6.2	1.598	17.88	-0.604
1	8	197.8	362.1	2.05	4.1	1.07	26.76	-0.610
2	7	175.15	320.6	1.82	3.63	0.935	30.4	-0.615

Table A- 12 Corrosion of carbon steel in 0.2 M Na₂SO₄ at 32 °C for immersion time of 2 h and velocity of 2000 rpm

Time, h	$i_L = i_{\text{corr}}$, A/m ²	CR, gmd	CR, mpy	N _{O₂} , ×10 ⁵ mol/m ² .s	N _{Fe} , ×10 ⁵ mol/m ² .s	K, ×10 ⁴ m/s	δ, ×10 ⁶ m	E _{corr} , V
0	15.5	387.4	709.2	4.02	8.03	2.18	13.6	-0.610
1	7.5	187.7	343.6	1.95	3.89	1	28.4	-0.671
2	6.75	168.4	308.3	1.75	3.49	0.9	31.72	-0.690

Table A- 13 Corrosion of carbon steel in 0.2 M Na₂SO₄ at 42 °C for immersion time of 2 h and velocity of 250 rpm

Time, h	$i_L = i_{\text{corr}}$, A/m ²	CR, gmd	CR, mpy	N _{O₂} , ×10 ⁵ mol/m ² .s	N _{Fe} , ×10 ⁵ mol/m ² .s	K, ×10 ⁴ m/s	δ, ×10 ⁶ m	E _{corr} , V
0	6.25	156.3	286.1	1.62	3.24	0.98	3.76	-0.623
1	4.35	108.6	198.8	1.13	2.25	0.68	5.44	-0.738
2	3	74.8	136.9	0.78	1.55	0.47	7.88	-0.740

Table A- 14 Corrosion of carbon steel in 0.2 M Na₂SO₄ at 52 °C for immersion time of 2 h and velocity of 250 rpm

Time, h	$i_L = i_{\text{corr}}$, A/m ²	CR, gmd	CR, mpy	N _{O₂} , ×10 ⁵ mol/m ² .s	N _{Fe} , ×10 ⁵ mol/m ² .s	K, ×10 ⁴ m/s	δ, ×10 ⁶ m	E _{corr} , V
0	5.5	137.5	251.7	1.43	2.85	0.93	48	-0.722
1	4.5	112.4	205.8	1.17	2.33	0.75	57.6	-0.750
2	3.1	77.68	142.2	0.58	1.16	0.52	84	-0.808

Table A- 15 Corrosion of carbon steel in 0.2 M Na₂SO₄ with addition of air bubbles at 32 °C
for immersion time of 2 h and velocity of 250 rpm

Time, h	$i_L = i_{\text{corr}}$, A/m ²	CR, gmd	CR, mpy	N _{O₂} ,×10 ⁵ mol/m ² .s	N _{Fe} ,×10 ⁵ mol/m ² .s	K,×10 ⁴ m/s	δ,×10 ⁶ m	E _{corr} , V
0	6	149.6	273.9	1.55	3.1	0.55	52	-0.588
1	4.75	120.6	220.8	1.25	2.5	0.43	68	-0.618
2	4.25	106.2	194.4	1.1	2.2	0.4	72	-0.630

Table A- 16 Corrosion of carbon steel in 0.2 M Na₂SO₄ with addition of air bubbles at 32 °C
for immersion time of 2 h and velocity of 750 rpm

Time, h	$i_L = i_{\text{corr}}$, A/m ²	CR, gmd	CR, mpy	N _{O₂} ,×10 ⁵ mol/m ² .s	N _{Fe} ,×10 ⁵ mol/m ² .s	K,×10 ⁴ m/s	δ,×10 ⁶ m	E _{corr} , V
0	9	226.8	415.2	2.35	4.7	0.7	40.8	-0.604
1	5.25	130.3	238.5	1.35	2.7	0.4	71.6	-0.663
2	4.5	110.9	203	1.15	2.3	0.35	79.6	-0.668

Table A- 17 Corrosion of carbon steel in 0.2 M Na₂SO₄ with addition of air bubbles at 32 °C
for immersion time of 2 h and velocity of 2000 rpm

Time, h	$i_L = i_{\text{corr}}$, A/m ²	CR, gmd	CR, mpy	N _{O₂} ,×10 ⁵ mol/m ² .s	N _{Fe} ,×10 ⁵ mol/m ² .s	K,×10 ⁴ m/s	δ,×10 ⁶ m	E _{corr} , V
0	16	400.5	733.1	4.15	8.3	1.13	25.2	-0.581
1	7.5	188.2	344.5	1.95	3.9	0.52	56	-0.632
2	6	149.6	273.9	1.55	3.1	0.43	68	-0.639

Table A- 18 Corrosion of carbon steel in 0.2 M Na₂SO₄ with addition of air bubbles at 42 °C
for immersion time of 2 h and velocity of 250 rpm

Time, h	$i_L = i_{\text{corr}}$, A/m ²	CR, gmd	CR, mpy	N _{O₂} ,×10 ⁵ mol/m ² .s	N _{Fe} ,×10 ⁵ mol/m ² .s	K,×10 ⁴ m/s	δ,×10 ⁶ m	E _{corr} , V
0	7	173.7	317.9	1.8	3.6	0.723	50.8	-0.59
1	4.5	110.9	203	1.15	2.3	0.47	78.8	-0.650
2	3.5	86.85	158.9	0.9	1.8	0.36	104	-0.711

Table A- 19 Corrosion of carbon steel in 0.2 M Na₂SO₄ with addition of air bubbles at 52 °C
for immersion time of 2 h and velocity of 250 rpm

Time, h	$i_L = i_{\text{corr}}$, A/m ²	CR, gmd	CR, mpy	N _{O₂} ,×10 ⁵ mol/m ² .s	N _{Fe} ,×10 ⁵ mol/m ² .s	K,×10 ⁴ m/s	δ,×10 ⁶ m	E _{corr} , V
0	6.5	162.6	297.65	1.69	3.37	0.87	49.6	-0.638
1	5	124.97	228.77	1.295	2.59	0.67	64.8	-0.679
2	3.5	87.33	159.86	0.91	1.81	0.47	92.4	-0.686

Table A- 20 Corrosion of carbon steel in 0.01 M Na₂SO₄ at different temperatures and
velocity of 750 rpm

T, °C	$i_L = i_{\text{corr}}$, A/m ²	CR, gmd	CR, mpy	N _{O₂} ,×10 ⁵ mol/m ² .s	N _{Fe} ,×10 ⁵ mol/m ² .s	K,×10 ⁴ m/s	δ,×10 ⁶ m	E _{corr} , V
32	5.75	139.9	256.1	1.45	2.9	0.63	44	-0.539
42	9	226.8	525	2.35	4.7	1.16	31.6	-0.505
52	7.75	193	353.3	2	4.0	1.08	40	-0.520

Table A- 21 Corrosion of carbon steel in 0.025 M Na₂SO₄ at different temperatures and velocity of 750 rpm

T, °C	i_L=i_{corr}, A/m ²	CR, gmd	CR, mpy	N_{O2},×10⁵ mol/m ² .s	N_{Fe},×10⁵ mol/m ² .s	K,×10⁴ m/s	δ,×10⁶ m	E_{corr}, V
32	7.25	181.4	332.1	1.88	3.76	0.85	33.6	-0.559
42	9.5	236.4	432.7	2.45	4.9	1.28	28.8	-0.541
52	7	173.7	317.9	1.8	3.6	1.03	42	-0.602

Table A- 22 Corrosion of carbon steel in 0.05 M Na₂SO₄ at different temperatures and velocity of 750 rpm

T, °C	i_L=i_{corr}, A/m ²	CR, gmd	CR, mpy	N_{O2},×10⁵ mol/m ² .s	N_{Fe},×10⁵ mol/m ² .s	K,×10⁴ m/s	δ,×10⁶ m	E_{corr}, V
32	9	226.8	415.2	2.35	4.7	1.09	26	-0.583
42	12.5	313.6	574.1	3.25	6.5	1.78	20.7	-0.571
52	9.1	226.8	415.2	2.35	4.7	1.39	31.1	-0.576

Table A- 23 Corrosion of carbon steel in 0.1 M Na₂SO₄ at different temperatures and velocity of 750 rpm

T, °C	i_L=i_{corr}, A/m ²	CR, gmd	CR, mpy	N_{O2},×10⁵ mol/m ² .s	N_{Fe},×10⁵ mol/m ² .s	K,×10⁴ m/s	δ,×10⁶ m	E_{corr}, V
32	7.5	188.2	344.5	1.95	3.9	0.96	29.7	-0.573
42	12	299.2	547.7	3.1	6.2	1.78	20.6	-0.570
52	11	275	503.4	2.85	5.7	1.7	25.4	-0.572

Table A- 24 Corrosion of carbon steel in 0.4 M Na₂SO₄ at different temperatures and velocity of 750 rpm

T, °C	i_L=i_{corr}, A/m ²	CR, gmd	CR, mpy	N_{O2},×10⁵ mol/m ² .s	N_{Fe},×10⁵ mol/m ² .s	K,×10⁴ m/s	δ,×10⁶ m	E_{corr}, V
32	4	101.3	185.4	1.05	2.1	0.57	50	-0.600
42	6.25	156.3	286.1	1.62	3.24	1.02	36.1	-0.595
52	6	149.6	273.9	1.55	3.1	1.05	41.3	-0.600

Appendix -B-

Table B-1 Corrosion of carbon steel in 0.01 M Na₂SO₄ + 1 % HCl

T, °C	u, rpm	u, m/s	Re	i_{corr}, A/m²	CR, gmd	CR, mpy	N_{Fe} × 10⁴ mol/m².s	β_a, v.m²/A	β_c, v.m²/A	E_{corr}, V
32	0	0	static	8	197.8	362	0.41	0.018	-0.00753	-0.555
	250	0.327	4663	23	579	1059.9	1.2	0.0193	-0.00588	-0.5
	750	0.982	14004	34	849.2	1554.5	1.76	0.025	-0.0047	-0.478
	2000	2.618	37334	50	1249	2287.5	2.59	0.038	-0.004	-0.476
42	250	0.327	5501	31	776.8	1421.9	1.61	0.0382	-0.0056	-0.498
52	250	0.327	6437	40	1013	1854.9	2.1	0.0641	-0.0054	-0.495

Table B- 2 Corrosion of carbon steel in 0.05 M Na₂SO₄ + 1 % HCl at velocity of 250 rpm

T, °C	Re	i_{corr}, A/m²	CR, gmd	CR, mpy	N_{Fe} × 10⁴ mol/m².s	β_a, v.m²/A	β_c, v.m²/A	E_{corr}, V
32	4657	33	825.1	1510	1.71	0.00982	-0.00741	-0.505
42	5526	45	1124	2058	2.33	0.0333	-0.00455	-0.490
52	6537	60	1501	2747	3.11	0.0339	-0.00136	-0.489

Table B- 3 Corrosion of carbon steel in 0.2 M Na₂SO₄ + 1 % HCl at velocity of 250 rpm

T, °C	Re	i_{corr}, A/m²	CR, gmd	CR, mpy	N_{Fe}, × 10⁴ mol/m².s	β_a, v.m²/A	β_c, v.m²/A	E_{corr}, V
32	4639	28	699.6	1281	1.45	0.00743	-0.00455	-0.480
42	5519	42	1052	1926	2.18	0.0092	-0.00357	-0.482
52	6492	49	1226	2243	2.54	0.0206	-0.00293	-0.488

Table B-4 Corrosion of carbon steel in 0.2 M Na₂SO₄ + 0.5 % HCl at velocity of 250 rpm

T, °C	Re	i_{corr}, A/m²	CR, gmd	CR, mpy	N_{Fe}, × 10⁴ mol/m².s	β_a, v.m²/A	β_c, v.m²/A	E_{corr}, V
32	4726	20	501.8	919	1.04	0.00471	-0.0065	-0. 516
42	5618	33	825	1510	1.71	0.00658	-0.0056	-0.515
52	6619	40	999	1828	2.07	0.0222	-0.00533	-0.508

Table B-5 Corrosion of carbon steel in 0.2 M Na₂SO₄ + 3 % HCl at velocity of 250 rpm

T, °C	Re	i_{corr}, A/m²	CR gmd	CR, mpy	N_{Fe}, × 10⁴ mol/m².s	β_a, v.m²/A	β_c, v.m²/A	E_{corr}, V
32	4776	34	849.2	1555	1.76	0.00769	-0.00681	-0. 440
42	5690	48	1291	2199	2.49	0.0325	-0.0033	-0.435
52	6642	56	1399	2562	2.9	0.0365	-0.00235	-0.429

Table B-6 Corrosion of carbon steel in 0.2 M Na₂SO₄ + 1 % HCl with addition of air bubbles

T, °C	u, rpm	u, m/s	Re	i_{corr}, A/m²	CR, gmd	CR, mpy	N_{Fe}, × 10⁴ mol/m².s	β_a, v.m²/A	β_c, v.m²/A	E_{corr}, V
32	0	0	static	29	724.7	1327	1.502	0.002	-0.0038	-0.531
	250	0.327	4639	40	1013	1855	2.1	0.00282	-0.00375	-0.494
	750	0.982	13931	55	1375	2517	2.85	0.018	-0.0037	-0.490
	2000	2.618	37139	68	1689	3092	3.5	0.027	-0.0029	-0.488
42	250	0.327	5519	58	1452	2659	3.01	0.0068	-0.00273	-0.492
52	250	0.327	6492	69	1727	3162	3.58	0.00844	-0.00276	-0.483

Appendix -C-

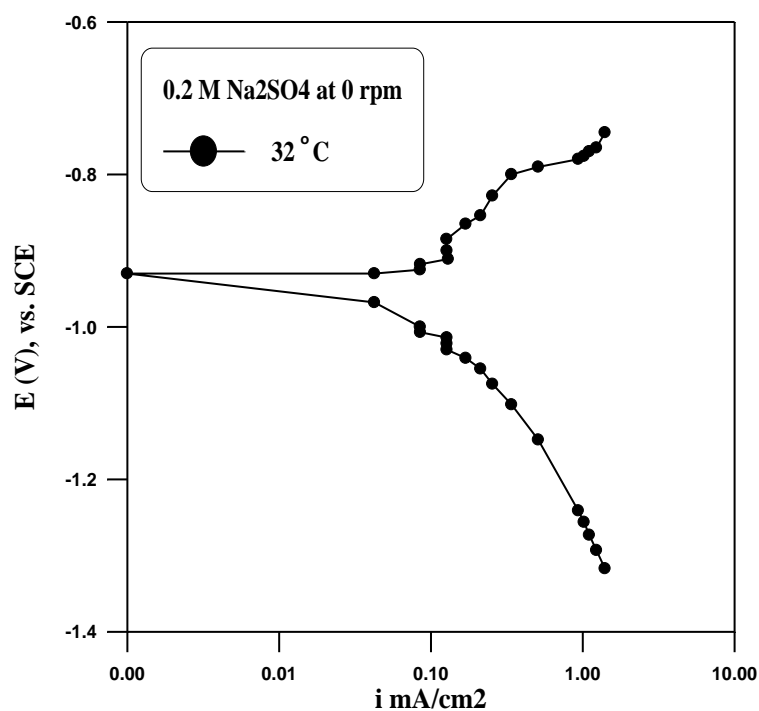


Figure C-1 Polarization curve in 0.2 M Na₂SO₄ at 32 °C and 0 rpm

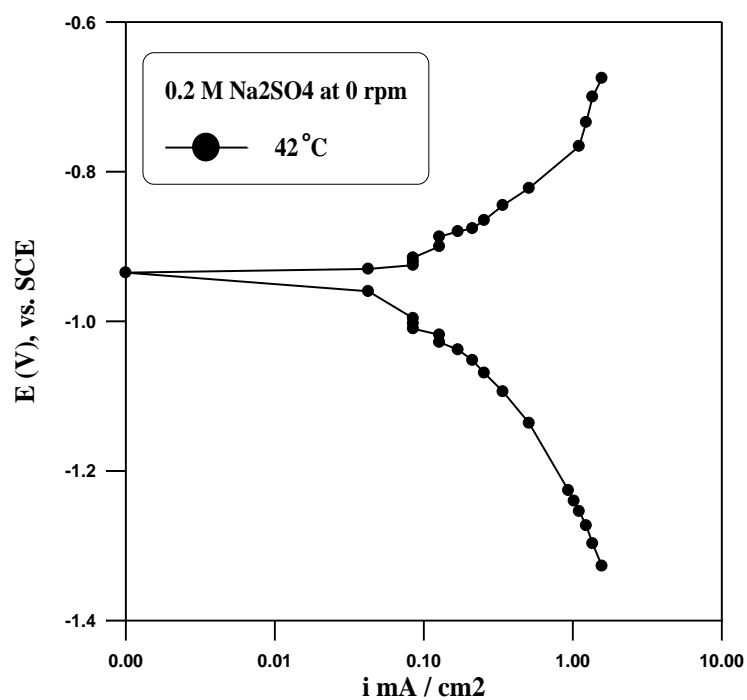


Figure C-2 Polarization curve in 0.2 M Na₂SO₄ at 42 °C and 0 rpm

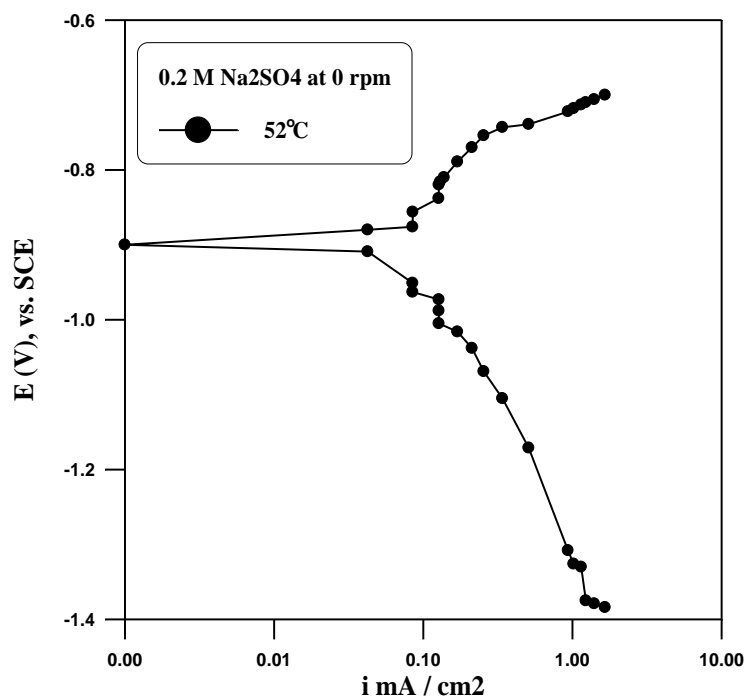


Figure C-3 Polarization curve in 0.2 M Na₂SO₄ at 52 °C and 0 rpm

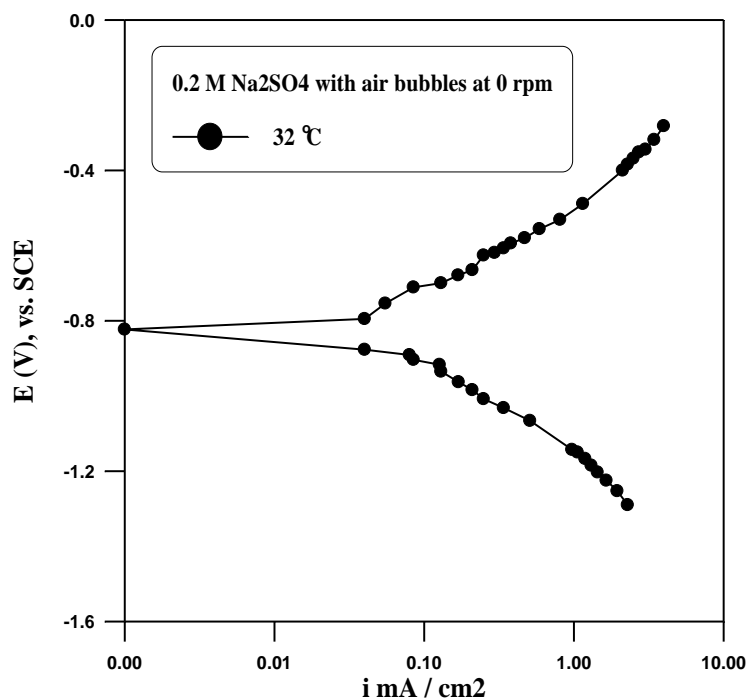


Figure C-4 Polarization curve in 0.2 M Na₂SO₄ with air bubbles at 32 °C and 0 rpm

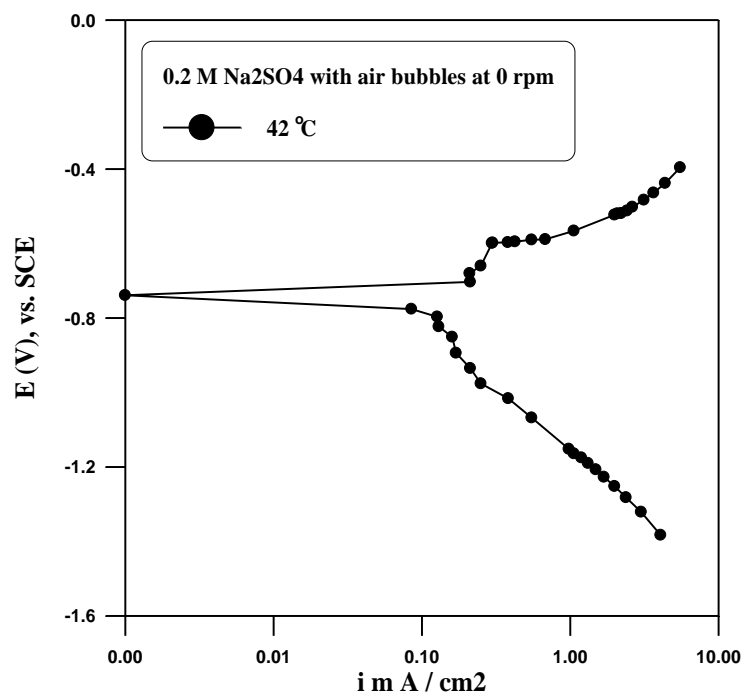


Figure C-5 Polarization curve in 0.2 M Na₂SO₄ with air bubbles at 42 °C and 0 rpm

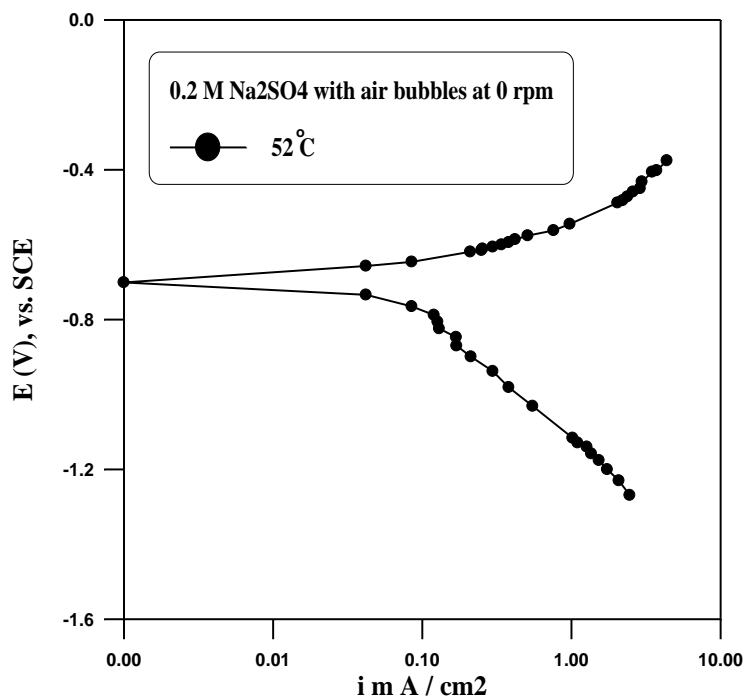


Figure C-6 Polarization curve in 0.2 M Na₂SO₄ with air bubbles at 52 °C and 0 rpm

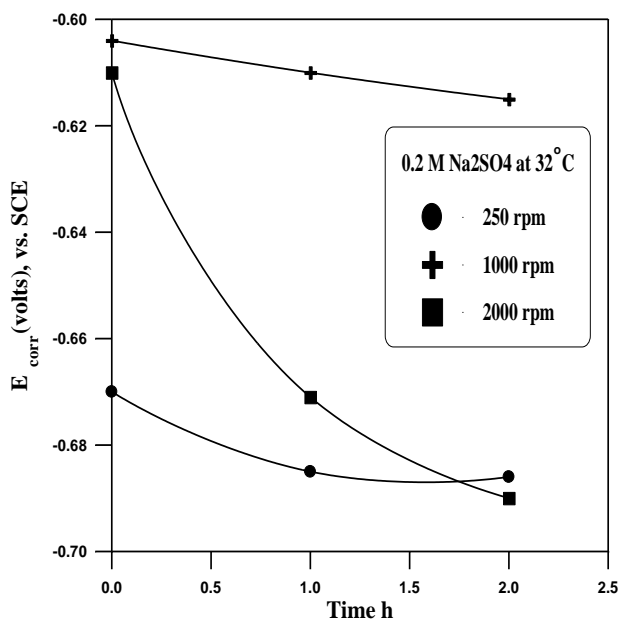


Figure C-7 Variation of E_{corr} with time at different u and $32\text{ }^\circ\text{C}$

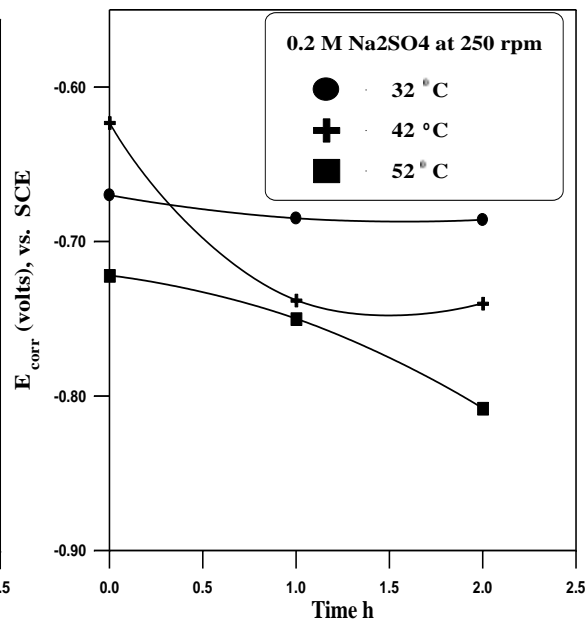


Figure C-8 Variation of E_{corr} with time at different T and 250 rpm

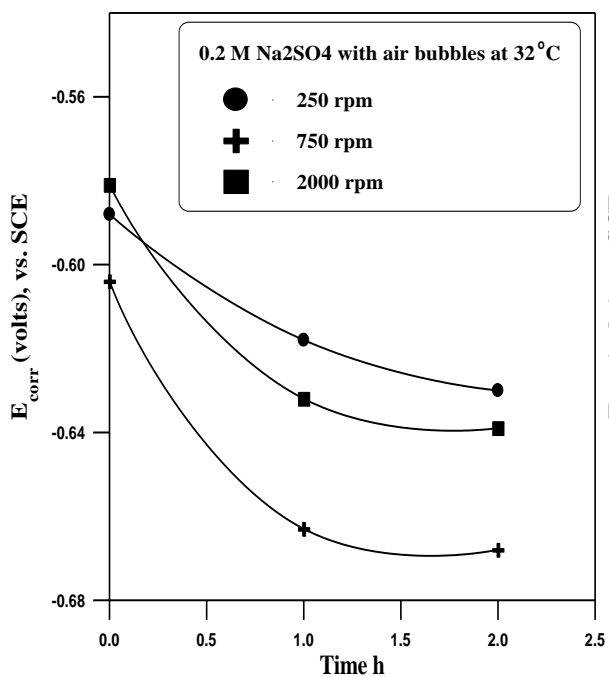


Figure C-9 Variation of E_{corr} with time at different u and $32\text{ }^\circ\text{C}$ in 0.2 M Na_2SO_4 with air bubbles

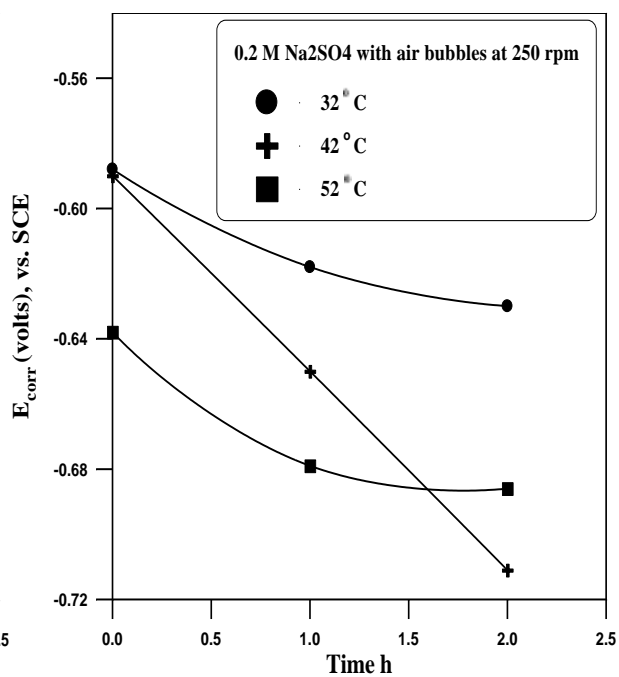


Figure C-10 Variation of E_{corr} with time at different T and 250 rpm in 0.2 M Na_2SO_4 with air bubbles

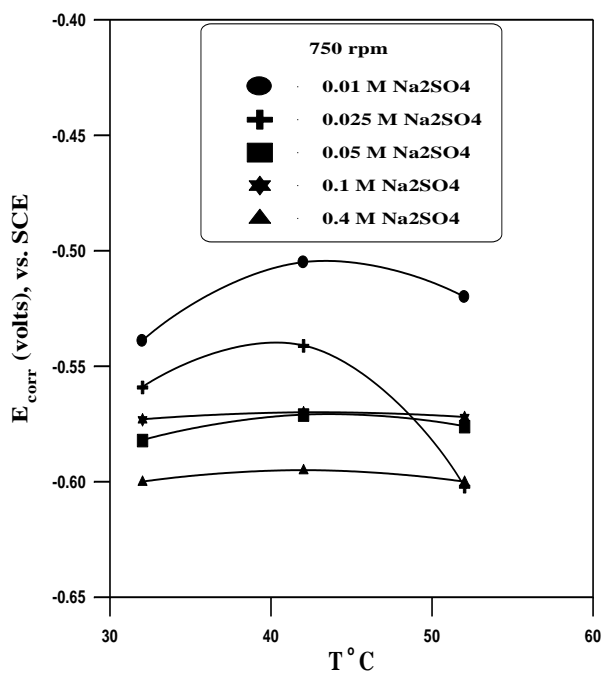


Figure C-11 Variation of E_{corr} with T at 750 rpm in different salt solutions

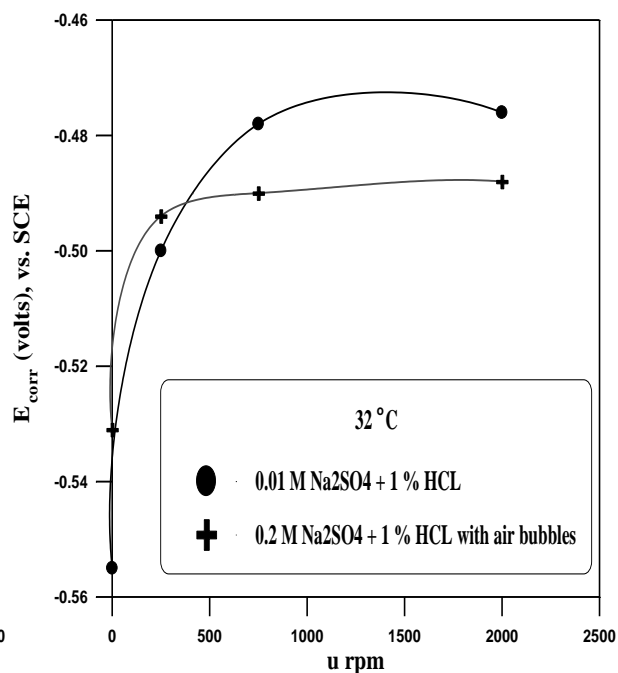


Figure C-12 Variation of E_{corr} with u at 32 °C

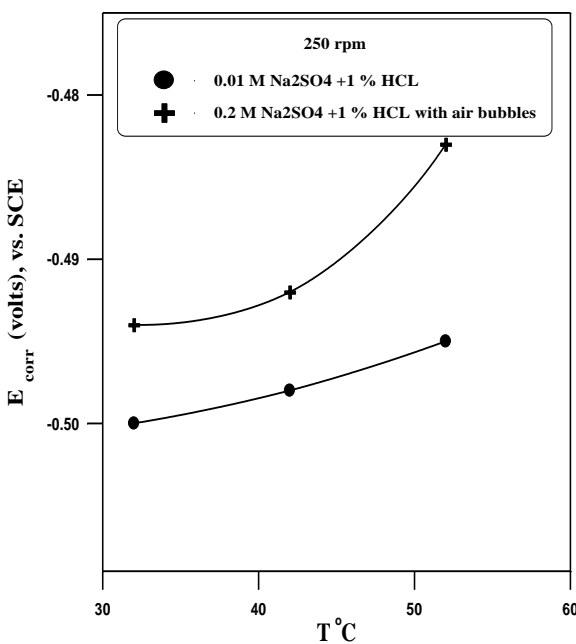


Figure C-13 Variation of E_{corr} with T at 250 rpm in different acid salt solution with and without air bubbles

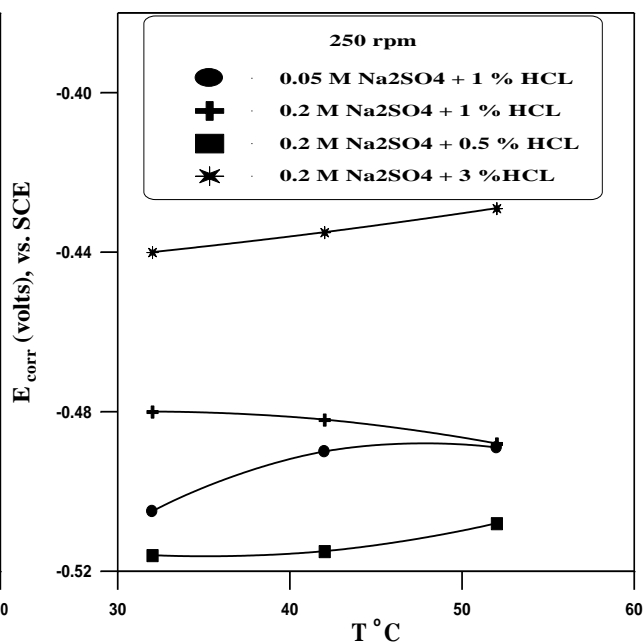


Figure C-14 Variation of E_{corr} with T at 250 rpm in different acid salt solution

Appendix -D-

Table D-1 Data for polarization experiments in 0.2 M Na₂SO₄ at 32 °C

0 rpm		500 rpm		1000 rpm		1500 rpm		2000 rpm	
i mA/cm²	E V								
1.4006	-1.317	2.2494	-1.388	5.3212	-1.391	5.342	-1.384	6.09	-1.334
1.2308	-1.293	1.8674	-1.339	2.3343	-1.291	3.0133	-1.301	2.9285	-1.246
1.1035	-1.273	1.6128	-1.303	1.9523	-1.238	2.3767	-1.243	2.3343	-1.167
1.0186	-1.256	1.4006	-1.272	1.6977	-1.19	1.9947	-1.204	1.9947	-1.1
0.9337	-1.241	1.2308	-1.247	1.4854	-1.146	1.6977	-1.164	1.7401	-1.02
0.5093	-1.148	1.1035	-1.226	1.3157	-1.099	1.4854	-1.126	1.5703	-0.937
0.3395	-1.102	1.0186	-1.208	1.1884	-1.051	1.3472	-1.06	1.4006	-0.875
0.2546	-1.075	0.9337	-1.192	1.1035	-0.993	1.209	-1.013	1.2732	-0.826
0.2122	-1.055	0.5093	-1.067	0.8765	-0.92	1.1213	-0.967	1.1884	-0.762
0.1698	-1.041	0.3395	-0.978	0.5521	-0.76	0.6554	-0.783	0.8913	-0.722
0.1273	-1.03	0.2546	-0.896	0.38197	-0.7009	0.48835	-0.712	0.5942	-0.651
0.1273	-1.022	0.2122	-0.827	0.2971	-0.675	0.3213	-0.675	0.4244	-0.629
0.1273	-1.014	0.1698	-0.77	0.2546	-0.65	0.2546	-0.66	0.2971	-0.62
0.085	-1.007	0.1486	-0.735	0.2122	-0.643	0.2122	-0.651	0.2546	-0.616
0.08488	-1	0.128	-0.718	0.1273	-0.64	0.1698	-0.646	0.2122	-0.613
0.04244	-0.968	0.1273	-0.703	0.08488	-0.636	0.1273	-0.643	0.1698	-0.611
0.000	-0.93	0.085	-0.69	0.04244	-0.632	0.1273	-0.64	0.1273	-0.61
....	0.08488	-0.679	0.000	-0.623	0.08488	-0.638	0.1273	-0.609
....	0.04244	-0.654	0.04244	-0.633	0.08488	-0.608
....	0.000	-0.639	0.000	-0.62	0.04244	-0.606
....	0.000	-0.604

Table D-2 Data for polarization experiments in 0.2 M Na₂SO₄ + 1 % HCl at 250 rpm

32 °C		42 °C		52 °C	
i (mA/cm ²)	E (V)	i (mA/cm ²)	E (V)	i (mA/cm ²)	E (V)
35.231	-1.449	57.8901	-1.54	34.987	-1.371
22.665	-1.309	34.8019	-1.489	27.502	-1.286
21.765	-1.215	27.502	-1.344	22.876	-1.214
16.543	-1.144	22.6637	-1.255	19.225	-1.162
12.987	-1.094	19.2259	-1.18	16.637	-1.116
11.765	-1.049	16.637	-1.113	14.7696	-1.078
11.231	-1.018	14.7696	-1.072	13.1564	-1.043
11.009	-0.994	13.1568	-1.03	11.9685	-1.015
10.987	-0.976	11.9685	-1.0002	11.234	-0.995
10.441	-0.964	11.035	-0.972	11.0099	-0.965
8.913	-0.933	10.228	-0.95	10.765	-0.943
8.488	-0.923	9.7615	-0.927	10.0032	-0.923
7.894	-0.906	9.0825	-0.905	9.998	-0.905
7.427	-0.897	8.5307	-0.898	9.342	-0.888
7.003	-0.886	8.0214	-0.877	8.887	-0.876
6.663	-0.873	7.597	-0.86	8.432	-0.858
6.451	-0.863	7.1726	-0.846	6.989	-0.844
6.069	-0.848	6.8331	-0.834	6.665	-0.833
5.729	-0.836	6.536	-0.824	6.334	-0.81
5.517	-0.827	6.239	-0.81	5.789	-0.808
5.39	-0.827	5.9418	-0.8	5.342	-0.79
5.178	-0.823	5.7296	-0.794	5.009	-0.782
4.966	-0.813	5.5174	-0.782	4.669	-0.771
4.796	-0.804	5.3052	-0.773	4.541	-0.766
4.669	-0.798	5.1354	-0.764	4.414	-0.758
4.498	-0.794	4.9232	-0.757	4.287	-0.751
4.329	-0.789	4.7534	-0.749	4.159	-0.744
4.202	-0.777	4.6261	-0.741	3.947	-0.732
4.117	-0.772	4.456	-0.735	3.819	-0.725
3.947	-0.769	4.3715	-0.729	3.735	-0.721
3.819	-0.756	4.2441	-0.721	3.565	-0.711
3.692	-0.754	4.117	-0.715	3.48	-0.707
3.608	-0.748	3.9895	-0.711	3.31	-0.699
3.523	-0.747	3.905	-0.703	3.226	-0.696
3.438	-0.746	3.819	-0.698	3.013	-0.685
3.353	-0.743	3.6499	-0.692	2.886	-0.678
3.268	-0.738	3.565	-0.688	2.801	-0.672
3.183	-0.735	3.4802	-0.685	2.631	-0.664
3.141	-0.735	3.395	-0.678	2.419	-0.651
3.056	-0.73	3.31	-0.673	2.334	-0.646

Table D-2 (Continued)

2.759	-0.717	3.268	-0.671	2.249	-0.642
2.716	-0.714	3.0558	-0.66	2.207	-0.64
2.589	-0.706	2.971	-0.657	1.995	-0.625
2.504	-0.7	2.928	-0.653	1.909	-0.621
2.207	-0.682	2.8011	-0.648	1.74	-0.61
2.165	-0.677	2.674	-0.641	1.698	-0.606
2.122	-0.668	2.631	-0.64	1.528	-0.595
1.825	-0.651	2.334	-0.624	1.358	-0.586
1.613	-0.64	2.2918	-0.621	1.231	-0.579
1.443	-0.626	2.249	-0.618	0.976	-0.562
1.316	-0.616	2.0796	-0.609	0.891	-0.554
1.188	-0.604	2.037	-0.606	0.764	-0.548
1.103	-0.594	1.9523	-0.604	0.679	-0.543
1.019	-0.592	1.9099	-0.602	0.6366	-0.541
0.934	-0.584	1.698	-0.59	0.4669	-0.531
0.891	-0.58	1.528	-0.58	0.4244	-0.528
0.806	-0.574	1.358	-0.571	0.297	-0.521
0.806	-0.568	1.2308	-0.564	0.2546	-0.517
0.722	-0.559	1.061	-0.554	0.2122	-0.514
0.6366	-0.551	0.9337	-0.546	0.1698	-0.513
0.467	-0.546	0.8064	-0.539	0.1273	-0.512
0.467	-0.539	0.6791	-0.532	0.1273	-0.511
0.4244	-0.538	0.6366	-0.531	0.1273	-0.51
0.297	-0.525	0.4244	-0.52	0.08488	-0.509
0.255	-0.517	0.2971	-0.512	0.0696	-0.5
0.2122	-0.51	0.2546	-0.508	0.0471	-0.496
0.1698	-0.509	0.2122	-0.506	0.0357	-0.49
0.1273	-0.506	0.1698	-0.504	0.002	-0.485
0.1273	-0.503	0.1273	-0.503	0.0000	-0.48
0.1273	-0.5	0.1273	-0.502	0.0255	-0.48
0.08488	-0.5	0.1273	-0.501	0.03	-0.48
0.0467	-0.492	0.08488	-0.501	0.039	-0.48
0.0352	-0.488	0.04244	-0.498	0.054	-0.48
0.0284	-0.486	0.0471	-0.497	0.0891	-0.479
0.0178	-0.484	0.0357	-0.496	0.1564	-0.479
0.0132	-0.484	0.0289	-0.49	0.1987	-0.478
0.0000	-0.484	0.0238	-0.488	0.2009	-0.478
0.025	-0.474	0.0204	-0.484	0.21243	-0.477
0.0344	-0.473	0.0178	-0.483	0.312	-0.477
0.0454	-0.472	0.0132	-0.482	0.332	-0.476
0.0675	-0.469	0.0000	-0.482	0.432	-0.476
0.0891	-0.466	0.1319	-0.482	0.538	-0.474

Table D-2 (Continued)

0.129	-0.461	0.249	-0.481	0.668	-0.466
0.249	-0.447	0.2737	-0.481	0.879	-0.454
0.273	-0.443	0.304	-0.48	1.282	-0.43
0.303	-0.439	0.341	-0.48	2.351	-0.371
0.339	-0.434	0.388	-0.479	2.534	-0.3617
0.387	-0.429	0.451	-0.478	2.776	-0.3504
0.449	-0.423	0.538	-0.473	3.073	-0.3364
0.535	-0.414	0.668	-0.467	3.4378	-0.3195
0.662	-0.396	0.879	-0.457	3.913	-0.295
0.866	-0.377	1.282	-0.438	4.545	-0.2667
1.2648	-0.3334	2.351	-0.389	5.348	-0.2268
2.3046	-0.254	2.534	-0.381	6.663	-0.1714
2.487	-0.2447	2.776	-0.373	9.846	-0.0455
2.725	-0.2307	3.073	-0.358	22.654	0.1642
2.996	-0.2109	3.4378	-0.3459	23.765	0.188
3.344	-0.15	3.913	-0.3255	25.321	0.2126
3.782	-0.118	4.545	-0.3009	27.654	0.236
4.431	-0.082	5.348	-0.268	30.654	0.2987
5.288	-0.018	6.663	-0.222	35.321	0.3653
6.578	0.041	9.846	-0.1154	44.5434	0.451
9.252	0.177	16.17	0.052	50.234	0.559
15.788	0.3855	16.17	0.0636	60.987	0.719
15.873	0.386	17.019	0.0885	67.765	0.925
16.807	0.388	18.335	0.1209	78.543	1.256
17.825	0.433	20.117	0.1692
19.099	0.45	22.621	0.229
20.329	0.506	25.974	0.301
22.494	0.594	30.643	0.385
26.568	0.673	37.475	0.528
31.534	0.798	50.081	0.703
42.017	0.941
60.352	1.254

الخلاصة

تم بحث تآكل الكربون الفولاذي في محاليل ملحية وحامضية تحت ظروف جريان لمعدل من السرعة الدوارانية يتراوح بين ٠ - ٢٠٠٠ دورة بالدقيقة و درجات حرارة ٣٢ - ٥٢ م° باستخدام القطب الاسطواني الدوار . تم حساب معدل التآكل باستخدام كلا من طريقة فقدان الوزن وتقنية الاستقطاب الكهروكيميائي. استخدمت تراكيز مختلفة من الملح والحامض تتراوح بين ٠,٠١ - ٠,٠٤ مولاري للملح ٠,٥% - ٥% للحامض. تم استخدام مانعات تاكل وهي الاندول و ستايلترايميثايل امونيوم برومايد بتراكيز ٠,٠٢٧٤ مولاري للستايلترايميثايل امونيوم برومايد و ٠,٠٠٧١ الى ٠,٠٠٣٤ مولاري للاندول. تم بحث تأثير الزمن أو تكوين طبقة نواتج التآكل على المحلول الملحي و تأثير تركيز الاوكسجين من خلال ضخ فقاعات من الهواء في المحاليل. أظهرت النتائج انه زيادة سرعة الجريان يؤدي الى زيادة معدل التآكل لجميع المحاليل التي تم استخدامها. ايضا معدل التآكل في المحاليل الملحية يتجه الى كونه غير مستقر مع زيادة تراكيز الملح والحرارة . في محاليل الحامض زيادة الحرارة وتراكيز الحامض يؤدي الى زيادة معدلات التآكل. بصورة عامة معدل التآكل الذي مثل بواسطة كثافة التيار المحدد يقل مع الزمن معتمدا على السرعة الدوارانية و الحرارة . لقد وجد انه اضافة فقاعات هواء باستخدام مضخة هواء يؤدي الى زيادة كبيرة في معدلات التآكل معتمدا على السرعة الدوارانية، الحرارة والزمن. اكبر تأثير لتركيز الاوكسجين لوحظ في حالة محاليل الحامض و في حالة السرعة العالية. تم الحصول على معادلات تربط بين معدل التآكل و المتغيرات الاخرى مثل السرعة ودرجة الحرارة والتركيز والزمن باستخدام الطريقة الاحصائية (STATISTICA version 5.0).

الاندول و ستايلترايميثايل امونيوم برومايد اظهرا كفاءة تثبيط عالية في معظم الظروف التي تم بحثها مع افضل كفاءة تثبيط التي وصلت الى ٨٨% عند السرعة الدوارانية الواطنة وتقل مع زيادة سرعة الجريان. بالاضافة الى ذلك، مانع التآكل اندول اظهر كفاءة تثبيط ممتازة مع درجات الحرارة العالية بينما في محلول ستايلترايميثايل امونيوم برومايد زيادة درجات الحرارة يؤدي الى نقصان في كفاءة التثبيط.

شكر وتقدير

أود ان أتقدم بخالص شكري و تقديري الى الأستاذ الدكتور باسم عبيد حسن لجهوده القيمة في الاشراف و المشورة العلمية و الوقت الوفير الذي قدمه لي خلال فترة البحث لأخراج هذا العمل في أفضل صورة ممكنة. وكذلك أتقدم بامتناني العميق الى قسم الهندسة الكيماوية في جامعة الزهرين لتقديمهم يد المساعدة وتسهيل اجراء التجارب في مختبراتهم. وكل من ساهم في انجاز هذا العمل.

ساره علي صادق

الباحثة

تآكل الكربون الفولاذي في محاليل حمضية ملحية تحت ظروف جريان

رسالة

مقدمة إلى كلية الهندسة في جامعة النهريين
و هي جزء من متطلبات نيل درجة ماجستير علوم
في الهندسة الكيمياءوية

من قبل

سارة علي صادق

(بكالوريوس علوم في الهندسة الكيمياءوية ٢٠١٠)

١٤٣٤

٢٠١٢

صفر
كانون الأول